REGULATION OF CELLULAR IRON HOMEOSTASIS: MULTIPLE ROLES OF HFE

by

Paige Shelton Davies

A DISSERTATION

Presented to the Department of Cell and Developmental Biology

and the Oregon Health & Science University

School of Medicine

in partial fulfillment of

the requirements for the degree of

Doctor of Philosophy

April 2004

Oregon Health & Science University

School of Medicine

CERTIFICATE OF APPROVAL

This is to certify that the Ph.D. thesis of

Paige Shelton Davies

has been approved

[redacted]

Professor in charge of thesis

[redacted]

Member

[redacted]

Member

[redacted]

Member

TABLE OF CONTENTS

LIST OF ILLUSTRATIONS AND TABLES ..... **iv**

ACKNOWLEDGEMENTS ..... **vi**

ABSTRACT ..... **viii**

ABBREVIATIONS ..... **x**

CELL LINES ..... **xii**

INTRODUCTION **1**
The Fundamental Need for Iron 1
Hereditary Hemochromatosis 1
Control of Iron Homeostasis at the Intestinal and Cellular Level 5
Effect of HFE on Cellular Iron Status 15

CHAPTER 1
Increased IRP1 and IRP2 RNA Binding Activity Accompanies a Reduction of the Labile Iron Pool in HFE-expressing Cells **23**

Summary 24
Introduction 25
Materials and Methods 27
Results 33
Discussion 40

CHAPTER 2
Evidence for the Interaction of the Hereditary Hemochromatosis Protein, HFE, with the Transferrin Receptor in Endocytic Compartments 50

Summary 51
Introduction 52
Materials and Methods 54
Results 62
Discussion 70

CHAPTER 3
Mechanisms of HFE-induced Regulation of Iron Homeostasis: Insights from the W81A HFE Mutation 80

Summary 81
Introduction 82
Materials and Methods 84
Results 87
Discussion 94

CHAPTER 4
Expression of the Hereditary Hemochromatosis Protein, HFE, Increases Ferritin Levels by Inhibiting Iron Export in HT29 Cells 103

Summary 104
Introduction 105
Materials and Methods 108
Results 115
Discussion 123
Supplementary Data 134
Rationale 134
Materials and Methods 136
Results and Discussion 139

SUMMARY AND CONCLUSIONS 145

HFE Expression Lowers Intracellular Iron Levels in HeLa Cells 145
Interaction of HFE and TfR1 148
Effect of HFE on Cellular Iron Status is Independent of TfR1 Association 149
HFE Increases Cellular Iron Levels when Expressed in Intestinal-like Cells ... 149
Multiple Roles of HFE in the Maintenance of Iron Homeostasis 151

APPENDIX I
Polarized HT29 Cells as a Model for Intestinal Villus Cells 154

Rationale 154
Materials and Methods 155
Results and Discussion 159

REFERENCES 168

LIST OF ILLUSTRATIONS AND TABLES

INTRODUCTION

Figure 0.1 *Crystal structure of HFE/β2m heterodimer* 19
Figure 0.2 *Proteins involved in iron absorption* 20
Figure 0.3 *Iron control of translation and mRNA stability* 21
Table 0.1 *Iron Uptake in HeLa and HT29 cells* 22

CHAPTER 1

Figure 1.1 *The rate of ^{35}S-methionine/cysteine incorporation into Ft is reduced in HFE-expressing cells* 44
Figure 1.2 *Total IRP RNA binding activity is increased in HFE-expressing cells* 45
Figure 1.3 *IRP1 and IRP2 RNA binding activity are increased in HFE-expressing cells* 46
Figure 1.4 *Steady state levels of IRP proteins are consistent with reduction of the labile iron pool in HFE-expressing cells* 47
Figure 1.5 *The rate of ^{35}S-methionine/cysteine incorporation into IRP1 does not change in HFE-expressing cells* 48
Figure 1.6 *Analysis of labile iron pools by Calcein in HFE+ cells and HFE- cells* 49

CHAPTER 2

Figure 2.1 *Inducible expression of HFE in fWTHFE/tTA HeLa and HFE–LAMP/tTA HeLa cells* 73
Figure 2.2 *Association of TfR1 and HFE in HFE–LAMP/tTA HeLa cells* 74
Figure 2.3 *Effect of HFE on TfR1 half-life* 75
Figure 2.4 *Tf competes with HFE for binding to TfR1 and increases TfR1 half-life in HeLa cells expressing HFE–LAMP* 76
Figure 2.5 *Immunofluorescence of HFE and TfR1 in HeLa cells expressing different forms of HFE* 77
Figure 2.6 *Measurement of endosome pH* 78
Figure 2.7 *Effect of fWTHFE expression on Tf-associated iron dissociation within endosomes* 79

CHAPTER 3

Figure 3.1 *Evidence for the competition between Tf and HFE for binding to the TfR1 in intact cells and cell lysates* 98

Figure 3.2 *Amount of Tf-mediated ^{55}Fe uptake at different concentrations of diferric-Tf by fWTHFE/tTA, fW81AHFE/tTA, and fC260YHFE/tTA HeLa cells* 99
Figure 3.3 *fW81AHFE/tTA HeLa cells have a low iron phenotype* 100
Figure 3.4 *Localization of HFE and TfR1 in fW81AHFE and fWTHFE/tTA HeLa cells* 101
Figure 3.5 *The effect of the level of HFE expression on Tf-mediated iron uptake into cells* 102

CHAPTER 4

Table 4.1 *Primer sets used for qRT-PCR* 127
Figure 4.1 *Establishment of HT29 cells as a system to study iron homeostasis* 128
Figure 4.2 *HFE expression in HT29 cells* 129
Figure 4.3 *HFE expression increases Ft independently of association with TfR1* .. 130
Table 4.2 *HFE does not alter Tf-mediated iron uptake in HT29 cells* 131
Figure 4.4 *HFE does not alter ^{55}Fe import, but inhibits ^{55}Fe export* 132
Figure 4.5 *Changes in mRNA levels in response to HFE expression* 133

Figure S4.1 *Transient transfection of FPN1 in fWTHFE/tTA HeLa cells* 142
Figure S4.2 *Transient transfection of FPN1 in fWTHFE/tTA HeLa cells in the presence of extracellular Tf* 143
Figure S4.3 *Transient transfection of FPN1 in fW81AHFE/tTA HeLa cells* 144

APPENDIX I

Table AI.1 *Primer sets used for qRT-PCR of mouse samples* 163
Figure AI.1 *Isolation of villus and crypt cells from mouse duodenum*..... 164
Figure AI.2 *Examination of villus and crypt fractions by Musashi-1 PCR* 165
Figure AI.3 *Both villus and crypt cells express mRNA of iron-related genes* 166
Figure AI.4 *Confocal microscopy of HT29 cells seeded on filter inserts* 167

ACKNOWLEDGEMENTS

All that encompasses the achievement of a graduate degree involves collaboration between many hard-working, intelligent, and generous people – all of which I have been privileged enough to work with while attaining this goal.

First, I would like to thank my advisor, Dr. Caroline Enns, for taking me on as a graduate student even though she was away on sabbatical when I wanted to join the lab. She is always enthusiastic about science and has consistently been positive about my project even throughout confusing results. Caroline has always encouraged me in my scientific endeavors and I have learned a great deal from her throughout my time spent in her lab.

I would also like to acknowledge Dr. David Haile, Dr. Anne Brown Mason, Dr. Prem Ponka, Dr. Pamela Bjorkman, Dr. Vonnie Landt, Dr. Rachel Ehrlich, Dr. Richard Eisenstein, Dr. Timothy McGraw, and Dr. John N. Feder who have all provided reagents, methods, and fruitful collaborations that are evidenced throughout this thesis.

Members of my thesis committee, Dr. Svetlana Lutsenko, Dr. Melissa Wong, and Dr. David Koeller, have provided much appreciated insight to my experiments, and have also been supportive in providing letters of recommendation, teaching me new techniques, and encouraging me throughout my research.

There have been many members of the Enns lab during my time here, and I would like to thank them for their technical insight and contributions and also for providing a fun work environment: Dr. An-Sheng Zhang, Martha Johnson, Todd Vogt, Dr. Bill Hooker, Tul-Dim Cing, Dr. Hanqian Carlson, Beatrice Pintea, Mastura Wahedi, Kristen

Bailey, and Fraser Marshall. Frank Green and Emily Anderson were present almost my entire time in the lab and I am grateful for their technical know-how and their always-smiling faces. I would especially like to thank Dr. Cindy Roy whom, though we only overlapped a few months in the lab, is a great model for maintaining excellence and keeping an amazing balance between science, family, and the outside world.

I am grateful to the Lord who has blessed me with so many wonderful people in my life, and their love and prayers carry me through all of my challenges:

Two fellow graduate students have become dear friends - Holly Rosenzweig and Janna Mundt have been steadfast in their support and I value their friendships immensely.

I am grateful that my parents, Dr. Stephen and Cindy Shelton, have always supported and encouraged me to reach for my goals, and stressed the importance of trying hard in all I do. My sisters, Sandy Shelton and Ashley Shelton, have grown up while I've been in graduate school and are now my role models. I appreciate the support from my extended family, Richard and Susan Davies, and Jana Davies who have always understood when I couldn't visit or go to family outings due to work constraints. I am truly blessed to have such wonderful family members and am thankful we remain close even as we spread ourselves across the country.

My husband, Michael H. Davies, has been my rock and strongest supporter for as long as I've known him. His continual encouragement and inspiration truly amaze me and gives me great confidence; and his ability to make me smile under any circumstance is a rare gift. I look forward to this next chapter in our lives together.

ABSTRACT

Hereditary hemochromatosis is an iron overload disease. Even though the gene mutated in the most common form of this disorder, *HFE1*, was identified eight years ago, its function is not understood. HFE does not transport iron and is not regulated by iron; however, its role in maintaining iron homeostasis in the body is clearly evident by the excess iron absorption that ensues when it is not functional. Paradoxically, iron levels in different cell types of the body respond differently to the expression of HFE. We have tested the effect of HFE expression on the iron status in cells of different origin and this thesis focuses on the cell-specific responses observed.

Previous studies showed that expression of HFE in HeLa cells results in lowered ferritin (Ft) and that HFE co-precipitated with transferrin receptor 1 (TfR1) when cells were solubilized. Using both gel shift assays to measure iron regulatory protein binding to the iron responsive element of Ft, and the fluorescent iron sensitive dye, Calcein, we have demonstrated that the decreased Ft is consistent with lower intracellular iron levels. In experiments with HeLa cells expressing a chimeric HFE protein with a lysosomal targeting signal, we show a decreased TfR1 half-life, implying that HFE and TfR1 interact in cells and are also associated in endosomes. The addition of Tf increased the TfR1 half-life, demonstrating that Tf competed with HFE for binding to the TfR1 at the cell surface.

HeLa cells continue to have decreased Tf-mediated iron uptake in the presence of Tf concentrations sufficient to dissociate HFE from TfR1, indicating that HFE's interaction with TfR1 is not essential for its ability to lower intracellular iron levels. To further test this hypothesis, an HFE mutant that has reduced affinity for the TfR1 was

examined. Cells expressing the mutant behaved similarly to cells expressing wild-type HFE with respect to decreased intracellular iron. These findings indicate that HFE can lower iron levels in HeLa cells independently of its interaction with TfR1, leading us to rethink the long-standing hypothesis that the basis behind HFE's function in iron homeostasis was due to its interaction with TfR1.

Although studies in HeLa cells gave insight into a mechanism for HFE, these cells lack many of the proteins involved in iron transport in the body, in particular those involved in the transport of iron across the intestinal epithelium. Using the HT29 cell line as a model more representative of intestinal absorptive cells, we detected endogenous mRNA expression of known genes involved in iron transport. When HFE is expressed in these cells, an iron phenotype opposite to that in HeLa cells was observed. HFE expression in HT29 cells led to increased intracellular iron levels accompanied by increased Ft due to inhibition of iron efflux. This distinction observed in HT29 compared to HeLa cells suggests a multifunctional role for HFE dependent upon expression levels of other proteins involved in iron transport.

ABBREVIATIONS

2-ME	2-mercaptoethanol
β2m	β2-microglobulin, the protein that complexes to MHC class-I-like molecules to allow for proper folding
BSA	Bovine serum albumin
Cp	Ceruloplasmin, a soluble multicopper ferroxidase present in serum
Dcytb	Duodenal cytochrome oxidase b, a ferrireductase found in the brush border membrane of the duodenum
Df	Desferal; an iron chelator
DMEM	Dulbecco's Modified Eagle's Medium
DMT1	Divalent Metal Transporter 1, transports ferrous ions into cells; also known as Nramp2 (Natural Resistance Associated Macrophage Protein 2 for its similarity to Nramp1) and DCT1 (Divalent Cation Transporter 1)
Dox	Doxycycline; an analog of Tetracycline
f	FLAG; an antigenic epitope tag containing 8 amino acids Asp-Tyr-Lys-Asp-Asp-Asp-Asp-Lys
FPN1	Ferroportin 1, a ferrous ion transporter that transports iron out of cells; also known as IREG1 (Iron-Regulated Gene 1) and MTP1 (Metal Transport Protein 1)
Ft	Ferritin; a cytosolic iron storage protein
GAPDH	glyceraldehyde 3-phosphate dehydrogenase
H-Ft	Heavy chain subunit of ferritin
Heph	Hephaestin, a protein with ferroxidase activity implicated in the export of iron from cells
HFE	Hereditary Hemochromatosis gene product; formerly known as HLA-H
HH	Hereditary Hemochromatosis
HLA	Human Leukocyte Antigen
HRP	Horseradish peroxidase
IRE	Iron Responsive Element; a portion of mRNA that forms a specific stem loop structure conferring iron sensitivity to the encoded protein
IRP	Iron Regulatory Protein; two isoforms (IRP1 & IRP2) that bind to IREs
kDa	Kilodaltons
LAMP-1	Lysosomal-associated membrane protein 1
L-Ft	Light chain subunit of ferritin
MHC	Major Histocompatibility Complex
mRNA	messenger RNA
NP	Non-polarized; cells seeded in dishes and not induced to polarize in culture
NTA	Nitrilotriacetic acid; a chelating reagent to keep Fe^{3+} in solution
qRT-PCR	Real-time quantitative reverse transcriptase polymerase chain reaction
PBS	Phosphate Buffered Saline
POL	Polarized; cells seeded on membrane filter inserts to induce polarization in culture
SDS	Sodium dodecyl sulfate
SDS-PAGE	SDS-polyacrylamide gel electrophoresis

SIH	Salicyladehyde isonicotinoyl hydrazone; a cell permeable iron-specific chelator
tet	Tetracycline
Tf	Transferrin, the major iron transport protein in the blood
TfR1	Transferrin Receptor 1, original transferrin receptor cloned in 1984; expressed in most cells and cell lines
TfR2	Transferrin Receptor 2, cloned in 1999 and is 68% identical to the ectodomain of TfR1; expressed mainly in liver and some hemopoietic progenitor cells and cell lines
tTA	Tetracycline Transactivatable
UTR	Untranslated Region

* The numbering system used for HFE in this thesis is based on the processed protein with the N-terminal signal sequence removed. As a result, the C260Y mutation refers to the most common mutation associated with Type 1 HH. In the literature it is often referred to as the C282Y mutation using the numbering sequence starting at the beginning of translation.

CELL LINES

HeLa	Human cell line derived from a cervical adenocarcinoma commonly used in cell culture studies
tTA HeLa	HeLa cell line stably transfected with the tet repressible activator
fWTHFE/tTA HeLa	Tet repressible HeLa cell line stably transfected with FLAG-tagged wild type human HFE under its control. In the presence of tet or dox, fWTHFE is not expressed and in the absence of either of these antibiotics, fWTHFE is expressed.
fW81AHFE/tTA HeLa	Tet repressible HeLa cell line stably transfected with FLAG-tagged W81A mutant HFE under its control. The W81A mutation causes a greatly reduced affinity of HFE for binding to the TfR1.
fC260YHFE/tTA HeLa	Tet repressible HeLa cell line stably transfected with FLAG-tagged C260Y mutant HFE under its control. The C260Y mutation disrupts a required disulfide bond critical for HFE folding; this mutation causes most cases of Type 1 HH
HFE-LAMP/tTA HeLa	Tet repressible HeLa cell line stably transfected with a chimera of wild type human HFE with its cytoplasmic tail replaced with that of the LAMP-1 protein under its control. The LAMP-1 cytoplasmic tail contains a lysosomal targeting motif.
HT29	Human cell line derived from a colorectal adenocarcinoma; forms microvilli upon differentiation
fWTHFE/HT29	Parent HT29 cells stably transfected with FLAG-tagged wild type human HFE
fW81AHFE/HT29	Parent HT29 cells stably transfected with FLAG-tagged W81A mutant HFE

INTRODUCTION

The Fundamental Need for Iron

Iron is essential to virtually all living systems and is a key component in multiple biological functions, such as oxygen transport, DNA synthesis, and respiration. However, if excess iron is present in the cell, hydroxyl radicals can be generated via the Fenton reaction. These free radicals can damage and oxidize lipids, proteins, and DNA (Park et al. 1987). Tight control of iron uptake, storage, and export is crucial in order to maintain balance.

Regulation of body iron homeostasis in humans is dictated at the level of absorption rather than excretion (Bothwell and Charlton 1979). Evidence for the control of iron uptake is demonstrated by the fact that individuals who are iron-replete absorb less iron from their diet than do iron-deficient people. This suggests that iron uptake is controlled at the intestinal level and that a distinct mechanism for sensing body iron needs exists. Inappropriate responses or lack of a response to body iron needs results in iron overload or anemia.

Hereditary Hemochromatosis

Hereditary Hemochromatosis (HH) is a disease of iron overload (for review see (Andrews 1999)). This disorder encompasses varying degrees of severity and can be due to defects in multiple genes. The most common form, Type 1 HH, is inherited in an autosomal recessive fashion and leads to iron deposition in major organs, contributing to their failure in the fourth or fifth decade of life (Bothwell and MacPhail 1998). Patients

with this form of HH experience a slow progression of symptoms due to increased intestinal iron absorption throughout their lifetime. Normally, ~30% of the serum iron transport protein transferrin (Tf) is saturated with iron in the blood (Edwards et al. 1988). Although increased Tf saturation (> 45%) may be observed in patients with Type 1 HH within the first two decades of life, most symptoms of the disease are subtle and include joint pain, hyperpigmentation of the skin, depression, and fatigue; all which do not present until much later in life (Bothwell et al. 1995). As tissues such as the liver, heart, and pancreas become overloaded with iron, patients can succumb to liver disease and hepatocellular carcinoma, cardiomyopathy and arrhythmias, as well as diabetes. Often, patients are not properly diagnosed due to the commonality of symptoms frequently associated with aging patient groups.

The defective gene in Type 1 HH is *HFE1*, located on human chromosome 6p21.3 (Feder et al. 1996). Eight years after its discovery, however, the function of the HFE protein remains unclear. Its expression, or lack thereof, has opposite effects on the iron status in different cell types (Gross et al. 1998; Corsi et al. 1999; Riedel et al. 1999; Roy et al. 1999; Montosi et al. 2000; Roy et al. 2000; Drakesmith et al. 2002; Roy et al. 2002; Davies and Enns 2004). When HFE is not expressed properly in humans, iron balance in the body becomes distorted, leading to disease. Further understanding of the role of HFE in maintaining cellular iron homeostasis is the topic of this thesis.

HFE belongs to the major histocompatibility complex (MHC) family of proteins and is most similar to non-classical class I MHC molecules. This is a family of glycoproteins whose main role is typically in the immune system involving presentation of peptide antigens to T-cells. Proteins in this family are comprised of three extracellular

domains (α−1, α−2, and α−3), a single membrane spanning domain, and a short cytoplasmic tail. They also form a heterodimer with β2-microglobulin (β2m), which is necessary for trafficking out of the endoplasmic reticulum to the surface of cells (Feder et al. 1996; Ehrlich and Lemonnier 2000). Prior to the cloning of *HFE1*, the gene responsible for the disease was proposed to be part of the MHC family due to observations made from the β2m knockout mouse. In addition to immunological defects, these mice are shown to have iron overload similar to HH patients (Rothenberg and Voland 1996; Santos et al. 1996). In MHC class I molecules, the peptide for antigen presentation sits in the peptide-binding groove formed between the helices of the α-1 and α-2 domains; but in the case of HFE, this groove is too narrow to bind peptide (Lebron et al. 1998). As a result, HFE does not bind to the T-cell receptor and affect immune capacity; instead, the alpha helices surrounding the groove can interact with the Tf receptor 1 (TfR1) (Bennett et al. 2000) (this interaction will be discussed in detail later).

Over 80% of patients with Type 1 HH carry a homozygous mutation in the α-3 domain of HFE, converting a cysteine to a tyrosine (C260Y; the numbering system used in this report for the amino acids in HFE reflects the amino acid position in the mature protein) (Feder et al. 1996). This mutation disrupts a disulfide bond necessary for proper folding of HFE, which in turn is needed for association with β2m and trafficking to the cell surface (Feder et al. 1997; Lebron et al. 1998) (Figure 0.1). Consequently, when this mutation is present, HFE remains in the secretory pathway and is subsequently degraded (Feder et al. 1997; Waheed et al. 1997). HFE knockout mice and mice that have a knockin mutation disrupting the disulfide bond in the α-3 domain, both show iron overload primarily in the liver (Zhou et al. 1998; Levy et al. 1999a).

While carrier rates of the C260Y mutation are quite prevalent (between 10% and 15%, and a homozygote frequency approximately 1 in 150 in people of Northern European descent), its penetrance may not be as high as once believed (Bomford 2002; Beutler 2003; Beutler et al. 2003). Although this mutation accounts for more than 80% of the cases of HH (Feder et al. 1996), some additional mutations in HFE are also implicated in the disease. Furthermore, recent observations evaluating the penetrance of mutations in HFE have begun to shed some light on other modifier gene mutations that might enhance disease when the HFE mutation is present (Bomford 2002). The extent to which these less common HFE mutations contribute to the disease state, however, remains unclear [H41D (Feder et al. 1996), S43C (Mura et al. 1999), I83T and G71R (Barton et al. 1999)].

There are also people who present clinically with HH, but do not have mutations in HFE at all. Type 2 HH, also known as juvenile hemochromatosis, whose gene has been known to be located on human chromosome 1q21 for quite some time (Roetto et al. 1999; Papanikolaou et al. 2001; Papanikolaou et al. 2002; Rivard et al. 2003) has just recently been cloned; its protein product is called hemojuvelin (Papanikolaou et al. 2004). This form of HH is much more severe than the Type 1 form and has clinical onset in the first or second decade of life (Camaschella et al. 2002; De Gobbi et al. 2002). Type 3 HH is caused by mutations in a newly identified Tf receptor (TfR2) on human chromosome 7q22, and is clinically similar to the HFE-form (Type 1) (Camaschella et al. 2000; Roetto et al. 2001; Mattman et al. 2002). The mutation responsible for an autosomal dominant form of the disease, Type 4 HH, is located in the putative iron transporter ferroportin 1 (FPN1) (Montosi et al. 2001; Njajou et al. 2001; Devalia et al.

2002; Wallace et al. 2002). In this form of the disease, selective iron overload of the Kupffer cells of the liver is coupled with normal Tf saturation, suggesting a defect in the release of iron from recycled red blood cells from the reticuloendothelial system to circulating Tf. Another autosomal dominant form of HH, Type 5, has also been described and affects the iron storage protein ferritin (Ft) (Kato et al. 2001). A point mutation in the iron responsive element (IRE) motif of the heavy chain subunit of Ft (H-Ft) leads to enhanced binding by the iron regulatory proteins (IRPs), thus decreasing Ft synthesis necessary for proper iron storage, and leading to iron overload in the body. Clearly, HH is a complex disease and more intricate than first expected. This report, however, will focus on the role of the protein implicated in the most common form of the disease, HFE.

Control of Iron Homeostasis at the Intestinal and Cellular Level

Dietary iron is absorbed into the body across the epithelium in the duodenum, the proximal portion of the small intestine. The cells in this region of tissue are polarized, differentiated epithelial cells, termed enterocytes, which transport dietary iron across the epithelial barrier (Conrad and Crosby 1963; Daniele and D'Agostino 1994; Hocker and Weidenmann 1998). To control the rate of iron absorption from the diet, the total body iron stores must be sensed, as well as the rate of erythropoiesis (red blood cell production), so that the appropriate amount of iron is absorbed. Because excess or insufficient amounts of iron in the body can be detrimental to the organism, regulation of iron levels must occur at the absorption stage since humans have no regulated means for iron excretion (Bothwell and Charlton 1979). The enterocytes have two distinct

membranes separated by tight junctions (Figure 0.2). The apical membrane faces the intestinal lumen and transports heme and other dietary nutrients, including non-heme iron, into the cell. The opposing basolateral membrane faces the blood plasma and iron is transported across this membrane to reach the rest of the body. Heme iron from the diet is absorbed more efficiently than non-heme iron, however, the molecular mechanisms of how heme crosses the apical membrane or traverses the enterocyte have not yet been determined (Wyllie and Kaufman 1982; Bezwoda et al. 1983; Monsen 1988). McKie and colleagues have presented unpublished work describing the isolation of a novel membrane protein whose mRNA is upregulated by hypoxia and hypotransferrinemia in the mouse duodenum, and exhibits protein expression localized to both vesicles and the apical membrane of enterocytes. They propose that this novel protein could be involved in either iron or heme transport or trafficking, however, no further conclusions have been elucidated regarding this data (Shayeghi et al. 2003).

The absorptive enterocytes take up ferrous iron (Fe^{2+}) via the divalent metal transporter (DMT1; discussed in detail later) (Fleming et al. 1997; Gunshin et al. 1997) (Figure 0.2). This occurs after the iron has been reduced from the ferric form (Fe^{3+}) by a brush border ferrireductase. A strong candidate for this function is named duodenal cytochrome b (Dcytb), for its similarity to cytochrome b reductase (McKie et al. 2001). After iron has been transported into the cell it can be stored in Ft, a cytoplasmic iron storage protein, or it can bind low molecular weight compounds and become part of the labile iron pool. Additionally, it can traverse the cell to the basolateral membrane and exit into the blood via the FPN1 transporter. In order to bind circulating Tf in the blood, iron must be oxidized. This process is believed to be facilitated by Hephaestin (Heph), a

protein with ferroxidase activity localized to the basolateral membrane as well as intracellular vesicles of enterocytes (Vulpe et al. 1999; Chen et al. 2004; Kuo et al. 2004). These two proteins, FPN1 and Heph, are hypothesized to coordinate iron export, however, the mechanism by which this occurs is not well understood (Chen et al. 2004; Kuo et al. 2004).

The distinction, by which iron is routed for storage in Ft versus traversing and exiting the cell, is not clear either. It could be caused by extracellular signals from the basolateral side of the enterocyte (Ten Elshof et al. 1999; Salter-Cid et al. 2000), or due to the gene expression profile previously determined in the undifferentiated crypt cells (Fleming and Sly 2002). Iron that is not exported out of the enterocyte is lost with exfoliation of the intestinal villi epithelium every three to four days (Geyer 1979; Lombard et al. 1997; Hocker and Weidenmann 1998).

Iron Regulatory Proteins –

In order to maintain proper iron balance in cells, tight control of iron uptake, utilization, and storage must be maintained. Much of this control is accomplished by the role of iron regulatory proteins (IRPs) (for review see (Hentze and Kuhn 1996; Eisenstein 1998)). IRPs are cytoplasmic proteins that specifically regulate the mRNA of iron-related genes by binding to iron responsive elements (IREs), which are stem-loop structures in the 5' or 3' untranslated regions (UTR) of certain mRNA (Aziz and Munro 1987; Casey et al. 1988b; Leibold and Munro 1988). This mode of gene regulation is one of the most striking examples of those that involve binding of protein to mRNA. There are two isoforms, IRP1 & IRP2, whose binding activity is influenced by intracellular free

iron levels of the labile iron pool (Casey et al. 1988a; Leibold and Munro 1988; Eisenstein 2000). IRP1 is bound to the IRE under low iron conditions, but binds iron and has aconitase activity when the intracellular iron environment is high (Haile et al. 1992a). This cytoplasmic aconitase contains an iron-sulfur cluster [4Fe-4S] in its active site (Kaptain et al. 1991). Under low iron conditions, a conformational change causes release of the cluster and increases mRNA binding function of the protein (Rouault et al. 1991; Haile et al. 1992b). IRP2 does not bind an iron-sulfur cluster, but under high iron conditions is ubiquitinated and degraded via the proteasome pathway, no longer available for IRE binding (Guo et al. 1994; Guo et al. 1995a; Iwai et al. 1995; Iwai et al. 1998).

Two classic examples of proteins regulated by IRPs are Ft and TfR1 (Figure 0.3). When the IRE is present in the 5'UTR of mRNA, such as Ft (Aziz and Munro 1987; Casey et al. 1988b; Leibold and Munro 1988), binding by the IRP prevents recruitment of the eIF4F cap-binding complex (Muckenthaler et al. 1998) leading to decreased synthesis of Ft protein (Rouault et al. 1988). Conversely, when iron levels are high and IRPs do not bind IREs, uninhibited translation of Ft is permitted leading to increased iron storage. TfR1, on the other hand, harbors multiple IRE sequences in its 3' UTR surrounding a rapid turnover determinant highly susceptible to nuclease activity. Under low iron conditions, IRP binding stabilizes the mRNA by protecting the nuclease site, thereby increasing TfR1 mRNA levels. When the intracellular iron levels increase, IRPs no longer bind to the stem-loop structures and the nuclease site of TfR1 mRNA is exposed causing destabilization of TfR1 message (Mullner and Kuhn 1988; Casey et al. 1989; Koeller et al. 1989; Mullner et al. 1989). Under these high iron conditions, IRP activity allows the cell to increase iron storage in Ft and decrease uptake by TfR1, which protects

the cell from detrimental iron overload and oxidative damage. When the cell is in need of iron, TfR1 levels rise to increase iron uptake and Ft synthesis is suppressed to prevent iron sequestration.

Interestingly, two iron transporters harbor putative IREs, which are located in the 5' UTR of FPN1 and the 3' UTR of DMT1. DMT1 has at least two mRNA splice variants; one contains the IRE and one does not (Lee et al. 1998; Canonne-Hergaux et al. 1999). While the IREs in both of these transporters have been shown to be functional *in vitro*, i.e. they bind IRPs and are regulated by iron, (Lee et al. 1998; Han et al. 1999; Wardrop and Richardson 1999; Tandy et al. 2000; Trinder et al. 2000; Lymboussaki et al. 2003), it remains unclear if these transport proteins are regulated by the established IRE/IRP mechanism *in vivo*. The binding affinity of IRP1 to the IRE sequence in DMT1 is approximately 10-fold lower than the IRP1/Ft-IRE interaction (Wardrop and Richardson 1999). Furthermore, no change in DMT1 mRNA half-life has been observed in the presence of iron as would be expected if regulation was through the IRE/IRP mechanism similar to TfR1 (Zoller et al. 2002). Thus, a functional role for the IRE sequences in the mRNA of these transporters remains unknown, suggesting that their control may be more complex than originally proposed (Zoller et al. 2002).

Tf-Mediated Iron Uptake -

The primary source of iron for most cells is from the serum protein Tf. Tf is ~80 kDa and can bind up to two ions of ferric iron (Fe^{3+}) with high affinity (Ka ~10^{-20}–10^{-23} M) (Leibman and Aisen 1979; Aisen 1998) and binds to cells via TfR1 (Zak et al. 1994; Mason et al. 1997). TfR1 is a Type II glycosylated single transmembrane protein ~97

kDa that forms a homodimer and is expressed on the surface of cells (reviewed in (Enns et al. 1996; Lok and Loh 1998)). At the neutral pH of the extracellular environment, the TfR1 binds its ligand, diferric-Tf, with high affinity (~10^{-8}–10^{-9} M) (reviewed in (Enns et al. 1996)). The binding constant for apo-Tf (Tf with no iron bound) at this pH is approximately 2,000-fold lower (Tsunoo and Sussman 1983). The specificity in pH associated with binding allows for iron-loaded Tf to bind the receptor for entry into the cell, thus increasing the efficiency of iron import (Dautry-Varsat et al. 1983; Klausner et al. 1983; Tsunoo and Sussman 1983). The receptor clusters in clathrin-coated pits on the plasma membrane that pinch off intracellularly into vesicles (Geuze et al. 1983; Gruenberg et al. 1989). Once inside the cell, the vesicle becomes uncoated and enters the endosomal pathway where the pH is decreased in an ATP-dependent manner by a membrane-bound H+/ATPase (Yamashiro et al. 1983; Schmid 1992; Forgac 1999). The iron is released from Tf in the slightly acidic endosome, but the apo-Tf remains associated with the receptor (Morgan 1979). The decreased pH causes conformational changes in both the TfR1 and Tf that increase the dissociation constant of Tf for iron to 10^{-7} M (Bali and Aisen 1991; Sipe and Murphy 1991), thus releasing iron into the endosome. The ferric iron must be reduced (presumably by an unidentified endosomal reductase) and is transported across the endosomal membrane into the cytosol of the cell most likely by the iron transporter DMT1 (Fleming et al. 1998). The apo-Tf remains bound to the receptor in the endosome due to its high dissociation constant at the low pH. The apo-Tf/TfR1 complex cycles back to the plasma membrane and upon the neutral pH of the extracellular environment, apo-Tf is released in order to bind more iron and in turn

frees the receptor to bind diferric-Tf and continue the endocytic/exocytic cycle (Morgan 1981; Young and Aisen 1981; Tsunoo and Sussman 1983).

The TfR1 has been studied extensively for many years, but a new TfR was identified in 1999, designated TfR2 (Kawabata et al. 1999; Fleming et al. 2000). This receptor shares 66% similarity with the ectodomain of TfR1 and also binds diferric-Tf, although with much lower affinity (Kawabata et al. 1999; Kawabata et al. 2000). It does not, however, form a stable complex with HFE (West et al. 2000) as has been shown for TfR1 (Feder et al. 1998; Bennett et al. 2000) (this interaction will be discussed in depth later). TfR2 has a specific expression pattern found virtually only in liver and hematopoietic cells, compared to the fairly ubiquitously expressed TfR1 (Gatter et al. 1983; Kawabata et al. 1999; Fleming et al. 2000). Unlike TfR1, there is no IRE sequence in the UTR of TfR2 mRNA, and accordingly, it does not appear to be iron regulated by IRPs (Fleming et al. 2000). The role of TfR2 is an area of active investigation, but there is not yet a clear idea of its function; however, mutations in this protein result in a rare form of HH (Type 3).

Non-Tf Mediated Iron Uptake -

Although quite efficient and widespread, Tf-mediated iron uptake is not the only iron uptake system in cells. Non-Tf bound iron uptake also takes place. Two animal models that exhibit the same single base pair naturally occurring mutation in DMT1 (also known as NRAMP2 (Gruenheid et al. 1995) and DCT1 (Gunshin et al. 1997)), emphasize the important role for this transporter in iron absorption. The microcytic anemia (*mk*) mouse and the Belgrade (*b*) rat both have a glycine converted to an arginine at position

185 in the coding region located in the putative transmembrane domain 4 of DMT1 causing these animals to experience severe defects in intestinal iron absorption (Garrick et al. 1993; Oates and Morgan 1996a; Fleming et al. 1997; Fleming et al. 1998). DMT1 is expressed on the apical membrane of villus cells and transports iron into the duodenum (Bowen and Morgan 1987; Oates and Morgan 1996a; Canonne-Hergaux et al. 1999; Trinder et al. 2000) and is also thought to transport iron released from Tf out of the endosome into the cytoplasm (Edwards et al. 1980; Garrick et al. 1993; Su et al. 1998; Garrick et al. 1999; Gruenheid et al. 1999). This putative 12-transmembrane protein is a proton symporter that is not specific for iron, but can also transport other divalent cations, such as zinc, cadmium, manganese, copper, and cobalt (Fleming et al. 1997; Gunshin et al. 1997). At the brush border membrane of villus cells, DMT1 takes up iron that has been reduced by the ferrireductase, presumably Dcytb (McKie et al. 2001). In its role in endosomal iron transport, DMT1 also requires the reduced form of iron, but the identity of the endosomal reductase is unknown.

Iron Storage -

Iron that is not immediately needed by the cell is stored in Ft, a cytosolic protein. This protein shell is a 430-460 kDa complex composed of a combination of 24 heavy chain (H-Ft, ~21 kDa) and light chain (L-Ft, ~19 kDa) subunits. The shell surrounds a semi-crystalline core of up to 4500 ferric ions (Mann et al. 1986). Ft is important for maintaining cellular iron balance because it serves as a source for iron mobilization when cellular iron needs increase, and it also stores the iron in order to protect the cell from oxidative damage from free iron within the cell. The ratio of H to L chain subunits in the

Ft complex is dependent upon specific iron needs and cell type. H-Ft has an oxidase activity useful for converting the ferrous iron to the ferric form, the state of the iron in the Ft core (Lawson et al. 1989). Complexes whose majority is composed of H-chains take up iron faster, suggesting a role for protection against toxicity rather than for efficient storage (Levi et al. 1988). The L-chain is directly involved in the formation of the iron core itself, implying a more long-term storage purpose (Levi et al. 1992). For example, H-Ft is more highly expressed in the heart, while L-Ft has greater expression in the liver and spleen. As discussed earlier, Ft is translationally controlled by IRPs but there are some forms of transcriptional control as well. For instance, H-Ft is transcriptionally controlled in response to cytokines and heme (Ponka et al. 1998), as well as inflammatory factors and oxidative stress (Torti and Torti 2002).

Iron Efflux -

Specialized cells in the body export iron. The protein implicated in iron efflux in the intestine as well as in macrophages is FPN1 (Donovan et al. 2000) (also known as iron-regulated gene 1 (IREG1) (McKie et al. 2000) and metal transport protein 1 (MTP1) (Abboud and Haile 2000)). FPN1 has 9 putative transmembrane regions and has been linked to an autosomal dominant form of HH (Type 4) (Montosi et al. 2001; Njajou et al. 2001; Devalia et al. 2002; Wallace et al. 2002). This protein is expressed on the basolateral membrane of enterocytes and is believed to transport iron across this barrier for eventual binding to Tf in the blood.

Oocyte experiments demonstrate the ability of FPN1 to transport ferrous iron (Donovan et al. 2000; McKie et al. 2000), but *in vivo* the ion must be oxidized prior to

binding circulating Tf. Evidence from the sex-linked anemia (*sla*) mouse suggests that Heph, a multicopper ferroxidase, accomplishes this task. These mice suffer from a paradoxical disorder where their enterocytes are iron-overloaded, but there is an insufficient amount of iron available for the production of red blood cells. The iron uptake into enterocytes is normal, but the efflux of iron across the basolateral membrane into the blood is impaired (Edwards and Bannerman 1970; Manis 1971; Bannerman 1976; Anderson et al. 1998). The *sla* mice produce a truncated version of Heph, decreasing the ferroxidase activity needed for iron efflux (Vulpe et al. 1999; Chen et al. 2004). This protein is highly homologous to ceruloplasmin (Cp), a soluble multicopper ferroxidase present in serum, that is necessary for efficient recycling of iron between storage and donation sites of the liver, reticuloendothelial system, and the blood (Osaki et al. 1971; Mukhopadhyay et al. 1998; Harris 1999). The identification of Heph emphasizes the link of copper to iron export (Askwith and Kaplan 1998). Unlike the soluble Cp, Heph has a membrane-spanning region at the C-terminus presumably expressing a short cytoplasmic tail. Thus, the multicopper ferroxidase activity is oriented on the surface of the cell or in the lumen of endocytic vesicles hypothesized to coordinate activity with the iron exporter, FPN1 (Vulpe et al. 1999; Chen et al. 2004; Kuo et al. 2004). The mechanism of how Heph and FPN1 accomplish the tasks needed for proper iron efflux have not yet been determined. However, there is strong evidence demonstrating the requirement of both of these proteins for the successful export of iron from the enterocyte.

Regulation of Body Iron Stores -

A newly identified 25 amino acid peptide synthesized by the liver, named hepcidin, is proposed to be an iron-regulatory hormone. Its synthesis is greatly increased by inflammation or iron overload and it is thought to be the main inhibitor of iron absorption in the small intestine (Ganz 2003), and possibly the long sought "iron stores regulator". Such a regulator has been thought to increase iron uptake when body iron levels are too low until the appropriate level is attained (Cox and Peters 1980; Nathanson et al. 1985; Gavin et al. 1994; Hunt and Roughead 2000). The stores regulator also has the job of preventing iron overload after reaching sufficient levels of body iron. Communicating body iron needs to the intestine is proposed to require a molecule that could signal between the liver, muscle, and intestine, implying a soluble molecule for such a task. Indeed hepcidin, a soluble peptide synthesized in the liver, has been shown to inhibit intestinal iron absorption and has decreased expression in HFE-associated HH (Park et al. 2001; Bridle et al. 2003; Gehrke et al. 2003). Mice lacking hepcidin suffer from severe iron overload and mice overexpressing hepcidin suffer from iron deficiency anemia (Nicolas et al. 2001). Although it is likely that hepcidin is the long awaited stores regulator, more experimental data is needed to fully characterize the intricacies of hepcidin's role in iron homeostasis.

Effect of HFE on Cellular Iron Status

Lack of functional HFE in humans causes opposite effects to iron levels in different cell types of affected tissues. Early in the disease, Kupffer cells of the liver and enterocytes of the duodenum are iron-poor (Francanzani et al. 1989; Pietrangelo et al.

1995; Brunt et al. 2000). On the other hand, at this same stage of disease, hepatocytes in the liver are iron-overloaded (Brunt et al. 2000). Notably, all of these cell types have detectable levels of HFE mRNA and protein in animal models (Muckenthaler et al. 2003; Zhang et al. 2004). Moreover, cell culture experiments have revealed distinct Ft phenotypes in response to HFE expression (Gross et al. 1998; Corsi et al. 1999; Riedel et al. 1999; Roy et al. 1999; Montosi et al. 2000; Drakesmith et al. 2002; Davies and Enns 2004).

Low Iron Phenotype –

The first link between HFE and its effect on iron homeostasis was the observation that it can tightly associate with the TfR1 when co-expressed in culture (Feder et al. 1998). Additionally, TfR1 and HFE co-localize on the cell surface and in endosomes (Gross et al. 1998; Corsi et al. 1999; Salter-Cid et al. 1999). The expression of HFE in HeLa or HEK293 cells results in lower intracellular iron levels. Experiments demonstrate that with HFE expression, Ft levels are decreased, TfR1 levels are increased, IRP/IRE binding is enhanced, Tf-mediated iron uptake is decreased, and the labile iron pool is lower than compared to untransfected cells (Gross et al. 1998; Corsi et al. 1999; Riedel et al. 1999; Roy et al. 1999; Roy et al. 2000; Roy et al. 2002; Zhang et al. 2003).

The association between HFE and TfR1 was originally thought to be the determinant that led to reduced Ft levels and lower Tf-mediated iron uptake in cell lines, such as HeLa. The ideas for a mechanism of how this interaction accomplished this task have evolved over the past six years as more and more data has been generated regarding HFE expression in cells. HFE competes with Tf for binding to TfR1 (Lebron et al 1999).

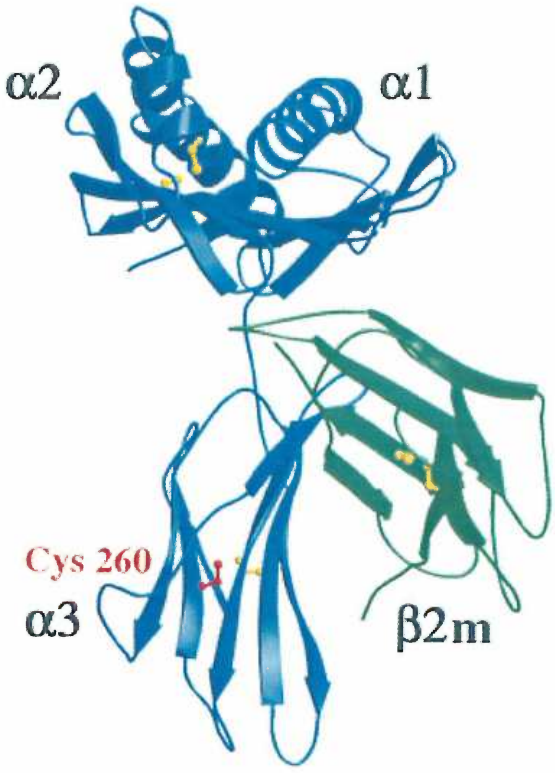
This competition, however, is not an acceptable explanation for the lowered iron uptake because the binding constant of Tf for its receptor is ~1-2 nM, while the binding constant of HFE for TfR1 is far less, ~60nM (Lebron and Bjorkman 1999). Furthermore, the concentration of diferric-Tf in the blood is ~10 μM, so it would not be expected that HFE ever associates with the TfR1 in the presence of physiological concentrations of Tf. Even at sub-physiological concentrations of diferric-Tf (100nM), the endocytic rates of TfR1 are unchanged in the presence or absence of HFE expression (Roy et al. 1999), but iron uptake from Tf is lowered by 30-40% (Riedel et al. 1999; Roy et al. 1999; Zhang et al. 2003). In this thesis, we put forth a new hypothesis that HFE has its effect on inhibiting iron uptake in HeLa cells from the site of the endosome, rather than by decreasing binding affinity at the cell surface, causing the low iron phenotype.

High Iron Phenotype -

Even though many reports have described the low iron phenotype imparted by HFE expression in HeLa and HEK 293 cells (Gross et al. 1998; Corsi et al. 1999; Riedel et al. 1999; Roy et al. 1999; Roy et al. 2000; Roy et al. 2002), some reports have also described HFE expression to cause an increased iron phenotype in cells, such as HFE infected monocytes from HH patients, or the macrophage-like cell line THP-1 (Cairo et al. 1997; Montosi et al. 2000; Drakesmith et al. 2002). Furthermore, studies in this thesis demonstrate that HFE expression in the intestinal cell line HT29 causes an increase in cellular iron accumulation and Ft levels due to an inhibition of iron efflux (Davies and Enns 2004). The ability of HFE to cause opposite changes in iron status in different cell types suggests that HFE's function is more complicated than originally considered.

We have tested HFE-specific regulation in both non-polarized and polarized cell culture systems to establish a mechanism for HFE's regulation of iron homeostasis, and this thesis demonstrates insights pertaining to the role of HFE in such regulation. Prior to transfection with HFE, cellular acquisition of iron via Tf-mediated or non-Tf-mediated iron uptake pathways are similar in HeLa and HT29 cells (Table 0.1). However, HeLa cells do not export iron as do HT29 cells. These differences in iron transport provide advantages to study HFE function in different cell types. Initial studies established that in HeLa cells, HFE expression causes a decrease in the labile iron pool (Roy et al. 2002). We next demonstrated that HFE and TfR1 co-traffick in the endocytic pathway in the absence of Tf. However, in the presence of physiological amounts of Tf, these two proteins do not associate (Davies et al. 2003). This raised the question as to whether HFE required association with TfR1 to impart its effect on intracellular iron levels. Indeed, our results exhibit that HFE can act independently of TfR1 to lower iron levels in HeLa cells (Zhang et al. 2003). These surprising results raised the possibility that HFE might affect other proteins besides TfR1.

When we expressed HFE in cells of intestinal origin, increased intracellular iron levels and an inhibition of iron efflux occurs (Davies and Enns 2004). This opposite iron phenotype, together with a role independent of TfR1 association, raised the possibility that HFE might interact with other proteins involved in iron transport. HFE appears to be a multifunctional protein with more than one target partner. Coordinating distinct roles in different cell types to maintain overall balance of iron in the body is a complex task. HFE does not bind iron, nor is it an iron transporter, but it is inherently involved in modulating iron homeostasis possibly via multiple roles as will be discussed in this work.



Lebron et al. (1998) Cell ***93****:111-123*

Figure 0.1. Crystal structure of HFE/β2m heterodimer. Ribbon diagram of the ectodomain of the HFE/β2m complex with the light chain (β2m) in green interacting with the α-3 domain of heavy chain (HFE) represented in blue. The groove formed by the α-1 and α-2 domains is too small to bind peptides for antigen presentation, as is typically the role for this region in other MHC class I molecules. Cys 260 (red) normally forms a disulfide bond with Cys 203 (yellow). But when the C260Y mutation is present, this bond cannot form, and HFE cannot bind β2m and is not trafficked to the cell surface.

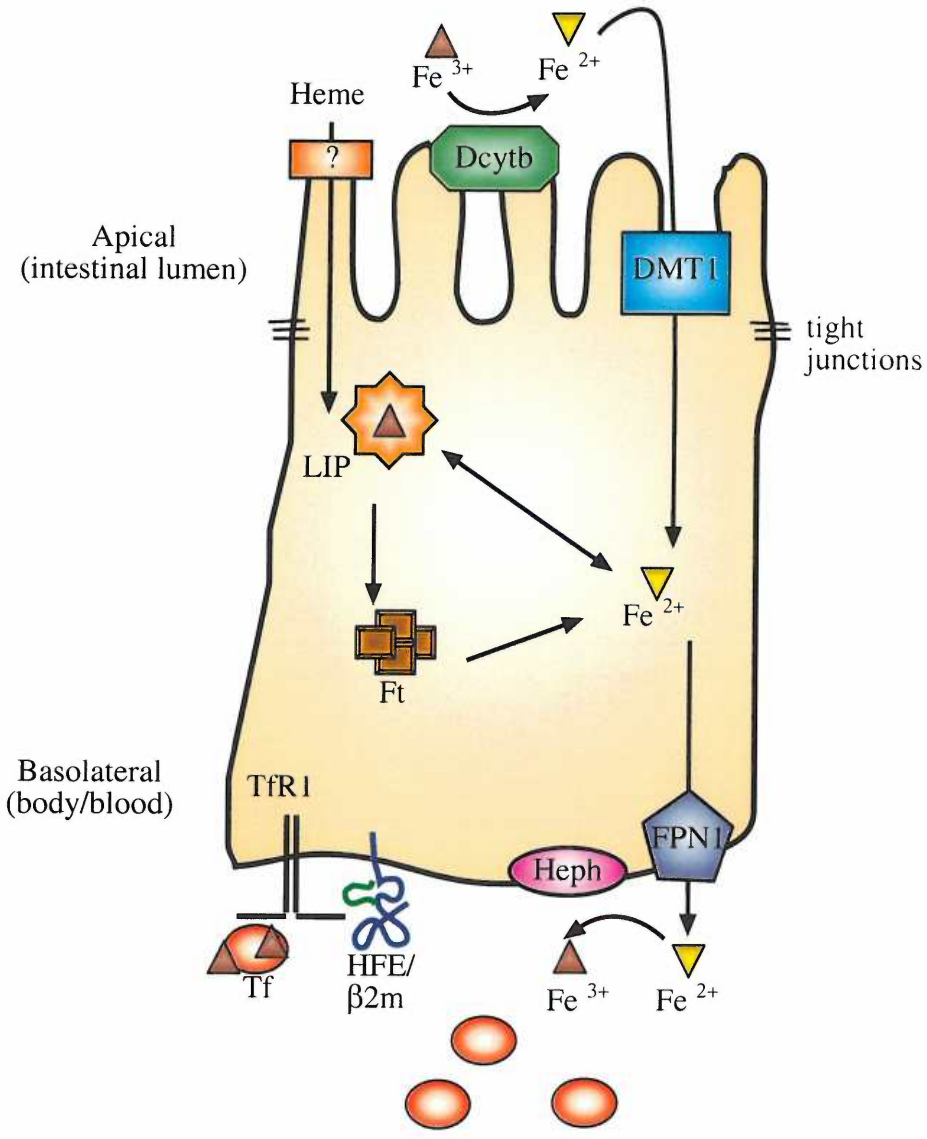


Figure 0.2. Proteins involved in iron absorption. Iron from the diet is transported across the apical membrane of the enterocyte. After entry, it can contribute to the labile iron pool (LIP) and alter the expression levels of genes involved in iron homeostasis, be stored in Ft, or be transported across the basolateral membrane to eventually bind circulating Tf in the blood.

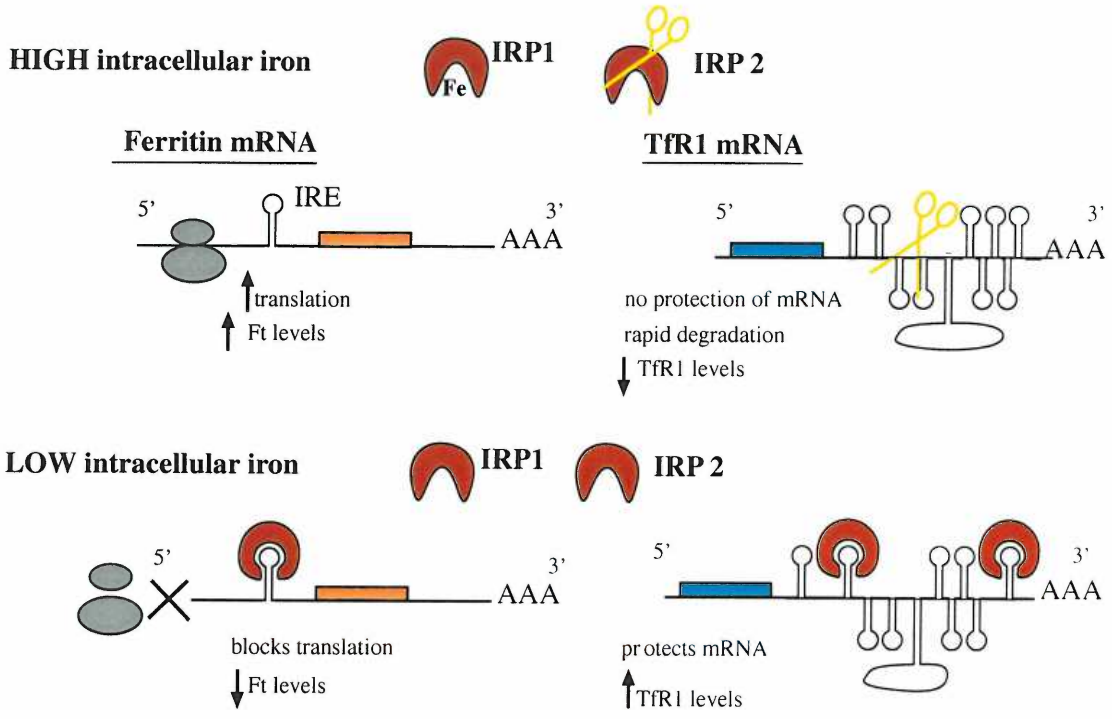


Figure 0.3. Iron control of translation and mRNA stability. Under high intracellular iron conditions, iron binds IRP1 allowing it to function as a cytosolic aconitase, while a ubiquitin-mediated degradation pathway degrades IRP2. When the IRPs are not bound to the IRE of Ft (upper left), this allows for normal translation of the mRNA and protein levels increase. On the other hand, when IRPs do not bind the TfR1 (upper right), a nuclease site is exposed leading to instability of the message. When the cellular iron levels decrease, the IRPs bind to the stem-loop structures in the untranslated regions of the mRNA causing a block in translation machinery for Ft (lower left) but a stabilization of the message in the case of TfR1 (lower right).

	RATES OF UPTAKE		
	pmole ^{125}I-Tf uptake/ min/10^6 cells	pmole ^{55}Fe-Tf uptake/ min/10^6 cells	pmole ^{55}Fe-NTA uptake/ min/10^6 cells
HeLa*	0.140	0.291	0.275
HT29	0.025	0.055	0.160

** Data from Roy et al. J. Biol. Chem. 274:9022-9028.*

Table 0.1. Iron uptake in HeLa and HT29 cells. Rates of ^{125}I-Tf uptake are greater in HeLa cells compared to HT29 cells; however, HeLa cells express a greater amount of receptors than HT29 cells. The mechanism of cellular iron acquisition from Tf between the two cells lines is equivalent (approximately two iron atoms are taken up per Tf endocytosed into the cells). The rate of non-Tf mediated iron uptake in both cell lines is similar. Iron efflux is difficult to measure in HeLa cells and is not thought to occur due to the absence or low expression of genes involved in iron export, but iron efflux can be measured in HT29 cells as demonstrated in Chapter 4.

CHAPTER 1

Increased IRP1 and IRP2 RNA Binding Activity Accompanies a Reduction of the Labile Iron Pool in HFE-expressing Cells

Cindy N. Roy*[1], Kenneth P. Blemings§[2], Kathryn M. Deck§, **Paige S. Davies***, Emily L. Anderson*, Richard S. Eisenstein§, and Caroline A. Enns*

*Department of Cell and Developmental Biology, Oregon Health & Science University, Portland, Oregon, 97239-3098, USA

§Department of Nutritional Sciences, University of Wisconsin, Madison, Wisconsin 53706, USA

[1]Present address: Harvard Medical School, Children's Hospital, Boston, MA 02115, USA
[2]Present address: West Virginia University, Division of Animal and Veterinary Sciences, Morgantown, WV 26505, USA

Published in *Journal of Cellular Physiology* (2002), **190:** 218-226

‡This work was supported by NIH DK 54488 (CAE) and DK 47219 (RSE). CNR and PSD were supported in part by the Training Program in Molecular Hematology, T32-HL00781, National Institutes of Health, National Heart, Lung, and Blood Institute. KPB was supported by USDA grant 96-35200-3273.

SUMMARY

Iron regulatory proteins (IRPs), the cytosolic proteins involved in the maintenance of cellular iron homeostasis, bind to stem loop structures found in the mRNA of key proteins involved iron uptake, storage, and metabolism and regulate the expression of these proteins in response to changes in cellular iron needs. We have shown previously that HFE-expressing fWTHFE/tTA HeLa cells have slightly increased transferrin receptor 1 (TfR1) levels and dramatically reduced ferritin (Ft) levels when compared to the same clonal cell line without HFE (Gross et al. 1998). While HFE does not alter TfR1 trafficking or non-Tf mediated iron uptake, it does specifically reduce ^{55}Fe uptake from Tf (Roy et al. 1999). In this report, we show that IRP RNA binding activity is increased by up to 5-fold in HFE-expressing cells through the activation of both IRP isoforms. Calcein measurements show a 45% decrease in the intracellular labile iron pool in HFE-expressing cells, which is in keeping with the IRP activation. These results all point to the direct effect of the interaction of HFE with TfR1 in lowering the intracellular labile iron pool and establishing a new set point for iron regulation within the cell.

INTRODUCTION

Biological systems maintain an appropriate iron balance through regulatory mechanisms that enable them to meet the iron demand, but prevent iron overload. Cytoplasmic iron regulatory proteins (IRPs) regulate the levels of several key proteins involved in iron uptake, storage and utilization by binding to iron responsive elements (IREs) in their respective mRNAs (reviewed in (Hentze and Kuhn 1996; Theil 1998; Eisenstein 2000)). The activities of the two IRP isoforms are primarily dependent on an elusive cytoplasmic pool of intracellular iron referred to herein as the labile iron pool. The iron-dependent RNA binding activity exhibited by both IRPs equips them to communicate the iron status of the cell to the cellular machinery involved in iron homeostasis.

Hereditary hemochromatosis is an autosomal recessive genetic disease that results from a defect in regulated iron transport across the intestinal epithelial cells. The disease is characterized by increased transport of iron from the enterocyte to the blood (McLaren et al. 1991). The transfer of iron across the duodenal epithelium is inversely proportional to the relative iron repletion of an organism (reviewed in (Bothwell et al. 1995)). Increasing evidence points to the involvement of IRP machinery, or at the very least the labile iron pool, in the regulation of dietary iron uptake and transfer across the enterocyte (Schumann et al. 1999; Garate and Nunez 2000). The specific effects of IRPs on enterocyte proteins of iron transport and homeostasis are just beginning to be investigated (Wardrop and Richardson 1999; Abboud and Haile 2000; Donovan et al. 2000; McKie et al. 2000).

Individuals who are homozygous for the most common mutation, C260Y, in the hereditary hemochromatosis protein, HFE (Feder et al. 1996), experience chronic increased dietary iron uptake, but the mechanism behind this increase is not yet known. HFE associates very tightly with the transferrin receptor 1 (TfR1) in cultured cells *in vitro* (Feder et al. 1998; Gross et al. 1998; Lebron et al. 1998; Bennett et al. 2000) as well as in the placental and duodenal extracts (Parkkila et al. 1997a; Waheed et al. 1999). Cells grown in culture that express HFE have increased TfR1 levels and decreased ferritin (Ft) levels suggesting an HFE-specific decrease in the labile iron pool (Gross et al. 1998; Corsi et al. 1999; Riedel et al. 1999). Consistent with these results is the finding that HFE specifically reduces iron uptake from transferrin (Tf) (Corsi et al. 1999; Riedel et al. 1999; Roy et al. 1999; Ikuta et al. 2000) and leads to activation of IRPs (Corsi et al. 1999; Riedel et al. 1999). Whether one or both IRP isoforms are activated has not been determined. Such information could shed light on whether increases in IRP activity are through an iron-mediated mechanism or by possible signal transduction pathways independent of intracellular iron levels.

To define the mechanism by which HFE expression leads to the activation of IRPs, we have characterized IRP activities in our cell line expressing wild type HFE under the control of the tetracycline (tet) transactivatable promoter (fWTHFE/tTA HeLa). We provide evidence that HFE expression increases both IRP1 and IRP2 RNA binding activity by reducing the labile iron pool.

MATERIALS AND METHODS

Cell Lines -

The fWTHFE/tTA HeLa cell line expressing FLAG epitope-tagged wild type HFE (fWTHFE) under the tet-responsive promoter has been previously described (Gross et al. 1998). Cells were grown in Dulbecco's modified Eagle's essential medium (DMEM) supplemented with 10% fetal bovine serum, 400 μg/ml G418 (Geneticin, Calbiochem), 200 ng/ml puromycin, and with (HFE-) or without (HFE+) 2 μg/ml tet. The tet-responsive promoter in our system (Warren et al. 1997) inhibits transcription of HFE (HFE-) in the presence of tetracycline and allows transcription of HFE (HFE+) in its absence.

^{35}S-methionine/cysteine Incorporation into Ft and IRP1 -

Subconfluent HFE- and HFE+ fWTHFE/tTA HeLa cells in 35-mm dishes were washed two times with sterile PBS and preincubated for 10 min at 37°C in DMEM without methionine or cysteine (Sigma) prior to labeling. After preincubation, the methionine and cysteine-free DMEM was removed and the cells were labeled for varying times with 100 μCi ^{35}S-Translabel (DuPont, New England Nuclear) in methionine and cysteine-free DMEM with 10% fetal bovine serum. After the indicated times, cells were put on ice and lysed as described above. Cell extracts were subjected to immunoprecipitation as described below and analyzed with denaturing SDS-PAGE under reducing conditions. Gels were fixed, treated with Amplify (Amersham, Pharmacia Biotech) for 30 min, dried and subjected to PhosphorImager analysis.

Immunoprecipitations -

For Ft immunoprecipitations, subconfluent ^{35}S-methionine/cysteine labeled HFE- and HFE+ fWTHFE/tTA HeLa cells were washed two times with 2 ml of PBS and lysed with NET-Triton on ice. Lysates of ~10^6 cells were preadsorbed for 1 h at 4°C with 30 μl of BSA-conjugated agarose. Preadsorbed lysates were incubated for 1 h at 4°C with 15 μl protein A Sepharose (50% suspension, Zymed) and 3 μl affinity purified rabbit anti-rat Ft antibody (Chen et al. 1997). The pellet was resuspended in 100 μl of NET-Triton and washed through 1 ml of radioimmune precipitation assay (RIPA) buffer (1% Triton X-100, 1% deoxycholate, 0.1% SDS, 50 mM Tris, 150 mM NaCl, and 0.2% sodium azide, pH 7.4) with 15% sucrose. Samples were eluted in 100 μl of 2X Laemmli buffer (125 mM Tris-HCl (pH 6.8), 4% SDS, 20% glycerol, and 10% 2-mercaptoethanol) (Laemmli 1970) and subjected to SDS-PAGE analysis on a 12% denaturing acrylamide gel under reducing conditions.

For IRP1 immunoprecipitations, HFE- and HFE+ subconfluent fWTHFE/tTA HeLa cells in 35-mm dishes were washed two times with 2 ml of sterile PBS (pH 7.4) and lysed with HEPES-citrate buffer (20 mM HEPES, 1 mM sodium citrate, 5 mM EDTA, 0.5% NP-40, 100 μg/ml leupeptin, 100 μg/ml pepstatin, 250 μg/ml soybean trypsin inhibitor, 200 μM phenylmethylsulfonyl fluoride, 10 μM MG132, pH 7.4) on ice. Lysates of ~10^6 cells were preadsorbed for 1 h at 4°C with 30 μl of BSA-conjugated agarose. Preadsorbed lysates were incubated for 1 h at 4°C with 15 μl protein A Sepharose (50% suspension, Zymed) and 30 μg rabbit anti-rat IRP1 antibody (Schalinske et al. 1997). The pellet was resuspended in 100 μl of NET-Triton, washed and eluted

with Laemmli buffer as described above. Samples were subjected to SDS-PAGE analysis on a 6% denaturing acrylamide gel under reducing conditions.

Electrophoretic Mobility Shift Assay -

RNA binding assays used the first 70 nucleotides of the rat L-Ft 5' untranslated region that contains the IRE. Internally ^{32}P labeled RNA was synthesized as described previously (Eisenstein et al. 1993). The RNA binding assay was performed as previously described (Eisenstein et al. 1993) with the following modifications. HFE- and HFE+ fWTHFE/tTA HeLa cells were harvested by trypsinization after they had been washed in Hanks balanced salt solution. Trypsinized cells were resuspended in Hanks and pelleted by centrifugation. The cell pellet was resuspended in 10 ml of Hanks and centrifuged again. The cell pellet was lysed in lysis buffer (Eisenstein et al. 1993) plus 2 mM DTT, 400 μM phenylmethylsulfonyl fluoride, leupeptin (40 μg/ml), pepstatin (4 μg/ml), soybean trypsin inhibitor (100 μg/ml), and MG132 (10 μM) by vortexing occasionally over a 10 min period. Lysates were clarified by centrifugation at 14,000 rpm in an Eppendorf model 3415C centrifuge at 4°C for 10 min. For the RNA binding assay, protein lysates were included at a concentration of 1-1.5 μg/30 μl reaction in the presence of binding buffer (Eisenstein et al. 1993) containing 0.6 μg nuclease free BSA, 2 mM DTT, and 1-1.2 nM RNA. IRE binding activity that was inducible by 2-ME was determined in the presence of 8% 2-ME. Lower concentrations (2%) had little effect on the activation of IRE binding activity of IRP in HeLa cell extracts and only partial effects on rat fibroblast (RF2) extracts (results not shown). Heparin was added (final concentration 0.45 μg/ml) just before loading the gel. Twenty-five microliters of each

reaction was loaded onto a gel shift (Eisenstein et al. 1993) and electrophoresed at 300 V constant voltage for 35 min at 4°C.

Human IRP1 and IRP2 co-migrate in gel shift assays. Antibody supershift experiments were performed to determine the contributions of IRP1 and IRP2 to the binding activity present in HeLa cells. For supershift analysis, 1 μg of HeLa cell lysate was incubated with 10 μg of antibody specific for IRP1 and IRP2 (Schalinske et al. 1997) for 2 h at 4°C. The antibody/lysate preparations were then incubated with IRE RNA and the RNA binding activity was determined as described above. Cytosol from the rat fibroblast cell line RF2 was used as standard for antibody specificity, since rodent IRP1 and IRP2 migrate separately in gel shift assays (results not shown). The contributions of IRP1 and IRP2 to the total binding activity in HeLa cell extracts was determined by the amount of binding activity that was not supershifted by a saturating concentration of antibody. This approach was taken because the polyclonal antibody against IRP2 is capable of both supershifting the RNA protein complex and inhibiting RNA binding by IRP2. Hence quantitation of the supershifted complex does not yield an accurate determination of the amount of IRP2 RNA binding activity.

PhosphorImager Quantitation -

IP Lab Gel 1.5 was used to quantitate immunoprecipitations by determining the volume within a region of fixed pixel number at each band of interest. A region of the same pixel number from an area within the same lane was subtracted from the band of interest as background. RNA binding activity was also quantified by phosphorimage analysis (Packard). The phosphorimage was calibrated (digital light units per fmole

RNA) using a standard curve of ^{32}P RNA in the phosphorimage coupled with scintillation counting of the RNA sample. Background was determined by running a lane with RNA alone. Data were analyzed by one-way analysis of variance using SAS version 8.0. Differences were considered significant at $P < 0.05$. Data are expressed as the means ± SEM for three independent experiments.

Immunodetection of IRPs -

Subconfluent HFE- and HFE+ fWTHFE/tTA HeLa cells were grown in 35-mm dishes. After 2 days, cells were treated with either 50 μM Df or 100 nM human diferric-Tf (Intergen Co.) overnight. Cells were lysed in NET-Triton after at least 12 h of treatment. Cell extracts from 1 x 10^6 HFE- or HFE+ cells were generated with IRP lysis buffer (20 mM HEPES, 1 mM sodium citrate, 5 mM EDTA, 0.5% NP-40, 100 μg/ml leupeptin, 100 μg/ml pepstatin, 250 μg/ml soybean trypsin inhibitor, 200 μM phenylmethylsulfonyl fluoride, 10 μM MG132, pH 7.4). Samples were diluted with 4X Laemmli buffer (Laemmli 1970) and subjected to electrophoresis on denaturing 6% SDS-polyacrylamide gels under reducing conditions. The proteins were transferred to nitrocellulose. Immunoblot analysis for IRP2 was performed using 780 ng/ml rabbit anti-rat IRP2 antibody (Schalinske et al. 1997) followed by goat anti-rabbit antibody conjugated to HRP (1:10,000 dilution; Roche Molecular Biochemicals). Immunoblots were developed using chemiluminescence (Super Signal, Pierce) per the manufacturer's directions.

Calcein Determination of Chelatable Intracellular Iron -

The acetoxymethyl ester of Calcein, Calcein-AM, was obtained from Molecular Probes and prepared as a stock solution of 1 mM in dimethyl sulfoxide (DMSO). The iron chelator SIH (salicylaldehyde isonicotinoyl hydrazone) was a generous gift from Dr. Prem Ponka (McGill University, Montreal, Quebec, Canada) and was prepared as a stock solution of 100 mM in 1 N NaOH. Trypan blue (0.4%) was purchased from Sigma and kept at a stock concentration of 500 μg/ml in PBS. Calcein measurements were modified from a previously published protocol (Konijn et al. 1999). HFE- and HFE+ fWTHFE/tTA HeLa cells were washed with PBS three to four times at room temperature and incubated in trypsin without EDTA at 37°C for 3-5 min. The cells were resuspended in 5 ml Hanks-HEPES buffer, centrifuged at 2,000 rpm for 5 min at room temperature, the resulting pellet was resuspended in 1 ml Hanks-HEPES buffer, and cells were counted on a hemocytometer. An aliquot of 1 x 10^6 cells was spun at 2,000 rpm for 5 min at room temperature. The resulting pellet was resuspended in 1 ml of 0.125 μM Calcein-AM Hanks-HEPES solution and incubated at 37°C for 10 min. Cells were washed twice with PBS to remove Calcein-AM and transferred to a stirred, thermostated cuvette. The fluorescence was monitored at an excitation of 488 nm and an emission of 517 nm on a fluorimeter at 25°C in a stirred cuvette. Trypan blue was added to a final concentration of 25 μg/ml to quench any extracellular Calcein-AM. SIH was added to a final concentration of 143 μM to release intracellular iron from the Calcein-AM. The increase in fluorescence was monitored until a steady signal was obtained (< 3 min). The average difference in fluorescence prior to and after the addition of SIH was plotted for both HFE+ and HFE- cells using Cricket Graph.

RESULTS

HFE Expression Reduces Ft Synthesis -

Ft expression is highly regulated at the translational level by IRP proteins. To verify that the reduced Ft protein levels observed in HFE-expressing cells was consistent with translational regulation by IRPs, we tested for a reduction in Ft synthesis in HFE-expressing cells (Figure 1.1). Under low intracellular iron concentrations, IRPs bind to the 5' IRE of Ft mRNA and prevent recruitment of the eIF3/40S ribosomal complex to the eIF4F cap-binding complex, thereby, reducing the rate of Ft synthesis (Muckenthaler et al. 1998).

Cells were labeled for 15, 30, or 45 min in the presence of 100 μCi of ^{35}S-methionine/cysteine, then immunoprecipitated with antibody against Ft. The incorporation of ^{35}S-methionine/cysteine into total protein as measured by trichloroacetic acid precipitable counts did not significantly differ between HFE- and HFE+ cells (data not shown), indicating that the rates of protein synthesis in the presence or absence of HFE are similar. The rate of ^{35}S-methionine/cysteine incorporation into Ft was 40% less for cells that express HFE (Figure 1.1B). A similar time course was performed at 5, 10, and 15 min with the same result (data not shown). These results suggest that the reduced Ft levels detected on immunoblot at steady state are the result of decreased Ft synthesis, which is consistent with an increase in IRP RNA binding activity.

IRP RNA Binding Activity is Increased in HFE-expressing fWTHFE/tTA HeLa Cells -

The decreased rate of ^{35}S-methionine/cysteine incorporation into Ft in HFE-expressing cells suggested that the IRP RNA binding activity in these cells might be increased. To determine the relative RNA binding activity of IRPs in HFE-expressing cells, we performed gel shift analysis on HFE- and HFE+ fWTHFE/tTA HeLa cell extracts. IRPs exist in spontaneously active as well as latent forms with respect to their ability to bind to IRE-containing RNA with high affinity. Factors that affect IRP function can alter either the distribution of IRP1 or IRP2 between active or latent forms and/or affect the total amount of the IRPs in the cell (reviewed in (Eisenstein 2000)). Therefore, in our studies, we felt that it was important to determine the abundance of the active and latent forms of IRP1 and IRP2 in the absence and presence of HFE in HeLa cells.

The species of IRP1 and IRP2 that bind to IRE RNA with high affinity in the absence of high levels of 2-ME are referred to as the spontaneously active forms. In the case of IRP1, this is the reduced form of the protein that is devoid of an iron-sulfur cluster (reviewed in (Eisenstein 2000)). For IRP2, the evidence indicates that the active high affinity form also must have certain Cys residues in a reduced state. In contrast, latent forms of IRP do not spontaneously bind to the IRE. However, they can be activated to do so *in vitro* by addition of high levels of 2-ME. The predominant latent form of IRP1 is the aconitase form. In iron replete cells a [4Fe-4S] iron-sulfur cluster is assembled in IRP1 and this results in a loss of high affinity RNA binding activity and the acquisition of aconitase activity. High levels of 2-ME can convert the aconitase form of

IRP1 into a form that binds IRE RNA. Therefore, in the presence of 2-ME the total (spontaneous plus latent) RNA binding activity of IRP can be determined.

IRE RNA binding activity was determined in extracts of HFE- and HFE+ fWTHFE/tTA HeLa cells (Figure 1.2). Initially, the combined contribution of IRP1 and IRP2 to the IRE binding activity was determined, since the two human IRPs co-migrate in gel shift assays. Cells expressing HFE had an RNA binding activity of 2,910 ± 270 fmole/mg protein. This was 4.6-fold higher than the IRE binding activity measured in fWTHFE/tTA HeLa cells not expressing HFE (640 ± 60 fmole/mg protein) (Figure 1.2). The addition of 2-ME to extracts from cells not expressing HFE increased IRE binding activity by about 2-fold (1,200 ± 60 fmole/mg protein). A rat fibroblast cell line, RF2, was used as a control to show a similar effect of 2-ME on IRP activation. There was, however, no effect of 2-ME on IRE RNA binding activity in HFE+ cell extracts (Figure 1.2), indicating that both IRPs were already in the spontaneously active RNA binding form. These results suggest that there is essentially no cytosolic-aconitase activity in HFE expressing cells. The IRE binding activity in 2-ME treated HFE+ cells is greater than that of 2-ME treated HFE- cells. This result suggests that HFE-expressing cells contain more total IRP (i.e., induced and uninduced IRP1 and IRP2), which could be attributable to increased expression of IRP1 and/or IRP2.

IRP1 and IRP2 RNA Binding Activity is Increased in HFE-expressing fWTHFE/tTA HeLa Cells -

Gel shift analysis revealed an increase in total IRP activity in HFE-expressing cells. A decreased intracellular labile iron pool would predict increased amounts of IRP2 resulting in increased IRP2 binding to the stem loop structure in the 5' untranslated Ft

message (Guo et al. 1995b; Guo et al. 1995a; Iwai et al. 1995; Iwai et al. 1998) and increased IRP1 RNA binding due to the loss of the iron sulfur cluster and no change in IRP1 levels (Haile et al. 1992b; Haile et al. 1992a). Alternatively, modifications to either IRP that were not iron dependent might lead to the activation of one IRP with no change in the other. We used gel supershift analysis to determine the relative activity changes in IRP1 and IRP2 isoforms (Figure 1.3). Saturating concentrations of antibodies specific for IRP1 or IRP2 were used (Schalinske et al. 1997). The intensity of the supershifted band for both IRP1 and IRP2 in HFE+ cells was increased over that of HFE- cells (Figure 1.3A, lane 2 vs. 5 and lane 3 vs. 6). The antibody specific for IRP2 is directed against the 73 amino acid sequence unique to this IRP. This polyclonal antibody can both supershift the IRP2/IRE complex as well as inhibit IRP2 RNA binding activity. Hence, we quantitated the amount of RNA binding activity that was not supershifted by an IRP-specific antibody and used that value as an indication of the contribution of the other IRP to the IRE binding activity present in these cells. Using this method, HFE+ cells had between 2 and 3 fold increased RNA binding activity over that of HFE- cells for both IRP1 and IRP2 (Figure 1.3B).

Expression of HFE was associated with an alteration of the relative contribution of IRP1 and IRP2 to the total spontaneous IRE binding activity present in the fWTHFE/tTA HeLa cells. In HFE- cells, IRP1 contributed slightly more than 50% of the total binding activity and the IRP1/IRP2 ratio was 1.2 ± 0.07 (calculated from Figure 1.3B). However, in HFE+ cells, IRP1 contributed about two-thirds of the total binding activity such that the IRP1/IRP2 ratio increased to 1.8 ± 0.14 (calculated from Figure 1.3B), which is significantly different from cells not expressing HFE ($P < 0.05$).

Citrate and other aconitase substrates block the ability of high levels of 2-ME to convert cytosolic aconitase into a high affinity RNA binding form of IRP1 (Haile et al. 1992a). In lysates from HFE- cells, citrate partially inhibited the effect of 2-ME (data not shown) suggesting that some of the 2-ME inducible activity in these extracts was due to activation of cytosolic aconitase into a high affinity RNA binding form. About half of the 2-ME inducible activity was not affected by citrate addition implying that 2-ME was also activating a latent form of IRP2 (data not shown) (Schalinske and Eisenstein 1996). Thus, our results suggest that expression of HFE leads to the conversion of IRP1 and IRP2 to fully active high affinity RNA binding proteins.

IRP Protein Levels are Consistent with Activity -

We tested HFE- and HFE+ cells for changes in steady state levels of the IRPs to determine whether the expression of IRP1 and IRP2 were consistent with the observed differences of the IRPs in their RNA binding. Immunoblot analysis was used to determine IRP1 and IRP2 protein levels in HFE- and HFE+ cells and their regulation with iron treatments. HFE- and HFE+ fWTHFE/tTA HeLa cells were treated overnight with standard growth medium (DMEM with 10% FBS) as a control or cells were treated in medium either containing 100 nM human Tf as an iron source or containing 50 μM Df to deplete the cells of iron. Immunoblots of cell extracts normalized for protein concentration were used to analyze relative amounts of IRP1 and IRP2. IRP1 levels did not change significantly with iron treatments or with HFE expression (data not shown), but IRP2 levels did respond to iron treatment and HFE expression (Figure 1.4). In the presence of the iron chelator Df, IRP2 levels increased (Figure 1.4, lane 1 vs. 2 and lane 4

vs. 5), while the addition of iron to the cells through Tf decreased IRP2 levels (Figure 1.4 lane 1 vs. 3 and lane 4 vs. 6). IRP2 levels responded to iron supplementation regardless of HFE expression, however, IRP2 levels were increased in HFE+ cells over that of HFE- cells with each treatment (Figure 1.4 lanes 4-6 vs. 1-3). Because iron regulates the stability of IRP2, but does not affect the stability of the IRP1 protein, these results suggest that the increased IRP activity observed in HFE+ cells is the result of a reduction in the labile iron pool rather than through iron-independent activation of IRP RNA binding activity such as phosphorylation of the IRP or modification of the [4Fe-4S] cluster by reactive oxygen and nitrogen species (Bouton et al. 1996; Pantopoulos et al. 1996; Brown et al. 1998).

Synthesis of IRP1 is Not Significantly Increased with HFE Expression -

Immunoblot analysis of IRP levels did not indicate a significant change for the IRP1 protein in HFE expressing cells. Since IRP1 is a relatively stable protein whose steady state levels do not change rapidly (Pantopoulos and Hentze 1995) we used a more sensitive assay for changes in protein level. The rate of ^{35}S-methionine/cysteine incorporation into IRP1 was determined for HFE- and HFE+ cells (Figure 1.5). Cells were labeled for 1, 2, 3, or 4 h in the presence of 100 μCi of ^{35}S-methionine/cysteine, then immunoprecipitated with antibody against IRP1 (Figure 1.5A). The rate of ^{35}S-methionine/cysteine incorporation into total cellular protein did not differ significantly between HFE- and HFE+ cells (data not shown).

Quantitation of ^{35}S-methionine/cysteine incorporation into IRP1 did not show a significant difference between HFE- and HFE+ cell lines (Figure 1.5B). These results are

consistent with immunoblot analysis of IRP1 levels and confirm that HFE increases IRP activity through post-translational modification of the IRP proteins.

Measurement of the Intracellular Labile Iron Pool by Calcein-AM -

Decreased Ft synthesis, and increased IRP levels and IRE binding activity in HFE-expressing cells indicated that the intracellular labile iron pool should be lower in HFE+ cells. To utilize the most direct technique available for quantitating this labile iron pool, we loaded HFE+ and HFE- cells with 0.125 μM of the fluorescent probe, Calcein-AM for 10 min at 37°C (Figure 1.6). Trypan blue (25 μg/ml) was added to quench any Calcein remaining on the cell surface to ensure that only the intracellular Calcein-AM was measured. The relative levels of labile iron were measured by the addition of SIH, an iron-specific cell permeable chelator to release iron from Calcein-AM. Calcein-AM's fluorescence is quenched when it is bound to iron, but when SIH chelates the iron, Calcein-AM is released and its fluorescence can be measured. Thus, we could measure the amount of iron within the cell by measuring the increase in fluorescence upon the addition of SIH. These experiments showed that the amount of SIH-sensitive iron in HFE+ cells was 45% less than in HFE- cells signifying a lower intracellular iron pool.

DISCUSSION

We and others have reported that the expression of HFE leads to lower Ft levels and activation of IRPs (Gross et al. 1998; Corsi et al. 1999; Riedel et al. 1999; Roy et al. 1999). IRPs are regulated by the labile iron pool, by stimuli from other processes such as kinase cascades (Schalinske and Eisenstein 1996; Brown et al. 1998) and in response to oxidative stress and nitric oxide (Drapier et al. 1993; Weiss et al. 1993; Bouton et al. 1996; Pantopoulos et al. 1996; Hanson et al. 1999). A direct relationship between HFE expression, the labile iron pool and IRP RNA binding activity has not been thoroughly examined. Therefore, we sought to characterize the activities of IRP1 and IRP2 in fWTHFE/tTA HeLa cells to test whether the mechanism by which HFE regulates iron homeostasis works through the labile iron pool or independent of it. Our results are consistent with HFE acting to lower the intracellular pool of labile iron.

Steady state levels of Ft are decreased in cells expressing HFE. IRP binding to the Ft IRE prevents translation by excluding the binding of the eIF3/40S ribosomal complex to the eIF4F cap-binding complex (Muckenthaler et al. 1998). To test whether Ft levels in HFE+ cells were reduced as a result of translational control, the rate of incorporation of ^{35}S-methionine/cysteine into Ft was determined in HFE- and HFE+ cells. The rate of Ft translation is reduced in HFE-expressing cells by approximately 40%. This result suggests that decreased Ft levels in HFE+ cells are the result of decreased translational efficiency, which is consistent with increased IRP RNA binding activity and a reduction in the labile iron pool.

Direct analysis of IRP RNA binding in fWTHFE/tTA HeLa cells indicated that HFE expression leads to an activation of IRP RNA binding. HFE+ fWTHFE/tTA HeLa cells exhibited an increase in IRE RNA binding of almost 5-fold more than HFE- cells. In our cell line, the difference between the IRE RNA binding in HFE- and HFE+ cell extracts was not equalized with 2-ME as previously reported (Corsi et al. 1999; Riedel et al. 1999). This is probably due to the increase in IRE RNA binding of both IRP1 and IRP2. This discrepancy with previously reported results may be due to the difference in levels of IRP2 between HeLa cell strains.

In the absence of HFE, fWTHFE/tTA HeLa cells contain a latent form of IRP1 presumably bound with an iron-sulfur cluster. Evidence from cell culture and animal experiments indicated that both IRP1 and IRP2 can exist in latent forms that are not able to bind RNA with high affinity unless 2-ME is added *in vitro*. A variety of physiological conditions including and in addition to iron deficiency can promote activation of these latent forms of IRP1 and IRP2. In characterizing the latent forms of IRPs present in fWTHFE/tTA cells not expressing HFE, we found that addition of 2-ME stimulated the IRPs binding to IREs in extracts of these cells. Aconitase substrates like citrate block the ability of 2-ME to activate RNA binding by cytosolic aconitase, the latent form of IRP1 (Haile et al. 1992b; Henderson et al. 1993; Henderson and Kuhn 1995; Schalinske and Eisenstein 1996). In cells not expressing HFE, only 50% of 2-ME inducible activity was blocked by citrate. This observation suggests that in the absence of HFE, the HeLa cells contain latent forms of IRP1 and IRP2. However, upon the induction of HFE expression, neither of these latent forms was present indicating full activation of IRP RNA binding activity in HFE+ cells. The enhanced RNA binding of IRP1 in HFE+ cells was due to a

relative increase in the proportion of IRP1 in the RNA binding form, rather than an increase in the amount of IRP1 protein. IRP2 protein levels, however, were increased in HFE+ cells over HFE- cells. This result is consistent with IRP2 regulation by a depleted labile iron pool, and is confirmed by the increased amount of calcein fluorescence in these cells. It explains why RNA binding activity is greater in extracts of HFE+ cells, even in the presence of 2-ME.

Expression of HFE was associated with a significant shift in the IRP1 to IRP2 ratio due to differences in the degree to which the RNA binding activity of each protein was increased. The IRP1/IRP2 ratio increased from 1.2 in HFE- cells to 1.8 in HFE+ cells, suggesting that IRP2 RNA binding activity was not induced as efficiently as was IRP1. The regulation of RNA binding of these two proteins occurs through different pathways, but they are believed to be dependent on the same labile iron pool. In light of this observation, it is interesting that in the presence of HFE, Ft expression appears to be more dramatically affected than does that of TfR1 (Roy et al. 1999). Multiple factors could influence the efficiency with which the two IRPs affect the utilization of specific mRNA. This includes the relative abundance of the two binding proteins and/or their mRNA targets, potential differences in their ability to bind to specific IRE-containing mRNA, and the activity of competing proteins such as certain protein synthesis initiation factors (Cairo et al. 1998; Ke et al. 1998; Recalcati et al. 1998). The molecular basis for the difference in the magnitude of activation of IRP1 and IRP2 in HFE+ fWTHFE/tTA HeLa cells and the extent to which it represents an important consequence of the expression of HFE in cells awaits further investigation.

In this study, we have investigated HFE's role in the coordination of intracellular iron sensing machinery, in particular through modulation of the labile iron pool. The results demonstrate that HFE establishes a new, lower steady state for the cellular labile iron pool. The HFE-induced reduction of this pool may be important for regulation of organismal iron homeostasis because despite the exquisite regulation afforded by IRPs, HFE's role in the maintenance of iron homeostasis remains indispensable. Individuals with hereditary hemochromatosis have reduced levels of functional HFE (Feder et al. 1996; Rothenberg and Voland 1996; Santos et al. 1996; Zhou et al. 1998; Levy et al. 1999b) and cannot appropriately regulate iron uptake despite functional IRPs (Cairo et al. 1997; Santos et al. 1998).

HFE-specific regulation of iron homeostasis may not be limited to regulation through the IRPs. We speculate that HFE's control of the labile iron pool may have further reaching effects on iron homeostasis through other regulatory mechanisms dependent on the labile iron pool such as iron-dependent transcription or iron-dependent protein trafficking. Experiments designed to test for the influence of HFE on the expression and activity of proteins involved in enterocyte-specific iron transport may clarify the purpose for HFE's hypothesized modulation of the labile iron pool in the enterocyte precursor cells of the crypt.

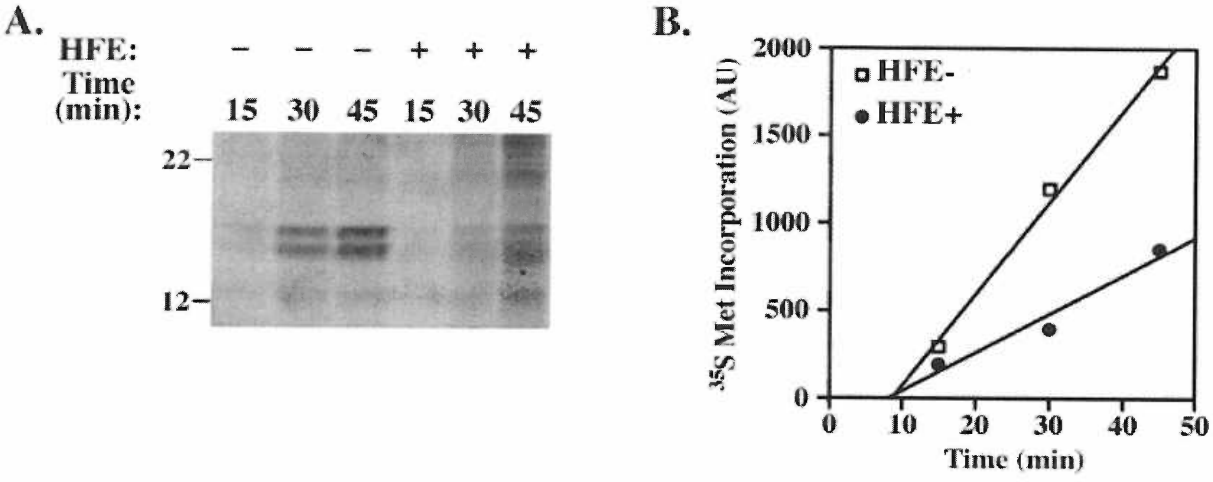


Figure 1.1. The rate of ^{35}S-methionine/cysteine incorporation into Ft is reduced in HFE-expressing cells. Approximately 6.5 x 10^5 cells were labeled over a 45 min time course with 100 μCi ^{35}S-methionine/cysteine. Ft was immunoprecipitated and run on a 12% polyacrylamide gel under reducing conditions. **A)** The autoradiograph shows a significant reduction in ^{35}S-methionine/cysteine incorporation in HFE-expressing cells. **B)** Quantitation of ^{35}S-amino acid incorporation in HFE- (open squares) and HFE+ (closed circles) by PhosphorImager analysis. These results are representative of three independent experiments without significant variation between results.

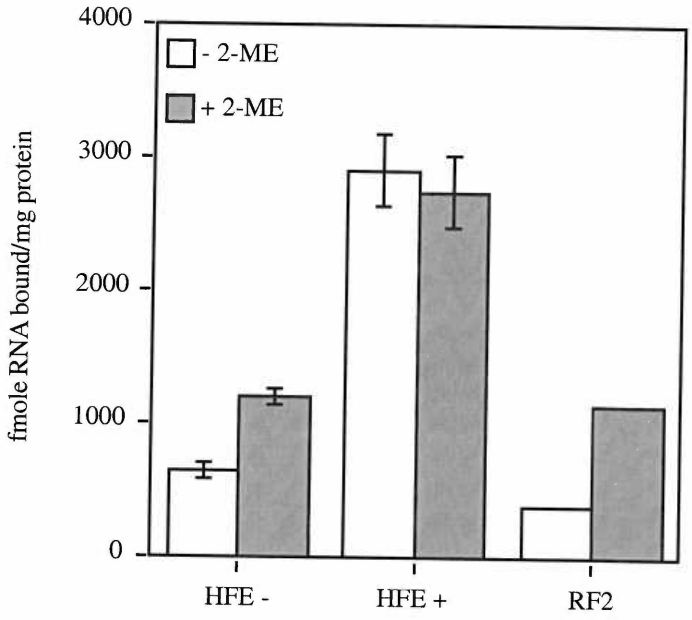


Figure 1.2. Total IRP RNA binding activity is increased in HFE-expressing cells. Between 1 and 1.5 μg clarified cellular protein was assayed for IRP RNA binding activity as described under Materials & Methods. RNA binding was performed without 2-ME (open bars) or with 2-ME (filled bars) in the assay buffer. HeLa IRP RNA binding activity was comparable to that of RF2 cells. HFE-expressing cells had increased IRP RNA binding activity in the presence or absence of 2-ME, and unlike RF2 or HFE- cell lysates, were not induced in the presence of 2-ME. These results are representative of those obtained in at least three independent experiments.

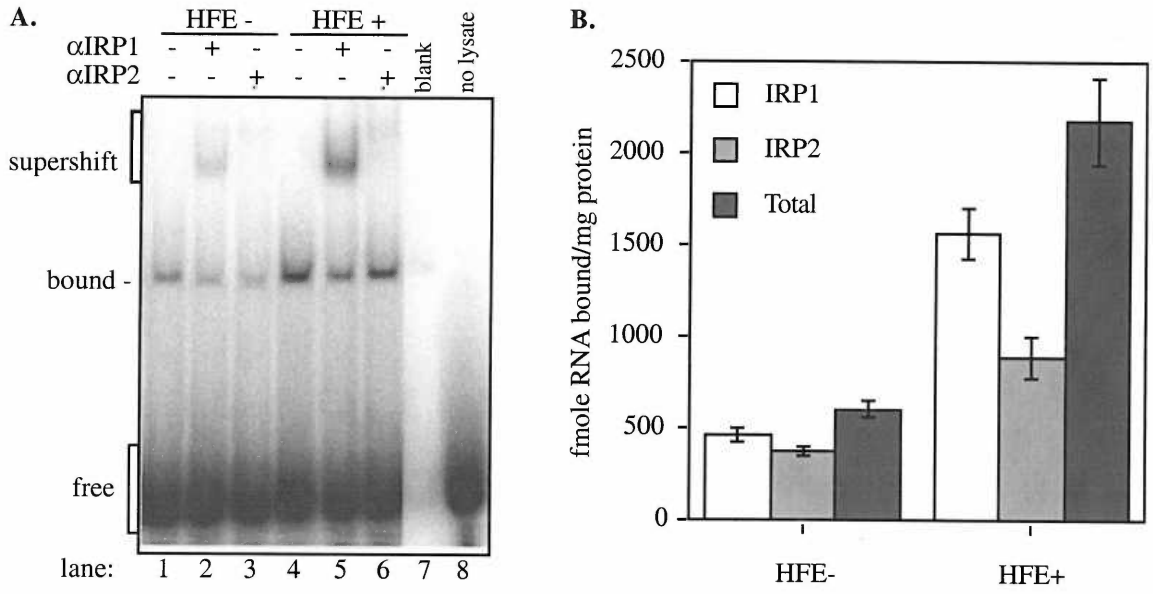


Figure 1.3. IRP1 and IRP2 RNA binding activity are increased in HFE-expressing cells. One microgram of cell extract was incubated with 10 μg IRP1 or IRP2 antibody, then assayed for IRP RNA binding activity as described under Materials & Methods. **A)** Binding of IgG to the protein-RNA complex results in supershifted RNA probe. HFE+ cells had increased IRP1 and IRP2 RNA binding activity. **B)** Quantitation of the IRP bound probe that was not supershifted by IgG indicates that HFE-expressing cells had 3.3-fold more IRP1 activity (open bars) and 2.3-fold more IRP2 activity (light gray bars), with total IRP activity increasing 3.6-fold (dark gray bars). These results are representative of those obtained in at least three experiments. The relative contribution of IRP1 and IRP2 to the total IRP binding activity in HeLa cell extracts was determined as follows. Saturating amounts of antibodies specific for IRP1 or IRP2 were used to individually supershift the binding activity for a given IRP. The amount of activity not supershifted by the IRP1 antibody was judged to be due to IRP2. The amount of activity not shifted by each antibody was summed and this was used to determine the percentage that each IRP contributed to the total activity. These values were determined from three independently prepared extracts of HeLa cells expressing or not expressing HFE. All values are reported as mean ± SEM.

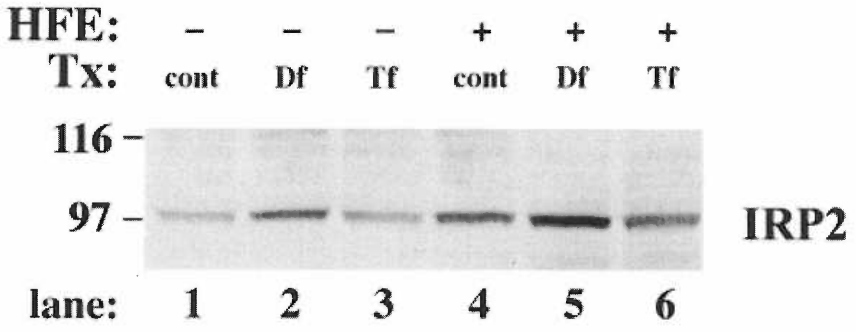


Figure 1.4. Steady state levels of IRP2 proteins are consistent with reduction of the labile iron pool in HFE-expressing cells. Approximately 500 μg of cellular protein was run on a 6% polyacrylamide gel under reducing conditions. Proteins were transferred to nitrocellulose and detected with rabbit anti-rat IRP2 antibody (1:5,000) and HRP conjugated goat anti-rabbit antibody (1:10,000). These results are representative of those obtained in multiple experiments.

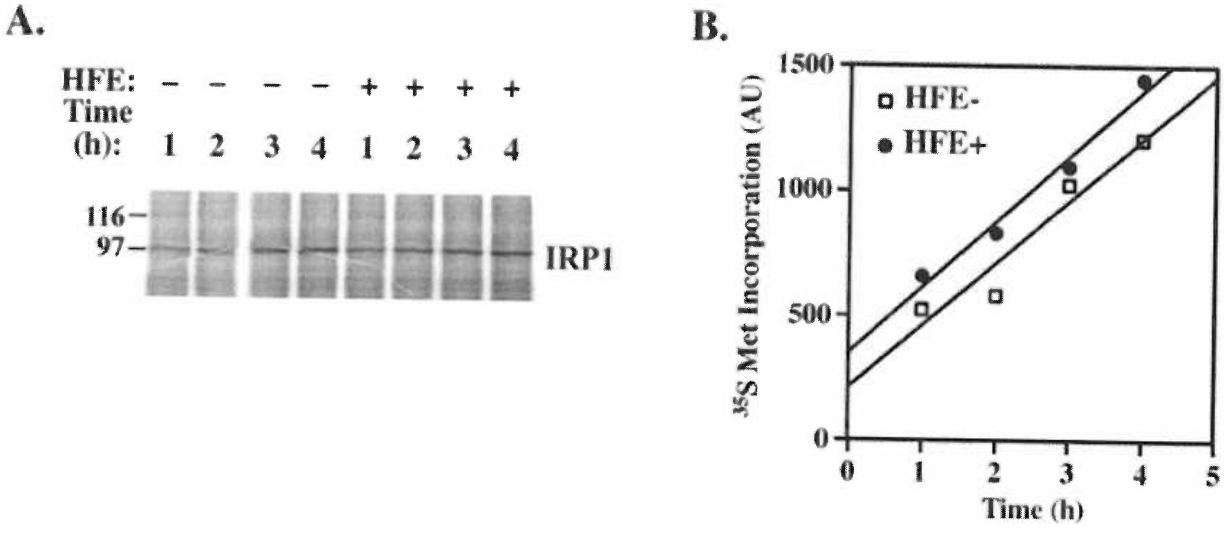


Figure 1.5. The rate of ^{35}S-methionine/cysteine incorporation into IRP1 does not change in HFE-expressing cells. Approximately 1 x 10^6 cells were labeled over a 4 h time course with 100 μCi ^{35}S-methionine/cysteine. IRP1 was immunoprecipitated and run on a 6% polyacrylamide gel under reducing conditions. **A)** The autoradiograph shows no significant change in ^{35}S-methionine/cysteine incorporation in HFE-expressing cells. **B)** Quantitation of ^{35}S-methionine/cysteine incorporation in HFE- (open squares) and HFE+ (closed circles) shows no significant change in IRP1 for HFE-expressing cells. These results are representative of multiple experiments without significant variation between results.

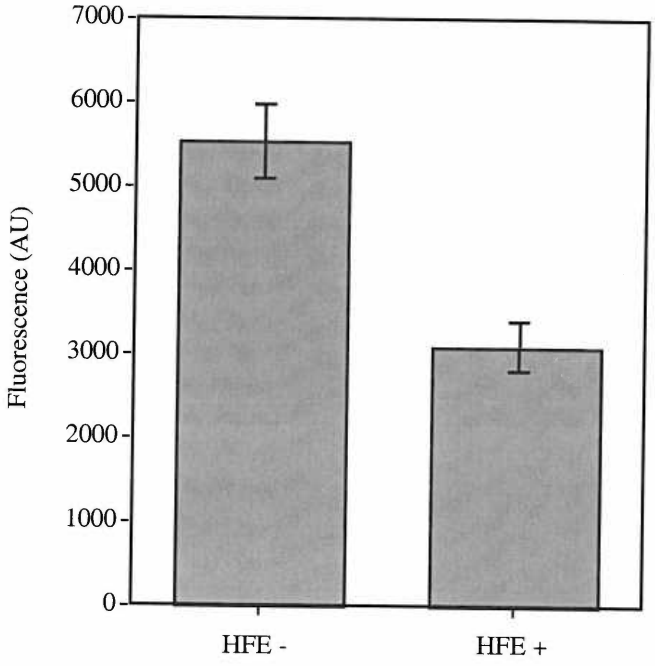


Figure 1.6. Analysis of the labile iron pool by Calcein in HFE+ cells and HFE- cells. The fluorescent probe Calcein-AM was used along with SIH, an iron chelator, to determine the relative level of free iron within fWTHFE/tTA HeLa cells. fWTHFE/tTA HeLa cells were incubated with 0.125 μM Calcein-AM for 10 min at 37°C and any unbound Calcein-AM was washed away. To ensure that the Calcein-AM was only binding to intracellular iron, 25 μg/ml Trypan blue was added to quench any Calcein-AM that may have bound to the outside of the cell. The iron chelator SIH was added to release intracellular iron from the Calcein-AM in order to measure the relative levels of intracellular iron chelated by the Calcein-AM. This increase in fluorescence upon addition of SIH is representative of how much intracellular iron was initially bound to Calcein-AM. These experiments showed that HFE+ cells had a lower change in fluorescence than HFE- cells, signifying a lower intracellular iron pool.

CHAPTER 2

Evidence for the Interaction of the Hereditary Hemochromatosis Protein, HFE, with the Transferrin Receptor in Endocytic Compartments

Paige S. Davies*, An-Sheng Zhang*, Emily L. Anderson*, Cindy N. Roy*[1], Michael A. Lampson§, Timothy E. McGraw§, and Caroline A. Enns*

*Department of Cell and Developmental Biology, Oregon Health & Science University, Portland, Oregon, 97239-3098, USA

§Department of Biochemistry and Structural Biology, Weill Medical College of Cornell University, New York, NY, 10021, USA

[1]Present address: Harvard Medical School, Children's Hospital, Boston, MA 02115, USA

Published in *Biochemical Journal* (2003) **373(Pt 1)**: 145-153

‡This work was supported by NIH DK 54488 (CAE). CNR and PSD were supported in part by the Training Program in Molecular Hematology, T32-HL00781, National Institutes of Health, National Heart, Lung, and Blood Institute.

SUMMARY

HFE, the protein mutated in hereditary hemochromatosis type 1, is known to interact with the transferrin receptor 1 (TfR1) on the cell surface and during endocytosis (Gross et al. 1998; Roy et al. 1999). However, whether they are capable of interacting with each other once inside the cell is not known. In the present study we present several lines of evidence that they do interact in endosome compartments. Cells expressing a chimera of HFE protein with the cytoplasmic domain of lysosomal-associated membrane protein 1 (LAMP1) in place of its own (HFE–LAMP) show a decrease in the half-life of the TfR1. This implies that the interaction between HFE and TfR1 in endosomes targets the TfR1 to lysosomal compartments. The interaction between TfR1 and HFE–LAMP was confirmed by immunoprecipitation, in addition to immunofluorescence studies. Addition of transferrin (Tf) to HFE–LAMP-expressing cells competes with HFE for binding to the TfR1, thereby increasing the half-life of TfR1 and confirming that the HFE–LAMP–TfR1 complex reaches the cell surface prior to entering the endosomal vesicles and trafficking to the lysosome. These results raise the possibility that interaction of HFE and TfR1 in intracellular vesicles may play an important role in determining the function of HFE in iron homoeostasis, which is still unknown. Analysis of endosomal pH and the iron content of internalized Tf indicated that HFE does not appear to alter the unloading of iron from Tf in the endosome.

INTRODUCTION

Hereditary hemochromatosis is an autosomal recessive disease that, over time, causes an accumulation of iron in the parenchymal tissues of affected patients. HFE is the protein that is mutated in the majority of hereditary hemochromatosis cases. Since its identification in 1996 (Feder et al. 1996), many insights regarding HFE have been elucidated, although its true role in iron homoeostasis remains unclear. Previous studies showed that HFE interacts with the transferrin receptor 1 (TfR1). Transferrin (Tf) is a serum protein that binds up to two molecules of ferric iron and subsequently binds to the TfR1 on the surface of cells. Once this complex is internalized, the acidic milieu of the endosome induces a conformational change in the TfR1, facilitating the release of iron from Tf (Bali and Aisen 1991; Bali et al. 1991; Sipe and Murphy 1991; Bali and Aisen 1992). The iron-free Tf (apo-Tf) stays bound to the TfR1 and is recycled to the cell surface where, in the neutral to slightly basic extracellular environment, the apo-Tf is released, allowing further binding of diferric-Tf to the receptor to continue the cycle.

When cells express HFE, the apparent affinity of the TfR1 for Tf is decreased (Feder et al. 1998; Gross et al. 1998). The reduction in apparent affinity is due to the competition of HFE and Tf for overlapping binding sites on the TfR1 (Lebron et al. 1998; Lebron and Bjorkman 1999; Lebron et al. 1999). Our lab and others have shown previously that HeLa cells expressing HFE have reduced iron levels (Gross et al. 1998; Corsi et al. 1999; Riedel et al. 1999; Roy et al. 2002), and that such reduction occurs through the Tf-mediated iron-uptake pathway (Roy et al. 1999). HFE expression does not affect either the kinetics of TfR1 cycling or the distribution of TfR1 within the cell

(Roy et al. 1999). Furthermore, we have shown that HFE and TfR1 are capable of interacting within 30 min of their synthesis. They are associated on the cell surface and also interact during endocytosis (Feder et al. 1998; Gross et al. 1998; Roy et al. 1999). Whether or not HFE and TfR1 remain associated once in the endosome is not known. *In vitro* studies using the soluble forms of both TfR1 and HFE lacking the transmembrane and cytoplasmic domains have over a 2,000-fold decrease in binding at pH less than or equal to 6.2 compared with pH 7.2 (Lebron and Bjorkman 1999). Whether the transmembrane and cytoplasmic domains play a role in the interaction, or whether the ionic environment of the endosome affects the interaction between these two proteins, has not been determined.

To study the possible interaction of HFE and TfR1 in cells, a chimeric HFE that has its cytoplasmic domain replaced with that of lysosomal-associated membrane protein 1 (LAMP1) was generated. LAMP1 is a lysosomal protein and its cytoplasmic domain contains the lysosomal-targeting motif YQTI, allowing it to traffic from the cell surface to lysosomes. Both LAMP1 and TfR1 endocytose via a common endocytic compartment (Warren et al. 1998); however, LAMP1 is targeted to lysosomes whereas TfR1 is recycled to the plasma membrane. An HFE–LAMP/tetracycline-transactivatable (tTA) HeLa cell line that can be induced to express HFE–LAMP was generated to determine whether TfR1 remains associated with HFE as it passes through the endosome. We show that induction of HFE–LAMP expression resulted in a decreased TfR1 half-life, due to its targeting to lysosomal compartments. Additionally, immunofluorescence showed TfR1 and HFE–LAMP co-localized in perinuclear compartments within the cell.

MATERIALS AND METHODS

Plasmids -

To create the pUHD 10-3 HFE–LAMP1 construct, the pUHD 10-3 fWTHFE plasmid (described in (Gross et al. 1998)) was linearized with the restriction enzyme *Sca*I. Primers were designed to replace the cytoplasmic domain of HFE and the FLAG epitope (RKRQGSRGAMGHYVLAEREDYKDDDDK) with the cytoplasmic domain of LAMP1 (RKRSHAGYQTI), which includes an internalization and lysosomal sequence. Both of these proteins have a membrane anchor of RKR, so the LAMP1 domain was added in place of the HFE domain following this motif. The reverse primer included a termination codon (5′-GCG-GCC-GCT-TAT-CAG-ATA-GTC-TGG-TAG-CCT-GCG-TGA-CTC-CTC-TTC-CTT-AAT-ATT-ATG-3′) and the forward oligonucleotide was designed from a nearby *Bam*HI site (5′-CCC-GGG-GAT-CCT-CTA-GCG-3′). We utilized the above primer pair to amplify and loop in the desired sequence, creating the HFE–LAMP cDNA in pUHD 10-3.

Subcloning -

The HFE–LAMP PCR product was ligated into the 3′ T-overhang of the pGEM-T vector (Promega). pGEM-T/HFE–LAMP and pUHD 10-3/fWTHFE plasmids were cut with *Not*I, gel purified and cut with *Bst*XI to yield the amplicon fragment (HFE–LAMP, 529 bp) and vector fragment (pUHD 10-3, 3698 bp). The amplicon and vector fragments were ligated, transformed and confirmed with *Not*I and *Bst*XI restriction digests in addition to sequence analysis.

The sequenced pUHD 10-3 HFE–LAMP plasmid revealed an A-to-T mutation in the LAMP1 domain, changing the amino acid sequence from RKRSHAGYQTI to RKRSHAGYQSI. The Tyr-Xaa-Xaa hydrophobic residue sequence at the C-terminus of the cytoplasmic domain of LAMP1 is necessary for internalization and essential for lysosomal targeting (Guarnieri et al. 1993). The mutation in our clone falls within this motif (YQTI to YQSI) but did not alter the ability of the protein to internalize or target to the lysosome.

Generation of the HFE–LAMP/tTA HeLa Cell Line -

The generation of the tetracycline-repressible HeLa cells that express FLAG-epitope-tagged wild-type HFE (fWTHFE/tTA HeLa) was described previously (Gross et al. 1998). The HFE–LAMP/tTA HeLa cell line was generated in an identical manner. Colonies were screened by Western analysis for expression of HFE using a rabbit anti-human HFE antibody (a gift from Dr. Pamela Bjorkman, California Institute of Technology, Pasadena, CA). The resulting HFE–LAMP/tTA HeLa cells were maintained in Dulbecco's modified Eagle's medium (DMEM) supplemented with 10% fetal bovine serum, 400 μg/ml G418 (Geneticin; Calbiochem) and 300 ng/ml puromycin, with or without 1 μg/ml doxycycline (Dox+ and Dox- respectively; Dox is an analogue of tetracycline). The HFE–LAMP protein was expressed in cells without Dox.

Western Immunodetection -

Cell extracts from ~6 x 10^5 cells were diluted with 4X Laemmli buffer (125 mM Tris/HCl (pH 6.8), 4% SDS, 20% glycerol and 10% 2-mercaptoethanol) (Laemmli 1970),

or immunoprecipitates were eluted with 2X Laemmli buffer and subjected to electrophoresis on SDS/polyacrylamide gels (8, 10 or 12%) under reducing conditions. The proteins were transferred to nitrocellulose (Nitropure 0.45 mm; Osmonics). Immunoblot analysis was performed using sheep anti-TfR1 serum (Williams and Enns 1991; Warren et al. 1997) (1:10,000 dilution), rabbit anti-HFE (EX1 #137; gift from Dr. John Feder, Bristol-Myers Squibb Co., Princeton, New Jersey; 1:10,000 dilution) and rabbit anti-human ferritin (Ft) (1:500 dilution; DAKO) followed by the appropriate secondary antibody conjugated to horseradish peroxidase and chemiluminescence (SuperSignal; Pierce) as per the manufacturer's directions.

Immunoprecipitation -

HFE–LAMP/tTA HeLa Dox- and Dox+ cells were washed three times with 2 ml of PBS (pH 7.4) and lysed with NET-Triton (150 mM NaCl, 5 mM EDTA and 10 mM Tris (pH 7.4) with 1% Triton X-100). Cell lysates were adsorbed for 1 h at 4 °C with 50 μl of donkey anti-mouse antibody (Jackson Laboratories)-coated Gamma Bind Plus Sepharose (Protein G–Sepharose; Amersham Biosciences) and 4 μl of monoclonal anti-HFE antibody (8C10 mouse anti-hHFE) (Ben-Arieh et al. 2001). After centrifugation in a microfuge for 2 min, the Protein G–Sepharose pellet was resuspended in 100 μl of 2X Laemmli buffer and subjected to SDS/PAGE analysis on an 8% acrylamide gel. Gels were transferred to nitrocellulose and immunodetected with sheep anti-TfR1 antibody or rabbit anti-HFE antibody as described above.

Immunofluorescence -

Subconfluent HFE–LAMP/tTA HeLa (Dox- and Dox+) cells grown on coverslips were washed three times with 2 ml of Hank's balanced salts modified medium (without sodium bicarbonate; pH 7.4; Sigma) at room temperature. All cells were fixed for 15 min in 4% paraformaldehyde (Electron Microscopy Sciences) at room temperature. They were washed twice for 1 min each with Hank's medium, permeabilized with 0.2% Triton X-100 in Hank's medium for 10 min at room temperature, and washed three times, for 5 min each, with Hank's medium. The cells were blocked for 1 h at room temperature in Hank's medium supplemented with 10% fetal bovine serum. The cells were incubated for 1 h at room temperature in sheep anti-TfR1 (1:800 dilution in blocking solution) or 8C10 mouse anti-HFE (1:1,000 dilution). Coverslips were then washed three times with Hanks and incubated again for 1 h at room temperature with Alexa 488 donkey anti-sheep secondary antibody (1:500 dilution) or Alexa 594 donkey anti-mouse secondary antibody (1:250 dilution; Molecular Probes). Cells were mounted with ProLong Antifade (Molecular Probes) and imaged by deconvolution microscopy (Deltavision) on a Nikon microscope (60x oil immersion lens).

Half-life Experiments -

Induced (Dox-) and uninduced (Dox+) subconfluent HFE–LAMP/tTA HeLa cells in 35 mM dishes were washed three times with sterile PBS (pH 7.4) and labeled with 50 μCi of [^{35}S]methionine/cysteine (Perkin Elmer Life Sciences) in DMEM minus methionine/cysteine (Invitrogen) medium supplemented with 20% fetal bovine serum overnight. The cells were washed three times with PBS and chased from 0 to 24 h with

complete medium. At the completion of the chase, all cells were lysed for 5 min on ice in NET-Triton. Cell lysates were preadsorbed for at least 45 min at 4 °C with 50 μl of Protein A–Sepharose 4B (Zymed) per ~6 x 10^5 cells to reduce precipitation of non-specific protein. Preadsorbed lysates were incubated for 1 h at 4 °C with 50 μl of Protein A–Sepharose and 1.4 μl of sheep anti-TfR1 serum. After incubation, the sample was spun down and the pellet was resuspended in 200 μl of NET-Triton and washed through 1 ml of NET-Triton containing 15% sucrose. Samples were eluted in 100 μl of 2X Laemmli buffer and subjected to SDS/PAGE analysis on 8% denaturing gel. Gels were fixed, treated with Amplify (Amersham Biosciences), dried and subjected to PhosphorImager analysis.

Tf Competition -

Subconfluent HFE–LAMP/tTA HeLa cells (Dox-) in 35 mm dishes were washed three times with sterile PBS (pH 7.4) and labeled with 50 μCi of [^{35}S]methionine/cysteine in DMEM minus methionine/cysteine medium with 20% fetal bovine serum overnight. After washing, the cells were incubated with or without 3 mg/ml diferric-Tf in complete medium for 0–24 h. Cells were washed and solubilized and the cell extracts were incubated with sheep anti-TfR1 to immunoprecipitate TfR1 as described above and analyzed by SDS/PAGE on an 8% acrylamide gel under reducing conditions. Gels were fixed, treated with Amplify, dried and subjected to PhosphorImager analysis.

PhosphorImager Quantification and Calculation of Half-lives -

IP Lab Gel 1.5 (Molecular Dynamics) was used to quantify images by determining the area within a region of fixed pixel number at each band of interest on the gel. Background of each lane was subtracted from the band of interest to obtain comparable values. Half-lives were calculated from analysis of the radioactive bands using a Molecular Dynamics PhosphorImager and Image 1.5 software. The values were plotted on a semi-log plot and slopes calculated using Cricket Graph.

^{55}Fe-Tf Uptake and ^{125}I-labeled Diferric-Tf (^{125}I-Tf) Preparation -

The procedures for ^{55}Fe loading on to human apo-Tf and ^{55}Fe-Tf uptake were essentially the same as described previously (Gross et al. 1998). The effect of monensin on ^{55}Fe-Tf was measured as described in the relevant figure legend. Human diferric-Tf was labeled with Na^{125}I using lactoperoxidase as described previously (Warren et al. 1997; Warren et al. 1998).

Urea/PAGE -

Urea/PAGE has the advantage that it can separate apo-, monoferric- and diferric-Tf based on their different rates of migration under this specific condition. It was performed as described previously (Makey and Seal 1976; Sipe and Murphy 1991) with the following modifications. Subconfluent Dox+ and Dox- fWTHFE/tTA HeLa cells in 35 mm wells were first incubated with 1 ml of pre-warmed incubation medium (DMEM with 20 mM HEPES and 2 mg/ml ovalbumin, pH 7.4) containing 100 nM ^{125}I-labeled diferric-Tf at 37 °C for 30 min to allow ^{125}I-Tf internalization and cycling. The externally

bound Tf was then stripped with an acidic buffer (0.5 M acetic acid and 0.5 M NaCl) for 2 min at 4 °C, followed by four washes with 2 ml of NET. Cells were lysed in 80 μl of NET-Triton. After mixing with an equal amount of 2x loading buffer (7 M urea, 1.25x TBE (100 mM Tris/10 mM boric acid/5 mM EDTA), pH 8.5, and 10% sucrose), samples were subjected to urea/acrylamide-gel electrophoresis (6 M urea, 6% acrylamide and 1x TBE, pH 8.5), and run at 4 °C at 100 V for 20 h. After fixation, the gel was dried and exposed to X-ray film at -80 °C. To avoid any residual amount of iron contamination, all the above solutions were pretreated with a de-ionization mix (AG 501-X8 resin; Bio-Rad) for at least 3 h with constant stirring at the ratio of 5 g of resin/100 ml of solution.

To show the efficacy of urea/PAGE in the separation of different forms of Tf and to ensure that the above procedure truly reflects the status of Tf within the endosome, we also ran samples prepared by incubating cells with ^{125}I-Tf at 4 °C without or with subsequent acid wash as controls, of which the former was expected to show only the cell-surface bound ^{125}I-Tf and the latter was expected to show no ^{125}I-Tf signal in the urea/PAGE. We also performed several positive controls by pre-incubating the cells with different concentrations of monensin (0, 20, 50 and 100 μM) for 30 min at 37 °C to inhibit the endosomal lumen acidification. ^{125}I-Tf (100 nM) was added and incubated for 30 min with the same concentrations of monensin as above. Cell lysates were subjected to urea/PAGE.

Immunofluorescence Analysis and Measurement of Endosomal pH -

The methods for measuring pH of endosomes have been described previously (Dunn et al. 1994). Briefly, subconfluent Dox+ or Dox- fWTHFE/tTA HeLa cells and

Dox+ or Dox- (mock-induced) tTA HeLa cells were seeded on a coverslip on the bottom of a dish and grown for 2 days. Cells were incubated with medium containing 10 μg/ml (125 nM) Tf labeled with both rhodamine and fluorescein. Fluorescence images were collected between 5 and 15 min of labeling with a Zeiss 63x planapochromat NA 1.4 oil immersion objective. Images were collected with a Zeiss Axiovert microscope using a Bio-Rad MRC-600 confocal attachment, with 515–545 nm fluorescein and 575 nm rhodamine emission filter sets, and 488 nm excitation. The rhodamine/fluorescein (R/F) ratio increases as the pH becomes more acidic because rhodamine fluorescence is pH-independent and fluorescein fluorescence is quenched as the pH decreases. Image processing was performed as described previously (Dunn et al. 1994). For each optical plane the ratios of R/F fluorescence were calculated for each pixel whose intensity for both fluorophore channels was above background. Histograms of pixel frequency of R/F ratio values were constructed. To confirm the pH-sensitivity of the probe, data were collected from cells in which the endosomes were alkalinized by incubating with 40 mM methylamine.

RESULTS

Identification of the HFE–LAMP/tTA HeLa Clone -

The tetracycline-responsive promoter system developed by Gossen and Bujard (Gossen and Bujard 1992) was used to create a cell line in which HFE expression could be tightly controlled. The expression of TfR1, HFE and Ft in this new cell line was compared against the previously characterized cell line fWTHFE/tTA HeLa (Gross et al. 1998; Roy et al. 1999; Roy et al. 2000) to confirm that the HFE–LAMP was functional; that is, its ability to decrease intracellular Ft levels. HFE expression was induced in cells in the absence of Dox (Dox-; Figure 2.1). HFE migrates as a broad heterogeneous band presumably due to heterogeneity in glycosylation, which has been noted previously (Gross et al. 1998; Riedel et al. 1999; Salter-Cid et al. 1999; Ben-Arieh et al. 2001). The apparent molecular mass of HFE–LAMP is slightly lower than fWTHFE because the LAMP1 cytoplasmic domain is only 11 amino acids compared with the 27 amino acids comprising the HFE cytoplasmic domain (19 amino acids) with a FLAG-tag epitope (8 additional amino acids) of the fWTHFE. It too migrates as a broad band that appears even broader than the wild-type HFE, perhaps due to the increased turnover of the lysosomally directed chimera. Both cell lines showed a decrease in the levels of Ft (19 and 21 kDa) in cells expressing fWTHFE and HFE–LAMP (Figure 2.1). These results imply that expression of HFE reduces the intracellular iron load. The iron-regulatory proteins (IRPs) modulate changes in TfR1 and Ft levels. At low intracellular iron concentrations, the IRP binds to the iron response element (IRE) stem loop structure in the 5′ untranslated region of Ft mRNA, blocking translation and lowering Ft levels. The

same reduction in intracellular iron load results in the binding of the IRP to the 3′ untranslated portion of the TfR1 mRNA, stabilizing the message and thus increasing the amount of TfR1 protein. In keeping with a low-iron phenotype generated by HFE, TfR1 levels increased in cells expressing fWTHFE. However, TfR1 levels did not increase in cells expressing HFE–LAMP. The lack of change of TfR1 expression in Dox-HFE–LAMP/tTA HeLa cells is probably due to increased lysosomal degradation of TfR1, as demonstrated in subsequent experiments.

Association of TfR1 and HFE in HFE–LAMP/tTA HeLa Cells -

We and others have shown previously that HFE and TfR1 can interact in cultured cells (Feder et al. 1998; Gross et al. 1998). To confirm this interaction in the HFE–LAMP/tTA HeLa cell line, immunoprecipitation experiments were carried out. Cells were immunoprecipitated with an HFE antibody (8C10 mouse anti-human HFE (Ben-Arieh et al. 2001)) followed by immunodetection with sheep anti-TfR1 and rabbit anti-HFE antibodies (Figure 2.2). In cells expressing the HFE–LAMP (Dox-), TfR1 was co-precipitated with HFE, providing evidence for the association of HFE and TfR1 in this cell line (Figure 2.2, lane 1). As expected, in cells that did not express HFE–LAMP (Dox+) no HFE–LAMP could be detected, no TfR1 was co-precipitated (Figure 2.2, lane 4) and TfR1 was only detected in the cell lysate (Figure 2.2, lane 6).

Half-life of the TfR1 in the Presence of HFE–LAMP -

To test our hypothesis that TfR1 and HFE interact in the endosome, we examined the half-life of TfR1 in the HFE–LAMP-expressing cells. If TfR1 is in fact being

targeted to the lysosome by interacting with the HFE–LAMP protein, the half-life of TfR1 should be less than its half-life in the absence of HFE–LAMP. The half-life of TfR1 was reduced from 14.7 to 7.9 h in the presence of HFE–LAMP (Figure 2.3 A&C). This reduction in half-life for the TfR1 supports the idea that HFE–LAMP is sorting TfR1 to the lysosome where it is being degraded, and this process is faster than the degradation rate of the typical recycling TfR1. Such a reduction in the half-life for TfR1 is not due to the association of TfR1 with the wild type HFE. We observed the opposite of what we measured in HeLa cells expressing wild-type HFE. In the fWTHFE/tTA HeLa cells, the half-life of TfR1 was doubled compared with these cells with fWTHFE turned off (Figure 2.3 B&C). The latter was a surprising result, in that we have previously shown that the expression of HFE in these cells has no effect on endocytosis, exocytosis or cellular distribution of the TfR1 (Roy et al. 1999). This result implies, however, that the interaction of HFE and TfR1 stabilized the TfR1 protein in some way.

Incubation of the HFE–LAMP/tTAHeLa cells with super-physiological levels of diferric-Tf (3 mg/ml) was used to determine whether Tf could increase the half-life of the TfR1 by competing for binding to TfR1. Tf competes with HFE for binding to TfR1, determined by surface plasmon resonance-based assays using the ectodomains of these proteins (Lebron et al. 1998; Lebron and Bjorkman 1999; Lebron et al. 1999; West et al. 2001). Our approach would also address whether the HFE–LAMP–TfR1 complex was getting to the cell surface prior to trafficking to the lysosome, and not being directly targeted to the lysosome after exit from the *trans*-Golgi network. If Tf competes with HFE–LAMP, then an increase in TfR1 half-life should occur. The addition of Tf resulted in an increase in the half-life of TfR1 from 9.1 to 13.6 h (Figure 2.4). This shift in half-

life upon Tf addition demonstrates that HFE and TfR1 are interacting on the cell surface and within intracellular compartments, and co-trafficking to the lysosome.

Localization of HFE–LAMP and TfR1 in HFE–LAMP/tTA HeLa Cells -

The intracellular localization of TfR1 and HFE–LAMP was examined by immunofluorescence to determine the extent of co-localization of these two proteins (Figure 2.5). In control fWTHFE-expressing cells, co-localization of HFE and TfR1 in punctate vesicles was visible (Figure 2.5A), which has been seen previously (Gross et al. 1998). Redistribution of HFE and TfR1 was seen in HFE–LAMP/tTA HeLa cells, whereby TfR1 and HFE–LAMP were detected co-localizing in perinuclear compartments (Figure 2.5B). This shift in distribution of both proteins confirms that TfR1 and HFE–LAMP are interacting within these cells and that the complex has a different trafficking pattern than control cells. Efforts to visualize TfR1 in lysosomal compartments show limited overlap, most likely due to the rapid degradation of the TfR1 once it reaches the lysosome (results not shown).

HFE Does Not Increase the pH of the Endosome -

Previous studies indicate that the expression of HFE in HeLa cells lowers the intracellular iron levels (Gross et al. 1998; Corsi et al. 1999; Riedel et al. 1999; Roy et al. 2002). Since HFE was capable of interacting with TfR1 in endosomal compartments, we wanted to determine which step of Tf-mediated iron uptake and release was altered by HFE. Tf-mediated Fe uptake by cells involves the binding of diferric-Tf to TfR1 on the cell surface followed by internalization of the complex into a low-pH endosomal

compartment. In the endosome, iron dissociates from Tf and is reduced and transported across the endocytic vesicle. The apo-Tf–TfR1 complex is recycled back to the cell membrane. The pH of the endosome regulates the efficiency of iron release from Tf (Sipe and Murphy 1991). HFE could alter iron homoeostasis of the cell by decreasing the acidification of the endosome, thereby lowering the efficiency of iron release from Tf.

The pH-sensitive fluorophore, fluorescein, bound to diferric-Tf in combination with a pH-insensitive probe, tetramethylrhodamine-labeled Tf, was used to measure intracellular pH of the HFE/TfR1-positive compartments. For these experiments, fWTHFE/tTA HeLa cells were used under both Dox- and Dox+ conditions, corresponding to with and without HFE expression, respectively. The R/F ratio of Tf-containing endosomes in both conditions was subsequently measured using microscopy (Dunn et al. 1994). To examine the pH of Tf-containing recycling endosomes, which accumulate in the pericentriolar region of cells, the R/F ratio of the pericentriolar endosomes was measured in two separate confocal planes from HFE-expressing and non-expressing cells (Figure 2.6A). The distribution of R/F ratios in these endosomes was unchanged by expression of HFE, indicating that HFE expression does not significantly alter endosome acidification. The rate-limiting step in return of Tf to the plasma membrane is movement from the recycling endosomes to the cell surface, and therefore Tf accumulates in recycling endosomes. To assess the pH of all endosomal compartments containing R/F-labeled Tf (e.g. early, sorting and recycling endosomes), the R/F ratios from two separate confocal planes from HFE-expressing and non-expressing cells were determined pixel by pixel. As was the case for recycling endosomes, there was no significant difference in the R/F ratios between cells expressing

or not expressing HFE (Figure 2.6B). The failure to observe any change in the R/F ratio strongly indicates that HFE expression has no effect on acidification of any of the Tf-containing endosomes. The R/F ratio in cells incubated with 40 mM methylamine, which alkalinizes endosomes, was significantly decreased, consistent with an increase in endosomal pH and thereby confirming the sensitivity of the assay (results not shown).

The Effect of HFE on Iron Dissociation from Tf within Endosomes -

HFE could be acting within the endosomal compartments to inhibit the release of iron from Tf. Previous studies by Murphy, Aisen and co-workers (Bali et al. 1991; Sipe and Murphy 1991) showed that at reduced pH, TfR1 facilitates the release of iron from Tf. The association of HFE with TfR1 could prevent this conformational change in TfR1. The amount of iron remaining bound to Tf within the endosome was measured by separation of apo-, monoferric- and diferric-Tf species on 6 M urea/PAGE gels as described by Makey and Seal (Makey and Seal 1976). These gels can separate the different forms of Tf molecules (diferric-, N-terminal monoferric-, C-terminal monoferric- and apo-Tf) into distinct bands on the basis of their different Stokes radii (Makey and Seal 1976). Taking advantage of this technique, we incubated non-transfected tTA HeLa cells and fWTHFE/tTA HeLa cells with or without inclusion of Dox in the presence of 100 nM ^{125}I-Tf for 30 min either at 37 °C to allow equilibration of Tf within the cell or at 4 °C to only allow binding to cell-surface TfR1 as a control. This Tf concentration was used because a 30% decrease in Tf-mediated ^{55}Fe uptake was seen but no difference in ^{125}I-Tf uptake was measured under these conditions (Roy et al. 1999). Surface Tf was removed by chilling cells and washing with neutral pH buffer, to remove

unbound Tf, followed by acidic buffer, to remove all surface-bound Tf. Cells were then lysed and subjected to 6 M urea/PAGE. In all the cell lines internalized Tf migrated predominantly as the apo-Tf band, with a small amount of monoferric-Tf and a very faint diferric-Tf band (Figure 2.7A). We were unable to distinguish between the two monoferric-Tf bands as described by Makey and Seal (Makey and Seal 1976). PhosphorImager analysis of the bands showed no significant difference with respect to the ratio of each Tf species from extracts of cells either expressing HFE or not. These results indicate that fWTHFE expression does not have any effect on iron dissociation from Tf within the endosome.

To demonstrate that only intracellular Tf was measured in this assay several controls were included. At 4 °C, the non-permissive temperature for endocytosis of the TfR1, the Tf that was bound to the cell surface migrated predominantly as diferric-Tf (Figure 2.7A, 4 °C). These results are consistent with results published previously that TfR1 has a high affinity for diferric-Tf, and a lower affinity for monoferric-Tf and no detectable binding to apo-Tf (Young et al. 1984; Mason et al. 1998; Yajima et al. 2000). Washing the cells with acid removes all of the surface-bound Tf (Figure 2.7B). These results indicate that acid wash is able to remove all cell-associated ^{125}I-Tf and also suggested that data obtained at 37 °C represent only the internalized ^{125}I-Tf (Figure 2.7 A&B). To exclude the possibility that acid washes could cause a loss of iron from Tf in the endosome, cells were treated with monensin, a weak base, to inhibit endosomal acidification (Yamashiro and Maxfield 1984). Monensin treatment is able to decrease the rates of ^{55}Fe-Tf uptake by 22, 33 and 34% at 20, 50 and 100 μM monensin, respectively, in comparison with the untreated cells (Figure 2.7C). The amount of inhibition of Tf-

mediated iron uptake at these concentrations of monensin was the same as that of HFE expression in cells (Roy et al. 1999). Under the same conditions, we performed the urea/PAGE gel analysis. Treatment of cells with monensin significantly increased the amounts of both monoferric- and diferric-Tf detected within the cell, indicating that we were able to observe changes in levels of iron-saturated Tf within the same range as we would expect for Dox- fWTHFE/tTA HeLa cells expressing wild-type HFE (Figure 2.7B). These results indicate that HFE does not inhibit the release of iron from Tf in endosomal compartments.

DISCUSSION

We and others have previously shown that TfR1 and HFE are capable of association soon after their synthesis in the endoplasmic reticulum and co-localize in endosomes. In this study, we demonstrate that these two proteins can remain associated as they pass through acidic vesicles inside the cell. Immunoprecipitation experiments show that a chimeric form of HFE used throughout our studies (HFE–LAMP) can co-immunoprecipitate the TfR1 when expressed in HeLa cells. The chimera is also capable of reducing Ft levels in the cells to the same extent as the FLAG-epitope-tagged wild-type form of HFE.

Alterations in the half-life of TfR1 in the HFE–LAMP/tTA HeLa cell line in the absence and presence of Dox were measured to determine whether TfR1 and HFE interacted within the endocytic compartments of the cell. The typical half-life for a normally recycling TfR1 has been reported to be anywhere from 14 to 24 h (Ward et al. 1982; Snider and Rogers 1985; Enns et al. 1988; Rutledge et al. 1991; Rutledge et al. 1994). In this cell line, the half-life was measured to be 14.7 h. When HFE–LAMP was induced by withdrawal of Dox, the half-life of TfR1 decreased to 7.9 h. Thus, interaction of TfR1 and HFE–LAMP causes a greater degradation rate for the TfR1 cycle that we have engineered than what a normally recycling TfR1 would incur. We conclude that the decrease in the TfR1 half-life is the result of its trafficking to the lysosome. Furthermore, when an excess of diferric-Tf is added to cells expressing HFE–LAMP, a longer half-life of TfR1 is observed. We conclude that competition of Tf and HFE for binding to the TfR1 allows the Tf–TfR1 complex to cycle through the endosome and circumvent the

lysosome. This result also confirms that the HFE–LAMP–TfR1 complex reaches the cell surface prior to endocytosis and sorting to the lysosome. Since lysosomal targeting is due to the motif on the HFE–LAMP protein, these results indicate that TfR1 is targeted to the lysosome through its interaction with HFE–LAMP.

Immunofluorescence was used to determine the co-localization of the TfR1 and HFE–LAMP in HeLa cells. Typically, immunofluorescence of TfR1 and HFE in HeLa cells reveals complete co-localization in a punctate pattern throughout the cell (Roy et al. 1999; Salter-Cid et al. 1999). In cells expressing HFE–LAMP, we also see co-localization of HFE–LAMP and TfR1. This localization, however, is redistributed to a perinuclear compartment distinct from the wild-type cells, confirming that TfR1 trafficking is altered due to its interaction with the HFE–LAMP.

A surprising result in our study was the observation of an increased half-life of TfR1 in fWTHFE/tTA HeLa cells. We found that the half-life of TfR1 in this cell line is nearly doubled from 25 to 44 h when fWTHFE is expressed. We have shown previously that the fWTHFE does not affect TfR1 recycling rates, or its cellular distribution (Roy et al. 1999); therefore, HFE must stabilize TfR1 in some manner. Such a stabilization could be key in determining the function of the HFE–TfR1 complex in iron homoeostasis and requires further experimentation.

Since HFE interacts with the TfR1 in endosomal compartments and specifically reduces iron uptake from Tf, we tested two hypotheses to explain the mechanism of HFE-mediated decreases in iron uptake. We found that HFE does not raise the intracellular pH of the endosome, nor does HFE inhibit the release of iron from Tf. Thus this study excludes the possibility that, in HeLa cells, HFE down-regulates Tf-associated Fe uptake

through inhibition of endosomal acidification or disruption of Fe dissociation from Tf within the endosome. Whereas competition of HFE and Tf for binding to the TfR1 at the cell surface could decrease Tf-mediated iron uptake at very low diferric-Tf concentrations, it does not explain differences in Tf-mediated iron uptake at normal diferric-Tf concentrations. We found that even sub-physiological concentrations of diferric-Tf (100 nM) allow for saturation of the TfR1 in the presence of HFE (Roy et al. 1999). If HFE expression does not change TfR1 cycling kinetics or Tf uptake, but does decrease Tf-mediated iron uptake, it must do so from the endosome. The data presented here argue that HFE does not mediate this decrease through changes in iron release from Tf. We speculate, therefore, that HFE or the HFE–TfR1 complex may act directly on the endosomal iron transporter that is responsible for the exit of iron from the endosome into the cytoplasm of the cell. Further studies will focus on this possibility.

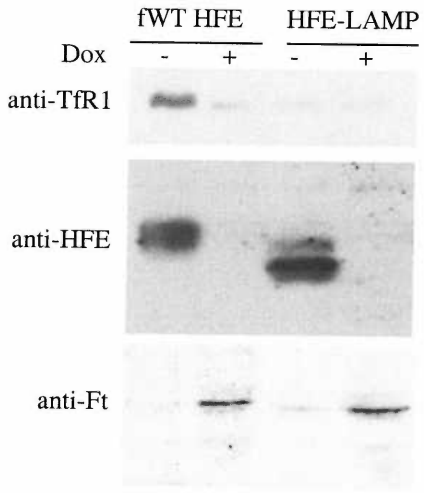


Figure 2.1. Inducible expression of HFE in fWTHFE/tTA HeLa and HFE–LAMP/tTA HeLa cells. Lysates of ~6 x 10^5 fWTHFE/tTA HeLa and HFE–LAMP/tTA HeLa cells, induced (Dox-) or uninduced (Dox+) for HFE expression, were run on a 12% denaturing acrylamide gel under reducing conditions. Proteins were transferred to nitrocellulose and detected with sheep anti-TfR1 (1:10,000), rabbit anti-HFE (1:10,000) or rabbit anti-Ft (1:500), and the appropriate horseradish peroxidase-conjugated secondary antibody (1:10,000). Chemiluminescence detected ~94-, ~43- and ~19/21-kDa bands representing TfR1, HFE and Ft respectively. The increased TfR1 expression (fWTHFE cells only) and decreased Ft expression in HFE-expressing cells (Dox-) are indicative of a decrease in intracellular iron load. The difference in molecular mass of HFE in the two different cell lines is due to the removal of its cytoplasmic domain (19 amino acids) and the FLAG tag (eight amino acids) in the fWTHFE cells and the addition of only 11 amino acids of the LAMP1 cytoplasmic domain, resulting in a decrease in molecular mass compared with fWTHFE. These results are representative of three experiments without significant variation between experiments.

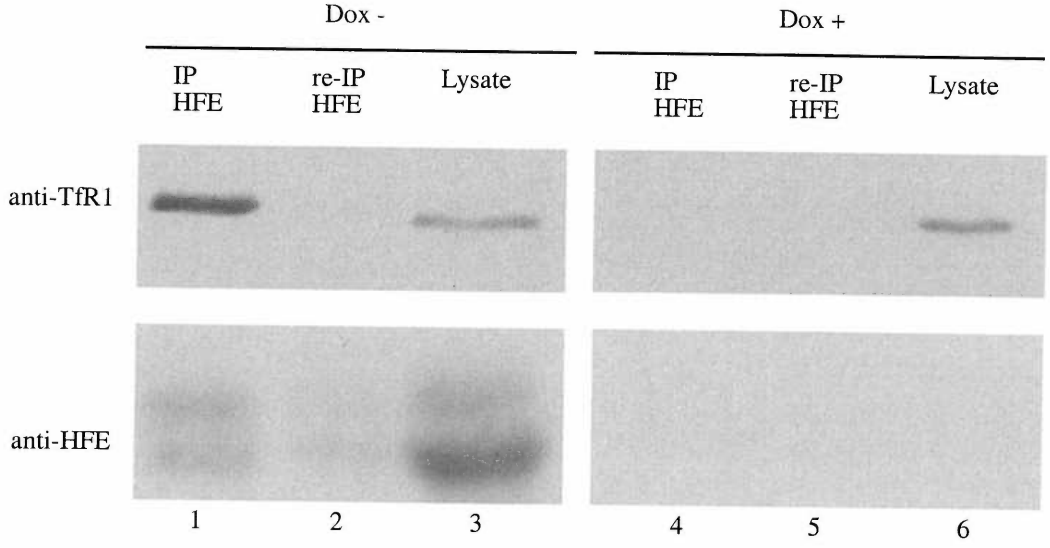


Figure 2.2. Association of TfR1 and HFE in HFE–LAMP/tTA HeLa cells. Lysates from ~6 x 10^5 HFE–LAMP/tTA HeLa Dox- or Dox+ cells were incubated with Protein G–Sepharose in the presence of 8C10 mouse anti-HFE antibody for 1 h at 4 °C. After pelleting and eluting the samples with Laemmli buffer, the eluants were subjected to SDS/PAGE. Immunodetection was carried out with sheep anti-TfR1 and rabbit anti-HFE (EX1 #137) antibodies followed by incubation with the appropriate horseradish peroxidase-conjugated secondary antibody. Chemiluminescence detected 97 kDa (TfR1) and 43 kDa (HFE) species upon immunoprecipitation (IP) with the HFE antibody, providing evidence for the association of HFE–LAMP and TfR1. Re-IP, re-immunoprecipitation control; these samples were immunoprecipitated a second time with the same antibody to confirm that all of the protein was pulled down in the initial immunoprecipitation.

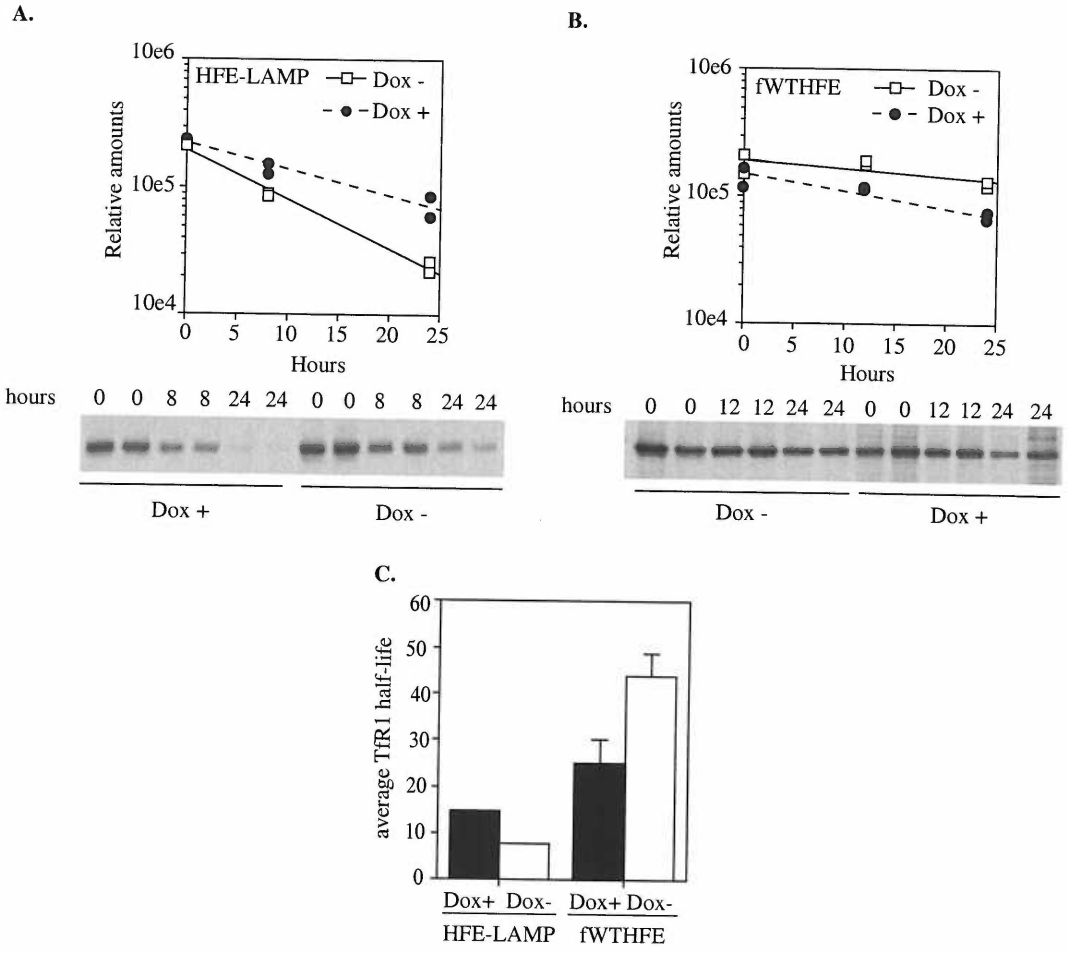


Figure 2.3. Effect of HFE on TfR1 half-life. **A**) HFE expression decreases TfR1 half-life in HFE–LAMP/tTA HeLa cells. Approximately 6 x 10^5 cells expressing HFE–LAMP (Dox-, ≤) or lacking HFE–LAMP expression (Dox+,) were labeled overnight with 50 μCi of [^{35}S]methionine/cysteine and chased for 0, 8 or 24 h with complete medium. Cell lysates were immunoprecipitated with anti-TfR1 antibody and subjected to SDS/PAGE on 8% acrylamide gels under reducing conditions. HFE–LAMP expression lowers the half-life of TfR1 from 15.1 to 7.7 h in this representative experiment as per the corresponding gel shown below. **B**) HFE expression increases TfR1 half-life in fWTHFE/tTA HeLa cells. Approximately 6 x 10^5 cells expressing fWTHFE (Dox-, ≤) and lacking fWTHFE expression (Dox+,) were labeled overnight with 50 μCi of [^{35}S]methionine/cysteine and chased for 0, 12 or 24 h with complete medium. Cell lysates were treated as described in panel **A**. fWTHFE expression increases the TfR1 half-life from 23 h (Dox+) to 50 h (Dox-) in this representative case as per the corresponding gel shown below. **C**) The half-lives of TfR1 were measured for HFE–LAMP and fWTHFE/tTA HeLa cells. These experiments were repeated three times each and the half-lives for each cell line under each condition were averaged (14.7 h for HFE–LAMP Dox+ and 7.9 h for HFE–LAMP Dox-; 25 h for fWTHFE Dox+ and 44 h for fWTHFE Dox-). Error bars cannot be seen for the HFE–LAMP samples because they were so slight. In all cases the half-life of TfR1 decreased when HFE–LAMP was expressed and increased when fWTHFE was induced.

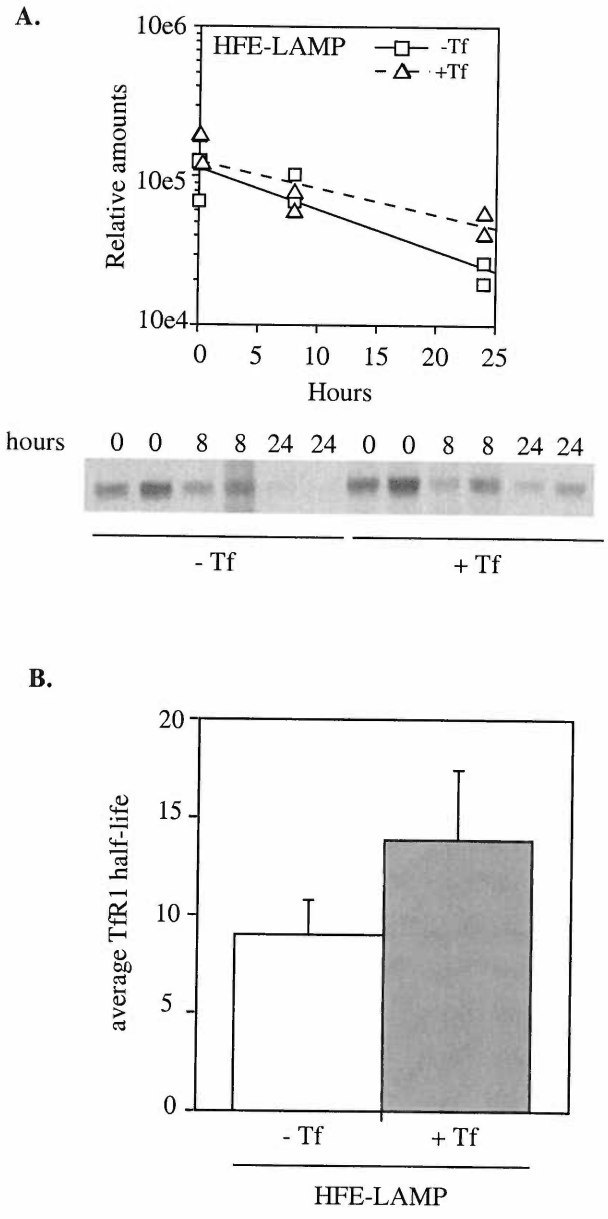


Figure 2.4. Tf competes with HFE for binding to TfR1 and increases TfR1 half-life in HeLa cells expressing HFE–LAMP. **A**) Approximately 6 x 10^5 HFE–LAMP/tTA HeLa (Dox-) cells were labeled overnight with 50 μCi of [^{35}S]methionine/cysteine. Cells were washed and either treated with 3 mg/ml diferric-Tf (Tf+; ρ) or given no treatment (-Tf; ≤) and chased up to 24 h. After immunoprecipitation with anti-TfR1, the samples were subjected to SDS/PAGE on 8% acrylamide gels under reducing conditions. Addition of Tf competes with HFE for binding to the TfR1, causing an increase in the half-life of TfR1 from 11.1 to 17.7 h in this representative experiment as per the corresponding gel below. **B**) The resulting half-lives from three experiments were averaged (9.1 h for -Tf and 13.6 h for +Tf). In all cases, the half-life of TfR1 was greater when cells were treated with Tf.

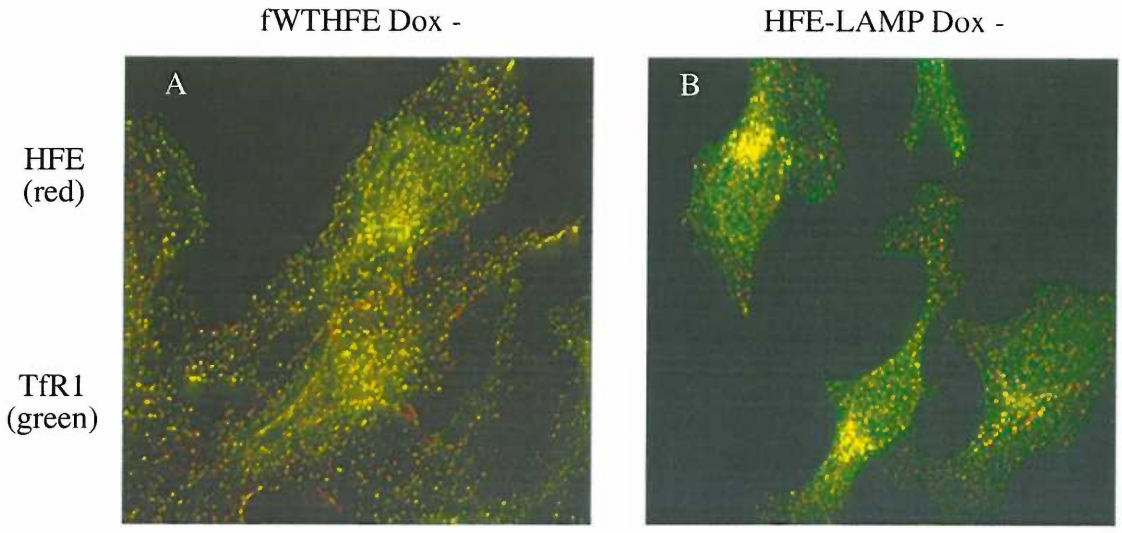


Figure 2.5. Immunofluorescence of HFE and TfR1 in HeLa cells expressing different forms of HFE. A) Co-localization of HFE with TfR1 in punctate vesicles throughout the cell in permeabilized fWTHFE/tTA HeLa (Dox-) cells stained with sheep anti-TfR1, mouse 8C10 anti-HFE, donkey anti-sheep (Alexa 488) and donkey anti-mouse (Alexa 594) antibodies. **B**) Permeabilized HFE–LAMP/tTA HeLa (Dox-) cells stained the same as in panel **A** show co-localization of TfR1 and HFE in a perinuclear region.

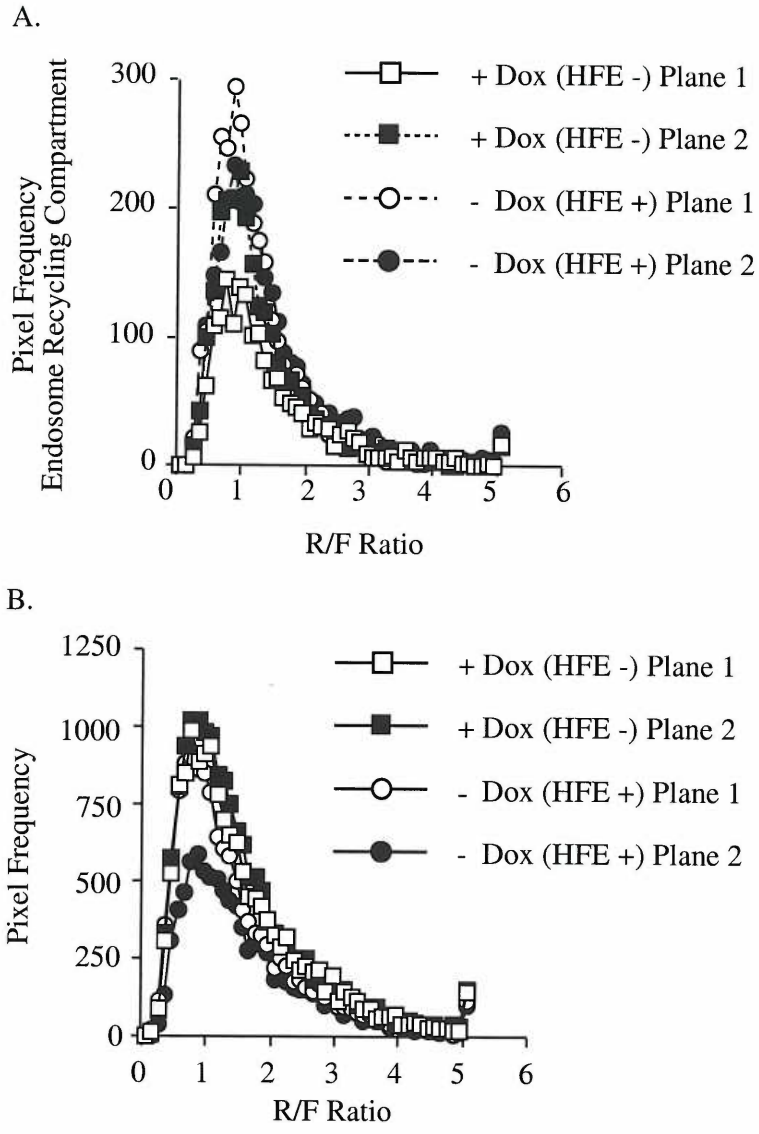


Figure 2.6. Measurement of endosome pH. Endosomal pH was quantified in two separate confocal planes of fWTHFE/tTA HeLa cells that do not (Dox+) or do (Dox-) express HFE. **A**) The R/F ratios of Tf in the recycling endosomes are shown. There is no difference between the distributions from cells expressing or not expressing HFE. There were fewer endosomes in 'plane 1' of the Dox-treated cells, accounting for the lower peak value. The R/F ratio distribution in this plane was similar to the distributions in the other planes. **B**) The R/F ratios of each pixel within the optical plane are shown. There is no difference between the distributions from cells expressing HFE or not, demonstrating that the pH of TfR1-containing endosomes is not altered by HFE expression. There were fewer endosomes in 'plane 2' of the cells not treated with Dox, accounting for the lower peak value. The R/F ratio distribution in this plane was similar to the distributions in the other planes. In all cases, only pixels above the background levels for both fluorophores were analyzed. These measurements were performed in duplicate. The data presented are from a representative of three experiments.

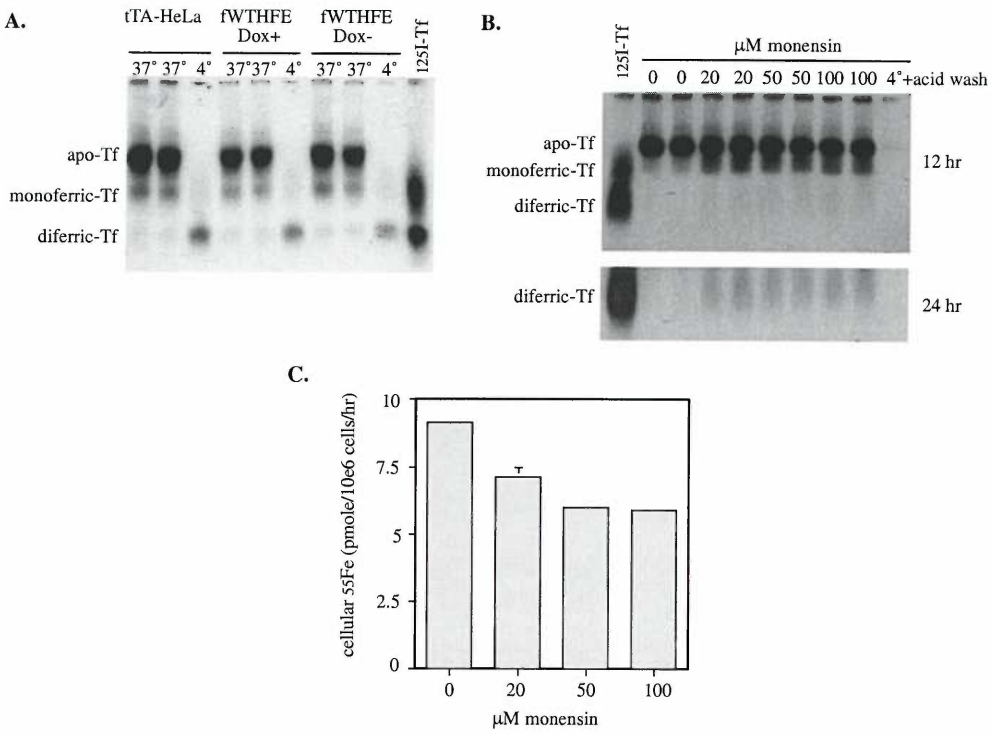


Figure 2.7. Effect of fWTHFE expression on Tf-associated iron dissociation within endosomes. A) Urea/PAGE analysis. fWTHFE/tTA HeLa cells (Dox+ and Dox-) and tTA HeLa cells were incubated in presence of 100 nM ^{125}I-Tf at 37 °C for 30 min to allow ^{125}I-Tf to bind to cell-surface TfR1, endocytose and cycle. This was followed by an acid wash to remove the fraction of cell surface-associated ^{125}I-Tf. Cell lysates were separated on urea/PAGE. The gels were fixed, dried and exposed to X-ray film. The samples were run in duplicate. In the meantime, we also ran two parallel controls of which one was cell-surface bound ^{125}I-Tf at 4 °C without acid wash and the other one was ^{125}I-Tf alone. **B**) Effects of monensin treatment on Tf-associated iron dissociation within endosomes. tTA HeLa cells were pretreated with different concentrations of monensin (0, 20, 50 and 100 μM) for 30 min at 37 °C, followed by addition of ^{125}I-Tf to the final concentration of 100 nM with the same concentrations of monensin. Cells were incubated for another 30 min at 37 °C, subjected to acid wash, run on urea/PAGE and exposed to X-ray film as above. All the samples were run in duplicate. Two more control samples were also included: (i) ^{125}I-Tf alone without any manipulation and (ii) tTA HeLa cells incubated with ^{125}I-Tf at 4 °C, followed by acid wash to remove the surface-bound ^{125}I-Tf to confirm that the samples incubated at 37 °C represented the true status of Tf within the endosome. The positions of apo-Tf, monoferric-Tf and diferric-Tf are marked on the left. As the diferric-Tf bands are weak for all the samples, a portion of an image from a longer exposure (24 h) is presented in the lower panel. **C**) Effect of monensin treatment on ^{55}Fe-Tf uptake. To further evaluate the effects of monensin on endosomal acidification, we examined its effects on the rate of ^{55}Fe-Tf uptake. The same cells were used and the experimental protocol was exactly the same as for panel **B** except that ^{55}Fe-Tf was used instead of ^{125}I-Tf. After a 30 min incubation at 37 °C, cells were subjected to acid wash and the intracellular ^{55}Fe was measured. The rate of ^{55}Fe-Tf uptake is expressed as pmole of ^{55}Fe/10^6 cells per h.

CHAPTER 3

Mechanisms of HFE-induced Regulation of Iron Homeostasis: Insights from the W81A HFE Mutation

An-Sheng Zhang, **Paige S. Davies**, Hanqian L. Carlson, and Caroline A. Enns

Department of Cell and Developmental Biology, Oregon Health & Science University, Portland, Oregon, 97239-3098, USA

Published in *Proceedings of the National Academy of Sciences U. S. A.* (2003) **100(16)**: 9500-9505

‡This work was supported by NIH DK 54488 (CAE). PSD and HLC were supported in part by the National Institutes of Health Training Grants T32-AI07472 and T-32-HL00781, respectively.

SUMMARY

The mechanisms by which the hereditary hemochromatosis protein, HFE, decreases transferrin-mediated iron uptake were examined. Coimmunoprecipitation studies using solubilized cell extracts demonstrated that transferrin (Tf) competed with HFE for binding to the transferrin receptor 1 (TfR1) similar to previous *in vitro* studies using soluble truncated forms of HFE and the TfR1. At concentrations of Tf approaching those found in the blood, no differences in Tf binding to cells were detected, which is consistent with the lower binding constant of HFE for TfR1 versus Tf. However, cells expressing HFE still showed a decrease in Tf-mediated iron uptake at concentrations of Tf sufficient to dissociate HFE from the TfR1. These results indicate that the association of HFE with TfR1 is not essential for its ability to lower intracellular iron stores. To test the effect of HFE on lowering intracellular iron levels independently of its association with TfR1, a mutated HFE (fW81AHFE) that shows greatly reduced affinity for the TfR1 was transfected into tetracycline-controlled transactivator HeLa cells. HeLa cells expressing fW81AHFE behaved in a similar manner to cells expressing wild-type HFE with respect to decreased intracellular iron levels measured by iron regulatory protein gel-shift assays and ferritin levels. The results indicate that HFE can lower intracellular iron levels independently of its interaction with the TfR1.

INTRODUCTION

Type 1 hereditary hemochromatosis (HH) is an autosomal recessive disorder with the clinical manifestation of severe iron overload in specific organs, including liver, heart, and pancreas. It is the most common inherited disease in people of northern European descent, affecting 1 in 400 individuals (reviewed in refs. (Andrews 1999) and (Enns 2001)). The HH gene encodes an atypical MHC class I-related protein named HFE. About 85% of Type 1 HH patients are homozygous for a single base pair mutation that results in a substitution of tyrosine for cysteine at amino acid position 260 (C260Y) (Feder et al. 1996). The C260Y mutation of HFE prevents the formation of a disulfide bond in its α−3 domain and abrogates its association with β2-microglobulin (β2m) as well as its subsequent trafficking to the cell surface (Feder et al. 1997; Waheed et al. 1997). The importance of functional HFE–β2m heterodimers for iron homeostasis is supported by the studies using gene-targeted animals. HFE (-/-) (Zhou et al. 1998), β2m (-/-) (Rothenberg and Voland 1996; Santos et al. 1996), and β2m (-/-)-HFE (-/-) double knockout mice (Levy et al. 2000) show similar patterns and extents of iron overload as individuals with HH.

Although HFE is expressed in most tissues (Feder et al. 1996), regulation of iron absorption in the intestine by HFE has been presumed to be the critical step to maintain the iron homeostasis (reviewed in ref. (Andrews 1999)). In HFE (-/-) knockout mice, intestinal iron absorption by divalent metal transporter 1 (DMT1) is enhanced (Oates et al. 2000a) and duodenal uptake of plasma transferrin (Tf) is impaired, but iron uptake by the kidney and liver is normal (Trinder et al. 2002).

How HFE regulates iron absorption at the molecular level still remains elusive. *In vivo* and *in vitro* studies show that HFE forms a complex with the Tf receptor (TfR1) at neutral pH (Feder et al. 1998; Lebron et al. 1998; Waheed et al. 1999). The binding sites on TfR1 for HFE and Tf overlap (West et al. 2001), which explains the observation that HFE is able to lower the apparent binding affinity of TfR1 to diferric-Tf (Feder et al. 1998; Gross et al. 1998). These results predict that, at circulating concentrations of diferric-Tf (10 μM), no HFE should be binding to the TfR1. Indeed, previous studies indicate that even at 100 nM to 1 μM Tf, no difference in Tf uptake was measured in cells expressing HFE compared with cells not expressing HFE (Roy et al. 1999). Despite this, cells expressing HFE have 30% less iron accumulation (Roy et al. 1999).

In this study we used a mutated HFE (W81A), which has a 5,000-fold lower affinity for the TfR1 than the WT HFE, to determine the effect of the HFE/TfR1 complex on Tf-mediated iron uptake. tTA HeLa cells expressing an epitope-tagged WT (fWT)-, fW81A-, or fC260Y-mutated HFE under the tight control of a tetracycline-repressible promoter were used. HFE expression was repressed in the presence of doxycycline (Dox, a tetracycline analog). Surprisingly, we found that the decrease in Tf-iron uptake upon HFE expression is independent of HFE binding to the TfR1.

MATERIALS AND METHODS

Cell Line Preparations and Western Analysis -

Both W81A and C260Y mutations of human HFE were made by using QuikChange XL Site-Directed Mutagenesis kit (Stratagene) following the manufacturer's instructions. The previously made fWTHFE/pUHD10-3 construct with a C-terminal FLAG tag (f) was used as a template (Gross et al. 1998). The primers used for the W81A mutation are 5'-GGG ATC ACA TGT TCA CTG TTG ACT TCG CGA CTA TTA TGG-3' (forward) and 5'-CCA TAA TAG TCG CGA AGT CAA CAG TGA ACA TGT GAT CCC-3' (reverse). The primers used for the C260Y mutation are 5'-GCA GAG ATA TAC GTA CCA GGT GGA GCA CC-3' (forward) and 5'-GGT GCT CCA CCT GGT ACG TAT ATC TCT GC-3' (reverse). The W81A and C260Y mutations in the resulting constructs were confirmed by DNA sequencing. No other new sequence changes were detected. Cells were transfected as described (Gross et al. 1998) and maintained in DMEM supplemented with 10% FBS, 400 μg/ml G418 (Geneticin, Calbiochem), and 300 ng/ml puromycin with or without 1 μg/ml Dox.

The expression of HFE in both fW81AHFE/tTA and fC260YHFE/tTA HeLa cells was found tightly controlled by Dox by Western blot analysis using rabbit anti-HFE antibody (1:10,000 dilution, #137, gift from J. Feder). These cell lines and our previously developed cell line fWTHFE/tTA HeLa (Gross et al. 1998) were all tested for the levels of β2m and Ft after turning off the HFE expression for different time intervals by adding Dox. The antibodies used were mouse anti-β2m antibody (1:1,000 dilution) and rabbit anti-Ft antibody (1:500 dilution, DAKO). The appropriate secondary

antibodies conjugated to horseradish peroxidase were applied, and the chemiluminescence kit (Super Signal, Pierce) was adopted to develop according to the manufacturer's directions. For all of the above analysis, 30 μg of protein from whole cell lysates were subjected to SDS/12% PAGE and transferred to nitrocellulose.

Immunoprecipitation –

Immunoprecipitation was performed as described (Gross et al. 1998). Mouse monoclonal antibodies, M2 to the FLAG epitope (Sigma) and 8C10 (gift of Dr. Rachel Ehrlich, Tel Aviv University, Tel Aviv, Israel), were used for immunoprecipitation of HFE. A mouse monoclonal anti-human TfR1 antibody 4091 (gift of Dr. Vonnie Landt, Washington University, St. Louis, MO) was used for TfR1.

Immunofluorescence -

Immunofluorescent analysis of HFE and TfR1 localization in both fW81AHFE/tTA and fWTHFE/tTA HeLa (Dox- and Dox+) cells was processed as described (Gross et al. 1998). Mouse anti-HFE (8C10, 1:1,000 dilution in blocking buffer) or sheep anti-TfR1 (1:800 dilution) antibody was used as the primary, and Alexa 594 donkey anti-mouse (1:250 dilution) or Alexa 488 donkey anti-sheep (1:500 dilution, Molecular Probes) was used as the secondary. Cells were mounted with ProLong Antifade (Molecular Probes) and imaged by the Oregon Health & Science University/Medical Marketing International Research Core Facility with the Applied Precision Deltavision image restoration system on a Nikon microscope (x60 oil immersion lens).

^{125}I-Tf Binding and ^{55}Fe-Tf Uptake -

Human diferric-Tf was labeled with Na[^{125}I] by using lactoperoxidase as described (Warren et al. 1997; Warren et al. 1998). ^{125}I-Tf binding assays of fW81AHFE/tTA and fWTHFE/tTA HeLa cells under both Dox+ and Dox- conditions were performed as described (Warren et al. 1997; Warren et al. 1998). All of the samples were assayed in triplicate. Results were expressed as fmole ^{125}I-Tf per 10^6 cells. ^{55}Fe loading onto human apo-Tf and the ^{55}Fe-Tf uptake were the same as described (Roy et al. 1999).

Electrophoretic Mobility Shift Assay -

Iron regulatory protein (IRP) binding to Ft iron-responsive element (IRE) mRNA was performed and quantitated as described (Eisenstein et al. 1993).

RESULTS

A series of experiments were done to reconcile the fact that, at concentrations of Tf that can effectively compete with HFE for binding to TfR1, less iron accumulates in cells expressing HFE. The rates of ^{55}Fe-Tf uptake and ^{125}I-Tf binding at various concentrations of human diferric-Tf were examined to compare the effect of HFE on Tf binding and Tf-mediated iron uptake. One way to account for these results would be if HFE has to be released from TfR1 by Tf to lower transferrin-mediated iron uptake into cells. A mutated HFE (fW81AHFE), which has greatly reduced affinity for TfR1 but is still able to bind β2m and be transported to the cell surface, was stably transfected into cells to test this possibility.

HFE Decreases Tf-Mediated Iron Uptake Independent of Its Competition with Tf for Binding to the TfR1 -

The W81AHFE mutation was originally designed to measure the contribution of specific amino acids to the HFE-TfR1 interface (Lebron and Bjorkman 1999). This previous study showed that the affinity of HFE for TfR1 decreased 5,000-fold with the W81A mutation. The W81AHFE is still able to bind β2m and form a heterodimer. The C260YHFE mutation, the most common mutation associated with HH, was generated as a control. This mutation disrupts HFE's association with β2m and TfR1 and does not alter the iron status of cells (Parkkila et al. 1997b; Feder et al. 1998; Lebron et al. 1998). W81A and C260Y mutations in HFE with a FLAG epitope tag were generated and stably transfected into the tTA HeLa cell line. The expression of HFE was repressed in the

presence of Dox (Dox+). The binding of ^{125}I-Tf to fW81AHFE and fWTHFE cells at 10, 20, and 100 nM Tf was measured. No inhibition of Tf binding to fW81AHFE cells or the control fC260YHFE cells (data not shown) was detected at any concentration of Tf (Figure 3.1A). In contrast, fWTHFE cells showed decreased ^{125}I-Tf binding at subsaturating concentrations of Tf. In agreement with plasmon resonance binding studies using truncated forms of the TfR1 and HFE, the lowered binding of Tf to cells expressing HFE at low concentrations but not at high concentrations of Tf is consistent with HFE and Tf competing for overlapping binding sites on TfR1.

Lower Tf binding by the fW81AHFE/tTA HeLa cells compared with fWTHFE/tTA HeLa cells under Dox repression of HFE expression was measured (Figure 3.1A). We attribute the lower binding to clonal variation and not to experimental variation or leakiness of the cells. This result was repeatable and did not appear to be caused by the inability to turn off expression because, as with the fWTHFE-expressing cells, no HFE could be detected by Western analysis when cells are incubated in the presence of 1 μg/ml Dox.

Coimmunoprecipitation was used to examine whether Tf is able to displace HFE from the TfR1/HFE complex. Cell lysates from [^{35}S]methionine-cysteine labeled cells were incubated with different concentrations of diferric-Tf (0–10 μM) for 30 min at 4°C, followed by immunoprecipitation of HFE or TfR1. A significant amount of HFE dissociated from TfR1 at the concentration of diferric-Tf as low as 10 nM (Figure 3.1B). The total amounts of TfR1 and HFE were unchanged. The same amount of TfR1 was immunoprecipitated by the anti-FLAG antibody as by the anti-TfR1 antibody, which indicated a relatively stable TfR1/HFE complex was formed and all of the TfR1 was

associated with HFE. However, the reverse was not true. The monoclonal antibody to TfR1 appeared to compete with the binding of HFE to TfR1 and little HFE was isolated with TfR1. The addition of Tf to the extracts followed by immunoprecipitation with anti-FLAG antibody and the ^{125}I-Tf binding studies indicated that Tf was able to displace HFE from the TfR1 in the context of the cell and cell lysates. The concentrations of Tf needed to displace HFE from the TfR1 were consistent with those of the competition studies between the ectodomain of HFE and Tf for binding to the ectodomain of TfR1 as measured by surface plasmon resonance (Lebron et al. 1998; West et al. 2001).

fW81AHFE could interact with TfR1 in the endosome. Isolation of fW81AHFE at pH 5.5–7.4 failed to detect TfR1 in the immunoprecipitates (Figure 3.1C). These results are not surprising in that an amino acid substitution of one neutral amino acid for another would not be expected to impart a pH-sensitive change in binding. The fact that Tf remains associated with TfR1 at endosomal pH and that no interaction between fW81AHFE and TfR1 was detected at low pH rules out the possibility that fW81AHFE exerts its effect on Tf-mediated iron uptake into cells through interaction with the TfR1 in the endosome.

The amount of ^{55}Fe taken up into cells via Tf at concentrations of diferric-Tf that saturate binding to the TfR1 (100 nM to 2 μM) was examined to determine whether the fW81AHFE cells showed altered Tf-mediated iron uptake. They exhibited a similar extent of inhibition (40% decrease) on Tf-meditated iron uptake compared with cells expressing fWTHFE at all of the examined Tf concentrations (0.1, 0.5, 1, and 2 μM) (Figure 3.2). These results suggest that HFE can function to lower iron levels in cells even in the absence of its association with TfR1.

fWTHFE- and fW81AHFE-Expressing Cells Show Decreased Intracellular Iron Levels -

We used three different methods to determine whether the cells expressing the different forms of HFE became iron deficient when HFE expression was induced. ^{55}Fe-Tf uptake over longer periods was measured to determine steady state levels of Tf-delivered iron in cells. Cells were grown for 20 h in complete medium supplemented with 25 nM to 5 μM ^{55}Fe-Tf, followed by acid wash to remove the membrane-associated ^{55}Fe-Tf. Consistent with the short-term uptake studies, cells expressing both the fWTHFE and fW81AHFE had lower accumulation of ^{55}Fe (Figure 3.3A). Gel-shift analysis of IRPs was used to further study the steady state levels of intracellular iron. At low intracellular iron concentrations, IRPs bind to the stem loop structure of the IRE in the untranslated region of mRNA, whereas at high intracellular iron concentrations the iron–sulfur complex in IRP1 and ubiquitin-mediated degradation of IRP2 precludes binding to the IRE stem loop structure. A ^{32}P-labeled Ft stem loop structure was used to assay IRP-binding from cell extracts of HFE expressing cell lines. Increases in the binding of IRPs to the IRE were detected in cells expressing fWTHFE and fW81AHFE (Dox-) over cells where the expression of HFE was suppressed (Dox+), indicating lower intracellular iron levels (Figure 3.3B). Quantitation of the IRP/IRE bands indicated that the ratio of IRP/IRE complex in the cells expressing versus not expressing fWTHFE was 1.7. Similarly, the ratio was 1.5 in the cells expressing versus not expressing fW81AHFE. As expected, fC260YHFE cells showed no changes in intracellular iron whether or not the fC260YHFE was expressed (ratio = 0.95). Furthermore, decreases in intracellular Ft levels were detected by western analysis when fWTHFE and fW81AHFE were induced by Dox withdrawal (Figure 3.3C). In contrast, the induction of

fC260YHFE had no effect on intracellular Ft levels consistent with its lack of function. These results are consistent with the low iron phenotype identified by gel-shift analysis and represent three independent tests for changes in the intracellular labile iron pool.

Subcellular Localization of fWTHFE and fW81AHFE -

The fW81AHFE/tTA HeLa cells gave different results in Ft expression compared with HuTu-80 cells expressing a similar construct (Ramalingam et al. 2000), so we decided to analyze the localization of HFE in fW81AHFE/tTA HeLa cells under Dox- conditions by using immunofluorescence labeling. In the duodenal epithelial cell line, HuTu-80, fW81AHFE does not alter Ft levels and is exclusively found on the cell surface (Ramalingam et al. 2000). In the fW81AHFE/tTA HeLa cell line, although fW81AHFE appeared extensively on the cell surface, it was also found in intracellular organelles positive for TfR1 (Figure 3.4). In contrast, the fluorescent pattern in fWTHFE/tTA HeLa cells showed almost a complete overlap between HFE and TfR1 containing compartments and little fWTHFE unassociated with TfR1 on the cell surface. fW81AHFE could be entering the endocytic compartments via a nonconcentrative uptake system or by interaction with another protein possessing an endocytic signal. The differences in the distribution of HFE in the HeLa and HuTu-80 cells could explain the differences seen in the effect of the fW81A mutation of HFE on iron homeostasis in that internalization may be critical for the effect of HFE in lowering intracellular iron levels.

Levels of HFE Required to Reduce Intracellular Iron Levels -

The amount of HFE required to inhibit Tf-mediated iron uptake was measured to determine the levels of HFE necessary to decrease intracellular iron levels and to determine whether HeLa cells could produce adequate amounts of β2m. A previous paper (Waheed et al. 2002) presented evidence that lack of β2m expression resulted in decreased iron uptake into cells, whereas when β2m was expressed, more iron was taken up into cells. To alter the levels of HFE in cells, Dox was added to the culture medium of fW81AHFE, fC260YHFE, and fWTHFE/tTA HeLa cells to turn off their expression at different time points (Figure 3.5A). The HFE protein levels are inversely correlated to the intervals of Dox inclusion in the medium with the highest at no Dox addition (0 h) and lowest with Dox present continuously (+). Visually, both fW81AHFE and fWTHFE show a similar half-life. In contrast, fC260YHFE disappears quickly after the addition of Dox, indicating that this misfolded form of HFE is more rapidly degraded. In addition to HFE, the levels of β2m and Ft were also visualized to examine the iron status of the cells and determine whether β2m levels paralleled increases in HFE levels (Figure 3.5A). Increases in β2m corresponded to increases in fW81AHFE or fWTHFE despite the fact that neither of these cell lines were transfected with β2m. This result could be due to the possibility that HFE expression itself could induce the expression of β2m. Alternatively, the expression of HFE and its association with β2m could result in more retention of β2m within the cells. Because β2m does not have a cytoplasmic domain, excess β2m would be secreted. In either case, HeLa cells appear to have sufficient amounts of β2m to complex with the transfected HFE. In contrast, cells that express the fC260YHFE show no measurable changes in β2m levels (Figure 3.5A). At all levels of HFE expression,

decreased Ft levels were observed in both fW81AHFE- and fWTHFE-expressing HeLa cells, but not in cells expressing the fC260YHFE.

The amounts of Tf-mediated iron uptake at different levels of HFE were measured to quantitate the effect of HFE expression on the inhibition of iron uptake. Both fW81AHFE and fWTHFE expressing cell lines showed lowered amounts of Tf-mediated iron uptake (Figure 3.5B). A striking difference between the decrease in Tf-mediated iron uptake is seen between the two cell lines. In fWTHFE/tTA HeLa cells, the extent of inhibition is proportional to the levels of HFE. In contrast, in fW81AHFE/tTA HeLa cells, Tf-mediated iron uptake remains depressed over a wide range of HFE levels. No change in Tf-mediated iron uptake was measured in fC260YHFE-transfected cells, consistent with the mutant HFE's lack of function. These results lead to the speculation that HFE interacts with another protein that is expressed at much lower concentrations in the cells than TfR1. The binding of Tf to the TfR1 would release HFE from the TfR1 and allow it to interact with the hypothetical protein, perhaps the endosomal iron transporter.

DISCUSSION

HFE down-regulates Tf-associated iron uptake and results in a low iron phenotype in a variety of cells (Corsi et al. 1999; Riedel et al. 1999; Roy et al. 1999; Salter-Cid et al. 1999; Ramalingam et al. 2000; Feeney and Worwood 2001). But the mechanism by which it down-regulates iron accumulation in cells is not well understood. Previous studies demonstrated that TfR1 has overlapping binding sites for both HFE and diferric-Tf (Lebron et al. 1999; West et al. 2001) and HFE expression lowers the binding affinity of TfR1 to diferric-Tf (Feder et al. 1998). We show that at low, subphysiological concentrations of circulating Tf (1–100 nM), Tf competed effectively with full-length HFE for binding to the TfR1. However, at physiological levels of diferric-Tf (10 μM), where no HFE would be expected to bind to TfR1, we still detected an inhibition of Tf-mediated iron uptake into cells. Both the short-term and long-term Tf-associated Fe uptake studies showed that the inhibition by HFE is independent of Tf concentration. Essentially the same extent of inhibition was observed from a low concentration (100 nM) to its physiological concentration in the serum (10 μM). Coimmunoprecipitation studies also confirmed the previous finding that inhibition of Tf binding to TfR1 by HFE only occurs when the concentration of Tf is <100 nM. These data exclude the possibility that the inhibition of Tf-associated iron uptake is through the decreased binding of diferric-Tf to TfR1 by HFE.

To further test the idea that HFE can act independently of TfR1 in decreasing iron uptake, new tTA HeLa cell lines with stably transfected fW81AHFE and fC260YHFE were generated by using the Tet-off regulatory system. The W81AHFE mutation was

originally designed to interfere with the interaction of HFE and TfR1 but still associate with β2m and fold correctly. Plasmon resonance binding studies demonstrated that the binding affinity of W81AHFE to TfR1 is 5,000-fold lower than that of the WT HFE (Lebron and Bjorkman 1999). In contrast, C260YHFE does not associate with either β2m or TfR1. fW81AHFE exhibits essentially the same effects when expressed in cells as its WT counterpart, which includes a decrease in Tf-associated iron uptake and Ft levels, and increased IRP/IRE binding. When a correlation between the levels of HFE expression and the amount of Tf-mediated iron uptake were compared, we found a distinct and interesting difference between the fWTHFE- and fW81AHFE-transfected cells. The extent of Tf-mediated iron uptake was inversely proportional to the levels of HFE in fWTHFE transfected cells, whereas in fW81AHFE transfected cells, the same amount of low levels of Tf-mediated iron uptake was observed over a wide range of fW81AHFE expression. As a control, no effect of fC260YHFE on iron homeostasis in transfected cells was detected. These results, therefore, support the hypothesis that HFE down-regulation of iron homeostasis can be independent of its association with TfR1.

Our present results are not completely consistent with a recent study in HuTu-80 cells (Ramalingam et al. 2000). Like the HeLa cells, the expression of WT HFE in HuTu-80 cells decreased intracellular Ft levels. However, unlike our present results, no decrease in Ft levels was detected when W81A HFE was expressed in HuTu-80 cells. One possible cause for this discrepancy might be the difference between the nonpolarized cells (HeLa) and polarized duodenal epithelial cells (HuTu-80) in terms of differences in the targeting of HFE in different cell types. Alternatively, the cell lines may differ in the expression of key proteins that could interact with HFE. For example, DMT1 mRNA

levels do not vary with iron loading in HeLa cells (A.-S.Z. and P.S.D., unpublished results) but do in other cell lines (Gunshin et al. 2001). HeLa cells show little iron efflux, whereas HuTu-80 cells, being an intestinal epithelial cell line, would be expected to export iron from its basolateral surface.

Other cells and cell lines do not respond to HFE expression in the same way that HeLa cells do. In monocytes from HH patients, expression of HFE results in iron accumulation rather than depletion (Montosi et al. 2000). Recent results of a monocytic cell line (THP1) transfected with HFE also indicates that expression of HFE results in iron accumulation (Drakesmith et al. 2002). The latter study demonstrated that iron accumulation within these cells was caused by a decrease in the efflux of iron from the cells. We have demonstrated that HFE inhibits Tf-mediated iron uptake into HeLa cells. If a cell line like HeLa takes up iron and does not release it through an efflux mechanism, then expression of HFE would result in a low iron phenotype. On the other hand, in cell lines where there is a large flux of iron through the cell, like monocytes and differentiated enterocytes, the net effect of HFE would be to inhibit iron efflux. Alternatively, if the binding of Tf to the TfR1 releases HFE to bind to another partner, then HFE could have different binding partners in different cell types and thus affect either the influx or efflux of iron.

In conclusion, this study excludes the possibility that in HeLa cells HFE down-regulates Tf-associated iron uptake through competition of binding to TfR1 with diferric-Tf. Instead, our results showed that HFE association with TfR1 is not required with respect to its function in the regulation of iron homeostasis. Therefore, we assume that HFE exerts its role through an uncharacterized partner(s). The challenge is to further

identify the possible binding partners of HFE and to determine how HFE affects both Tf-mediated iron uptake and iron efflux.

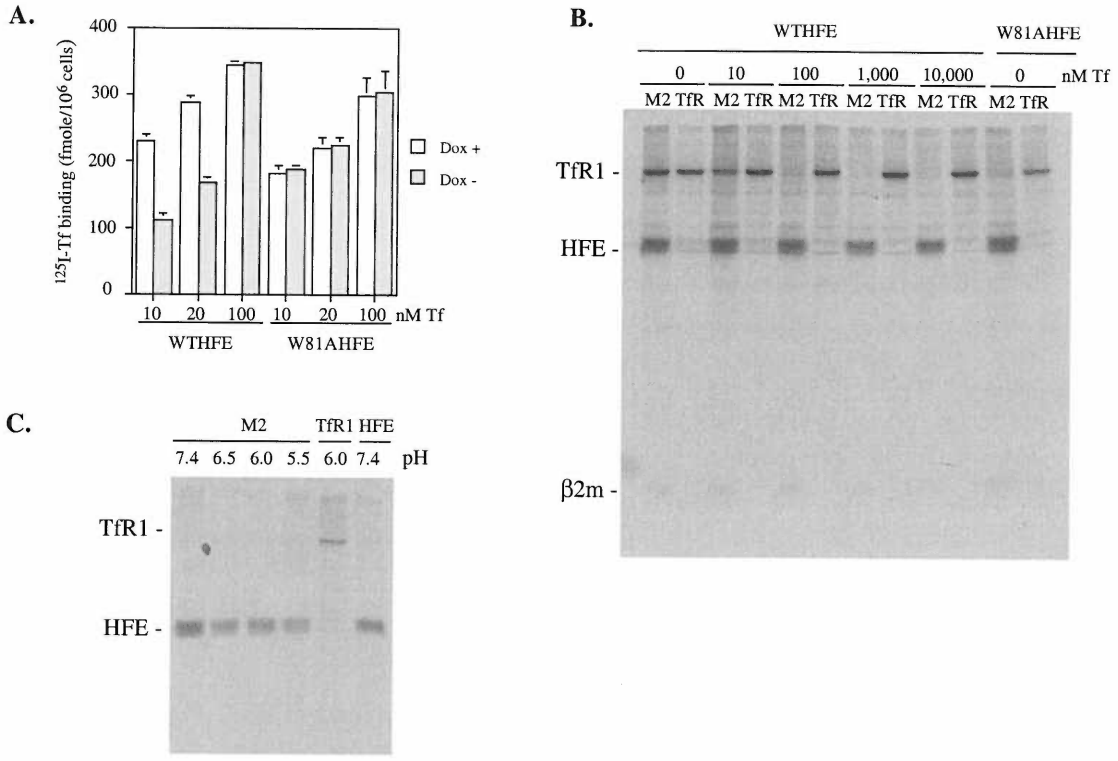


Figure 3.1. Evidence for the competition between Tf and HFE for binding to the TfR1 in intact cells and cell lysates. A) Binding of ^{125}I-Tf to cells. fWTHFE/tTA and fW81AHFE/tTA HeLa cells expressing HFE (Dox-) or not (Dox+) were incubated with 10, 20, and 100 nM ^{125}I-Tf for 90 min at 4°C to allow binding to cell surface TfRs. Excess unlabeled diferric-Tf (200x) was added to measure nonspecific binding. Samples were done in triplicate. **B)** Coimmunoprecipitation of HFE in the presence of Tf. fWTHFE/tTA HeLa cells expressing HFE (Dox-) were labeled overnight with 50 μCi/ml [^{35}S]methionine/cysteine (1 Ci = 37 GBq). Cell lysates were preabsorbed with protein A beads, and diferric-Tf was added for 30 min at 4°C, followed by immunoprecipitation with an anti-FLAG antibody (M2) for HFE or a mouse monoclonal TfR1 antibody. The experiment was repeated twice with similar results. **C)** Coimmunoprecipitation of fW81AHFE at pH 7.4, 6.5, 6.0, and 5.5. fW81AHFE/tTA cells (Dox-) were labeled with [^{35}S]methionine/cysteine as described above. For each sample, pH was kept the same throughout the entire immunoprecipitation and washes. The same antibodies were used as above except in the last lane, where a mouse monoclonal (8C10) against HFE was used as a control.

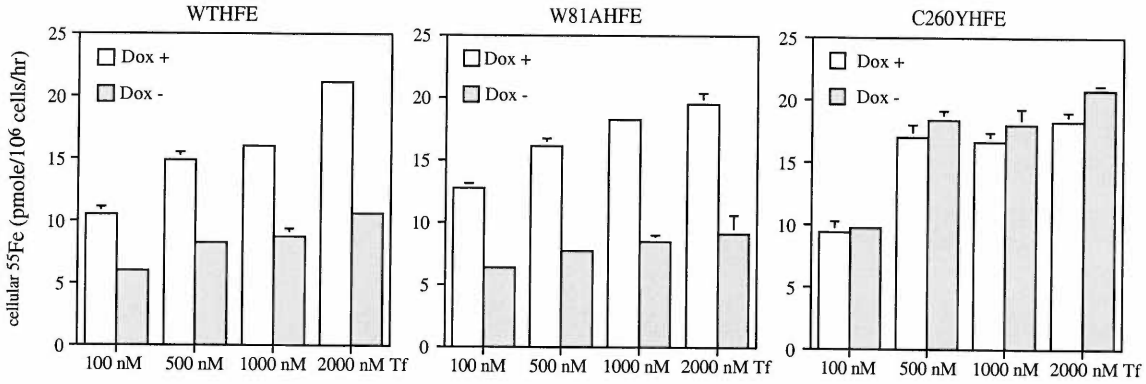


Figure 3.2. Amount of Tf-mediated ^{55}Fe uptake at different concentrations of diferric-Tf by fWTHFE/tTA, fW81AHFE/tTA, and fC260YHFE/tTA HeLa cells. ^{55}Fe-Tf was incubated with cells for 1 h at 37°C at 5% CO_2 in medium without FBS. For each cell line, cells were expressing (Dox-) or not expressing (Dox+) HFE. The experiment was repeated twice with similar results.

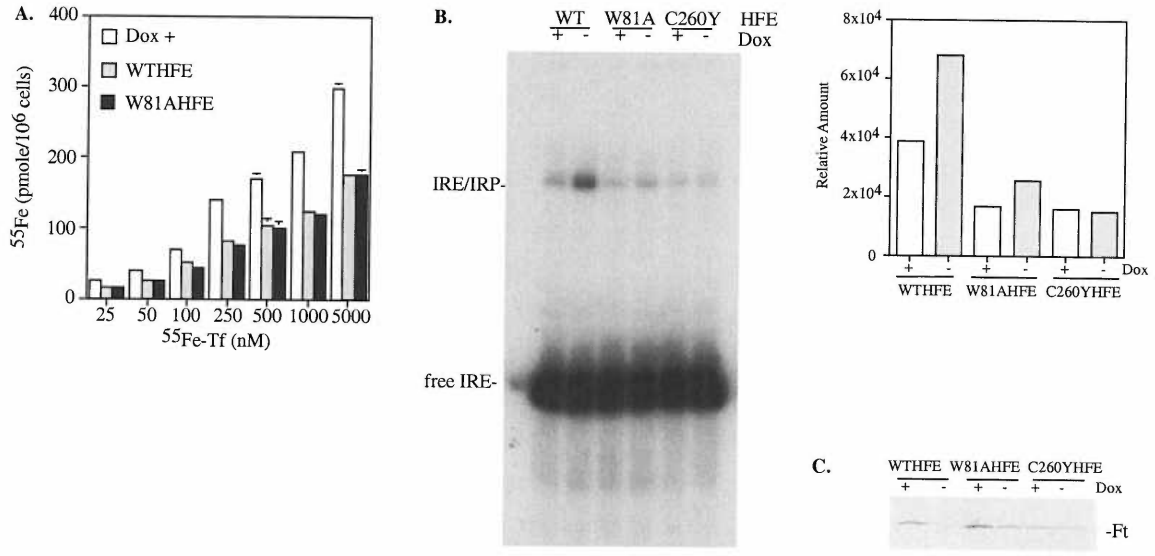


Figure 3.3. fW81AHFE/tTA HeLa cells have a low iron phenotype. A) ^{55}Fe-Tf accumulation in cells. ^{55}Fe-Tf was added to the complete culture medium of cells expressing (Dox-) or not expressing (Dox+) HFE to the final concentrations of 25, 50, 100, 250, 500, 1,000, and 5,000 nM. Cells were incubated for 20 h at 37°C at 5% CO_2. They were solubilized after acid wash at 4°C to strip off surface-bound Tf. The internal levels of ^{55}Fe were expressed as pmole per 10^6 cells. Because of the similar uptake rates between fW81AfHFE/tTA and fWTHFE/tTA HeLa (Dox+), the results were averaged together and labeled Dox+. The experiment was repeated with similar results. **B)** Gel-shift analysis of IRP binding to IREs by fWTHFE/tTA (WT), fW81AHFE/tTA (W81A), and fC260YHFE/tTA (C260Y) HeLa cell extracts. Extracts from cells expressing (Dox-) or not expressing (Dox+) HFE were incubated with ^{32}P-labeled IRE as described in Materials & Methods and subjected to PAGE. Quantitative analysis of the IRE/IRP complexes was done by using a PhosphorImager. **C)** Western blot of Ft levels using the same cell extracts as for IRP binding analysis in panel B. Thirty micrograms of protein lysate was loaded onto each lane. Blots were probed with an antibody to Ft as described in Materials & Methods. The experiments shown in panels B and C were repeated with similar results.

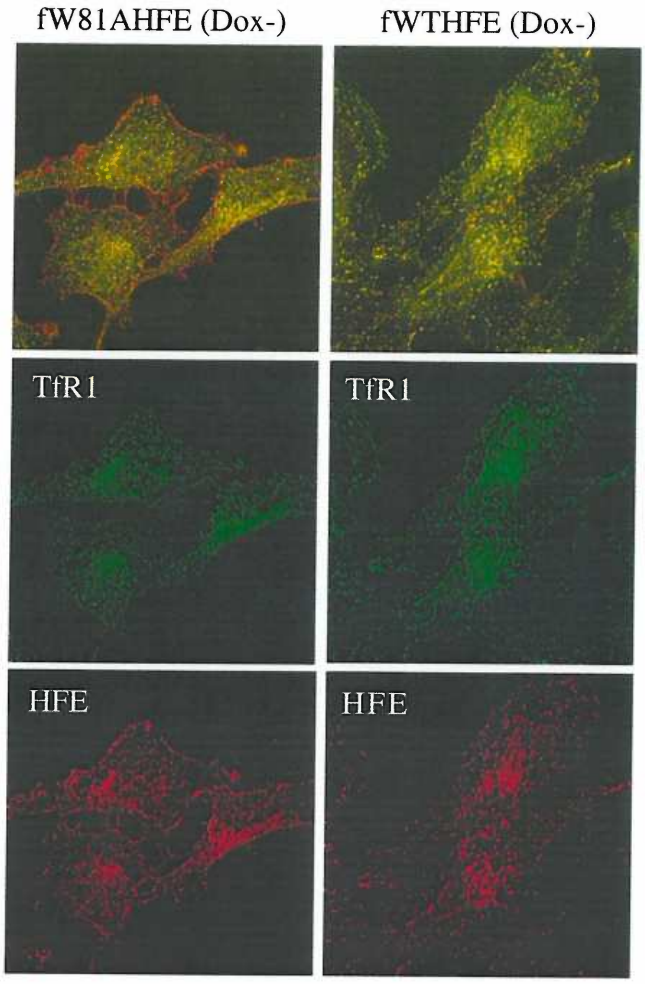


Figure 3.4. Localization of HFE and TfR1 in fW81AHFE and fWTHFE/tTA HeLa cells. Permeabilized cells were visualized with sheep anti-TfR1, mouse anti-HFE, donkey anti-sheep (Alexa 488), and donkey anti-mouse (Alexa 594) antibodies as described in Materials & Methods.

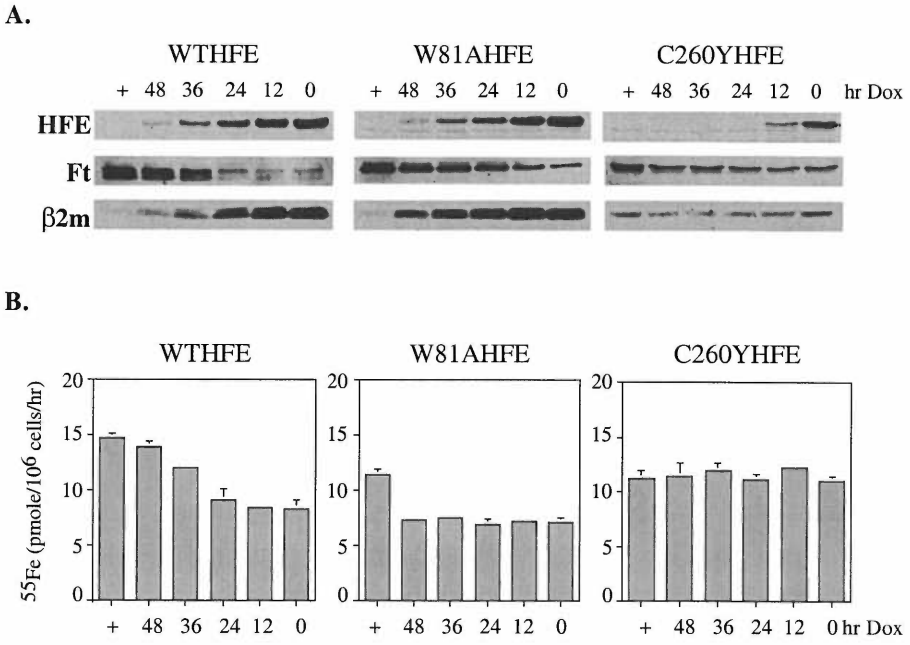


Figure 3.5. The effect of the level of HFE expression on Tf-mediated iron uptake into cells. A) Western blots of HFE, Ft, and β2m. Cell lines expressing HFE were treated for 0–48 h or maintained continuously with Dox (1 μg/ml) to turn off HFE expression. At each time point they were solubilized and subjected to western analysis with the indicated antibodies. For all of the western blots, 30 μg of protein was loaded into each lane. **B)** ^{55}Fe-Tf uptake. ^{55}Fe-Tf uptake was measured after cells were incubated with Dox to turn off HFE expression for the same time points as in A. ^{55}Fe-Tf (100 nM) was used. The results of the 1-h incubation at 37°C are presented for simplicity, although linear uptake was always observed for at least 3 h. The rates of uptake are expressed as pmole ^{55}Fe per 10^6 cells per h. Nonspecific background was performed the same as above except that the incubation was performed on ice. Samples were always in triplicate and the experiment was repeated with similar results.

CHAPTER 4

Expression of the Hereditary Hemochromatosis Protein, HFE, Increases Ferritin Levels by Inhibiting Iron Export in HT29 Cells

Paige S. Davies and Caroline A. Enns

Department of Cell and Developmental Biology, Oregon Health & Science University, Portland, Oregon, 97239-3098, USA

Published online ahead of print in *The Journal of Biological Chemistry,* March 25, 2004 (Scheduled for print in the June/July 2004 issue)

‡This work was supported by NIH DK 54488 (CAE). PSD was supported in part by National Institutes of Health Training Grant T32-AI07472.

SUMMARY

Iron is essential for life in almost all organisms and, in mammals, is absorbed through the villus cells of the duodenum. Using a human colonic carcinoma cell line that has many duodenal characteristics, HT29, we show that genes involved in intestinal iron transport are endogenously expressed. When stably transfected to express the hereditary hemochromatosis protein, HFE, these cells have increased ferritin (Ft) levels. We demonstrate that this is not due to an effect on the transferrin (Tf)-mediated iron uptake pathway, but rather due to inhibition of iron efflux from the cell. The effect of HFE was independent of its interaction with Tf receptor 1 (TfR1) as indicated by similar results using both the wild type HFE and the W81A mutant that binds TfR1 with greatly reduced affinity. HFE expression did not affect the mRNA levels of most of the genes involved in iron absorption that were tested, however, it did correspond to a decrease in hephaestin message levels. These results point to a role for HFE in inhibition of iron efflux in HT29 cells. This is a distinct role from that in HeLa and HEK293 cells, where HFE has been shown to inhibit Tf-mediated iron uptake resulting in decreased Ft levels. Such a distinction suggests a multifunctional role for HFE that is dependent upon expression levels of proteins involved in iron transport.

INTRODUCTION

Dietary iron absorption occurs in the duodenum via villus cells, a differentiated cell type involved in the transport of a variety of nutrients in the body. In mammals, iron homeostasis is controlled at the level of iron uptake rather than excretion, making iron absorption across the intestinal epithelial cell a key control point for iron homeostasis (reviewed in (Andrews 1999)). Disruptions in iron homeostasis result in a variety of diseases, the most common being Type I hereditary hemochromatosis (HH). Approximately 80% of Type 1 HH cases are due to a missense mutation in the HFE protein whereby a cysteine is mutated to a tyrosine in the α-3 domain of this MHC-related protein (Feder et al. 1996). This mutation disrupts a disulfide bond required for proper folding of HFE, preventing it from binding to β2-microglobulin and trafficking to the cell surface (Feder et al. 1997). People with Type 1 HH, an autosomal recessive disorder, absorb too much iron across the intestine, which eventually leads to excessive iron deposition in the liver, heart, and pancreas (Powell et al. 1970).

The mechanisms by which HFE regulates iron homeostasis at the cellular level are not known. HFE has been shown to interact with TfR1, but mutations in HFE that abrogate this interaction still cause changes in iron homeostasis leaving open the possibility that HFE interacts with other proteins involved in iron uptake, storage, or efflux (Zhang et al. 2003). Many of the essential proteins involved in the control of iron absorption have been identified. Ferric iron (Fe^{3+}) is reduced to the ferrous form (Fe^{2+}) prior to absorption into the duodenum. The duodenal cytochrome b (Dcytb) reductase is a strong candidate for this function (McKie et al. 2001). Evidence from two anemic

animal models bearing the same naturally occurring mutation in a divalent metal transporter, the Belgrade (*b*) rat and the microcytic anemia (*mk*) mouse, indicate that DMT1 (Fleming et al. 1997) (also known as DCT1 (Gunshin et al. 1997) and NRAMP2 (Gruenheid et al. 1999)) is involved in iron uptake across the apical portion of villus cells. Once inside the enterocyte, iron can be stored in ferritin (Ft), a cytosolic iron storage protein, or transported out of the absorptive enterocyte via the basolateral side by the ferrous iron transporter ferroportin 1 (FPN1) (Donovan et al. 2000) (also known as IREG1 (McKie et al. 2000) and MTP1 (Abboud and Haile 2000)). Evidence from the sex-linked anemia (*sla*) mouse indicates that hephaestin (Heph), an iron oxidase, facilitates the export of iron out of the villus cell for eventual incorporation into transferrin (Tf), the serum iron transport protein (Vulpe et al. 1999; Chen et al. 2004).

The effect of HFE expression on iron homeostasis in cell lines remains controversial and its effect in different cell types within organs appears to vary. In some cell lines such as HeLa, HEK293, and H1299, HFE expression results in decreased intracellular iron levels (Gross et al. 1998; Corsi et al. 1999; Roy et al. 1999; Roy et al. 2000; Wang et al. 2003), while in another other cell line such as THP-1, HFE expression leads to increased intracellular iron levels (Drakesmith et al. 2002). Similar to cell lines, lack of functional HFE in humans causes opposite effects on iron levels in different cell types of affected tissues. Early in Type I HH, Kupffer cells of the liver and intestinal enterocytes of the duodenum are iron-poor (Francanzani et al. 1989; Pietrangelo et al. 1995; Brunt et al. 2000). On the other hand, hepatocytes in the liver are iron-overloaded (Brunt et al. 2000). Notably, animal models reveal that all of these cell types have detectable levels of HFE mRNA and protein (Waheed et al. 1999; Muckenthaler et al.

2003; Zhang et al. 2004).

The aim of this study was to examine the effect of HFE expression on iron homeostasis in HT29 cells, a human colonic carcinoma cell line. These cells were chosen as a cell culture model to study the mechanism of HFE because our initial experiments demonstrated negligible expression of HFE but endogenous expression of the other genes involved in intestinal iron absorption and transport. We found that expression of HFE in this cell line led to both increased Ft and steady state iron levels. The increased intracellular iron level was not due to an effect on Tf-mediated iron uptake, as has been observed in HeLa cells expressing HFE (Riedel et al. 1999; Roy et al. 1999). Rather, HFE inhibited iron efflux from the cells, eventually leading to increased intracellular iron stores. This effect in HT29 cells, not observed in studies of HFE expressed in HeLa and HEK293 cells (Gross et al. 1998; Roy et al. 1999; Roy et al. 2000; Feeney and Worwood 2001), but shown in THP-1 cells (Drakesmith et al. 2002) suggests that HFE has multiple roles in the maintenance of iron homeostasis in the body. Furthermore, these results give insight to the observation that different cell types in the body respond differently in their iron status when HFE is not functionally expressed (Francanzani et al. 1989; Pietrangelo et al. 1995; Brunt et al. 2000).

MATERIALS AND METHODS

Cell Culture -

The human colon adenocarcinoma cell line HT29 (ATCC#38-HTB) exhibits an undifferentiated phenotype under standard growth conditions. When these cells are grown without glucose, but in the presence of galactose, on porous membrane inserts they form tight junctions and an apical microvillus brush border membrane (Godefroy et al. 1988; Godefroy et al. 1990). HT29 cells were seeded in six-well culture dishes in Dulbecco's modified Eagle's medium (DMEM) supplemented with 10% fetal bovine serum (FBS), pH 7.4 *(non-polarized)* or on cell culture inserts (0.4 micron pore size, clear polyester membrane; Costar Inc.) with DMEM without glucose, supplemented with 5 mM galactose and 10% FBS, pH 7.4 on either side of the insert *(polarized).* Cells were fed fresh medium every two days.

Iron Treatment -

Non-polarized cells: HT29 cells ($2x10^5$) were seeded in six-well culture dishes and two days later treated for 24 hours with one of the following: 10 μM $FeCl_3$ complexed to nitrilotriacetic acid (NTA)/1 mM ascorbate (Fe-Asc), 10 μM diferric-Tf (Tf), 100 μM Df, or no treatment. The pH of the medium was 7.4 for Df and Tf treatments and 5.5 for Fe-Asc treatments. The low pH was used to facilitate the function of the DMT1 transporter and mimic the acidic environment of the intestinal lumen. Untreated wells were included as controls at each pH.

Polarized cells: HT29 cells ($1x10^6$) were seeded onto 24 mm membrane inserts in 6-well dishes. After 15-18 days of culture on the inserts, they were treated for 24 hours with one of the following: 100 μM Df on both the apical and basolateral sides, 10 μM Fe-Asc on the apical side, 10 μM Tf on the basolateral side, or no treatment. The apical side of the insert contained buffer at pH 5.5 (25 mM HEPES, 140 mM NaCl, 5.4 mM KCl, 5 mM glucose, 1.8 mM $CaCl_2$) and the basolateral side contained the galactose-supplemented medium mentioned above. The cells maintained tight barriers as indicated by the maintenance of a pH differential between the basolateral and apical media.

Generation of HFE-expressing Cell Lines -

The plasmids containing either cDNA for the wild type HFE or the W81A HFE mutation, both fused to the octapeptide FLAG sequence at the C-terminus (fWTHFE/pcDNA3.1+ and fW81AHFE/pcDNA3.1+), have been previously described (Feder et al. 1997; Zhang et al. 2003). HT29 cells were seeded in 35 mm dishes at 2 x 10^5 cells/well one day prior to calcium phosphate transfection. Two hundred μl of HEPES-buffered saline solution (280 mM NaCl, 50 mM HEPES acid, 1.5 mM Na_2HPO_4, pH 7.05) was added to 200 μl of 0.25M $CaCl_2$ and 3 μg of plasmid while vortexing. The DNA solution was incubated for 20 minutes at room temperature, added to 1.6 ml fresh DMEM supplemented with 10% FBS per well, and incubated with cells for 16 hours at 37 °C, 5% CO_2. The medium was aspirated, replaced with fresh medium, and cells were incubated for an additional 48 hours. Cells were split 1:4 into 100 mm dishes with medium containing 400 μg/ml G418 (Geneticin, Calbiochem) for selection. Colonies were selected approximately 4 weeks later and screened by western analysis for

expression of HFE using rabbit anti-HFE (1:10,000 dilution, EX1 #137, gift from J. Feder) and goat anti-rabbit HRP (1:10,000 dilution, Chemicon). The resulting fWTHFE/HT29 and fW81AHFE/HT29 cells were maintained in DMEM supplemented with 10% FBS and 400 μg/ml G418.

Real-time Quantitative RT-PCR -

RNA was isolated from HT29 cells using the RNeasy RNA Isolation Kit (Qiagen) and treated with 10 units of DNaseI (Roche) to remove any contaminating genomic DNA. cDNA was synthesized using Oligo dT primers and Superscript II Reverse Transcriptase (Invitrogen). Samples were diluted 1:5 after cDNA synthesis and PCR using GAPDH primers spanning an intron/exon junction was performed to check cDNA yield and confirm the absence of genomic DNA contamination in samples containing no reverse transcriptase. Real-time qRT-PCR was carried out in triplicate on each sample for each gene in at least three independent experiments using the SYBR Green detection system on an ABI PRISM 7900 machine (Applied Biosystems). Melting curve experiments established that the fluorescent signal for each amplicon was derived from product only and not from primer dimers. The primer pairs used were designed with the Primer Express Software (Applied Biosystems), synthesized by IDT Technologies, and are shown in Table 4.1.

Data were analyzed by both the ΔC_T method described previously (Zhang et al. 2004) and the $\Delta\Delta C_T$ method (Applied Biosystems User Bulletin #2, p.11). Briefly, the threshold cycle (C_T) indicates the fractional cycle number at which the amount of amplified target reaches a fixed threshold. The difference in threshold cycles for target

(gene of interest) and reference (GAPDH) ($C_{T\text{-Target}}$ - $C_{T\text{-Reference}}$) is ΔC_T. The difference between the ΔC_T of interest and that of a baseline cDNA calibrator is $\Delta\Delta C_T$. The fold-change in mRNA expression between these two, the amount of target normalized to an endogenous reference and relative to a baseline cDNA calibrator normalized to an endogenous reference, is given by $2^{-\Delta\Delta CT}$.

In order for this calculation to be valid, the efficiencies of target and reference amplifications must be approximately equal across a range of template concentrations. All primer sets used in these studies were validated against the reference primers (GAPDH) to ensure such efficiency. Validation was determined by plotting the log of template concentration versus the ratio of the C_T of the gene of interest to the C_T of GAPDH. A slope less than or equal to 0.1 indicated an acceptably low variation between the amplification efficiencies of the target and reference.

Western Blot Immunodetection -

HT29 cells were lysed with NET-Triton (150 mM NaCl, 5 mM EDTA, and 10 mM Tris (pH 7.4) with 1% Triton X-100) to make whole cell extracts, and protein concentrations were determined by BCA assay (Pierce). Whole cell lysates (30 μg) were diluted with 2X Laemmli buffer (125 mM Tris-HCl (pH 6.8), 4% SDS, 20% glycerol, and 10% 2-mercaptoethanol) (Laemmli 1970), boiled for 5 minutes, subjected to electrophoresis on 12% SDS-polyacrylamide gels under reducing conditions, and transferred to nitrocellulose. Immunoblot analysis was carried out using rabbit anti-Ft antibody (1:500 dilution, DAKO) or rabbit anti-HFE antibody (1:10,000 dilution, EX1

#137) followed by goat anti-rabbit secondary antibody conjugated to HRP (1:10,000 dilution, Chemicon) and detected by ECL (SuperSignal, Pierce).

Immunoprecipitation -

Immunoprecipitation was carried out on stably transfected fWTHFE/HT29 cells as previously described (Davies et al. 2003) with slight modifications. Cell lysates were incubated for one hour at 4 °C with 50 μl protein G sepharose (Amersham Pharmacia Biotech) coated with either 4 μl of monoclonal anti-HFE antibody (8C10 mouse anti-hHFE (Ben-Arieh et al. 2001)) or 2 μg of monoclonal anti-TfR1 antibody (#4091, gift of V. Landt). Re-immunoprecipitation of duplicate samples was carried out by incubating the supernatant of the first immunoprecipitation with the second antibody. The samples were subjected to SDS-PAGE analysis on an 8% acrylamide gel, transferred to nitrocellulose, and immunodetected with sheep anti-TfR1 antiserum (1:10,000) (Williams and Enns 1991; Warren et al. 1997) or rabbit anti-HFE antibody (1:10,000; #137 EX1).

^{125}I-Tf Binding and ^{55}Fe-Tf Uptake -

Human diferric-Tf (Intergen, Co.) was labeled with Na [^{125}I] (NEN Life Science Products) using lactoperoxidase as described previously (Warren et al. 1997). The rate of ^{125}I-Tf uptake in parent, fWTHFE, and fW81AHFE/HT29 cells was determined as previously described (Roy et al. 1999). ^{55}Fe loading onto human apo-Tf and ^{55}Fe-Tf uptake and steady state labeling was also performed as previously described (Roy et al. 1999; Zhang et al. 2003).

^{55}Fe-NTA Uptake -

^{55}Fe-NTA uptake procedures were modified from a previously described protocol (Roy et al. 1999). Sub-confluent HT29 cells (parent, fWTHFE, and fW81AHFE) grown in 6-well dishes were washed twice and equilibrated in DMEM/20 mM HEPES for 15 minutes at 37 °C, 5% CO_2. Wash medium was replaced with 1ml of 200 nM ^{55}Fe-NTA (NTA in 40-fold excess) in DMEM/20 mM HEPES supplemented with 2 mg/ml ovalbumin. After 5, 10, 15, 30, or 60 minutes of uptake at 37 °C, 5% CO_2, excess ^{55}Fe was stripped from the cell surface by washing twice with 2 mL of 5 mM EDTA/PBS at room temperature. Solubilization detergent (0.1% Triton X-100, 0.1% NaOH) was added to the cells, mixed with 6 ml of UniverSol scintillation fluid (ICN), and counted for 10 minutes in a scintillation counter (Beckman LS 6000SC).

^{55}Fe-NTA Efflux -

Sub-confluent HT29 cells (parent, fWTHFE, and fW81AHFE) grown in 6-well dishes were washed twice with DMEM/20 mM HEPES and equilibrated at 37 °C, 5% CO_2 for 15 minutes. Medium was replaced with 200 nM ^{55}Fe-NTA (NTA in 40-fold excess) in DMEM/20 mM HEPES supplemented with 2 mg/ml ovalbumin and incubated at 37 °C, 5% CO_2 for 3 hours. This time point was chosen to allow sufficient time for iron transport across the cell, but not long enough for Ft synthesis to begin. After 3 hours of uptake, the radioactive medium was removed, cells were quickly washed twice at room temperature with 5 mM EDTA/PBS to remove extracellular or non-specific ^{55}Fe from the cell surface, and 1 ml of efflux medium (DMEM/20 mM HEPES/1 mM non-radioactive Fe-NTA) was added to the cells and incubated at 37 °C for 0, 5, 15 or 30

minutes. The plates were quickly washed twice with room temperature 5 mM EDTA/PBS to again remove any extracellular ^{55}Fe, and the cells were solubilized as described above. Six ml of UniverSol (ICN) were added to both the efflux media samples and the solubilized cells and counted as described above.

Statistical Analysis –

Average values are represented ± standard deviation (SD). Statistical significance was determined by unpaired *t* tests using the GraphPad Prism software. $P > 0.05$ was not considered significant.

RESULTS

Establishment of HT29 Cells as a System to Study Iron Homeostasis -

To determine if HT29 cells endogenously express the key genes involved in iron absorption in the intestine, mRNA expression of these genes was examined by qRT-PCR and normalized to the internal standard, GAPDH. In non-polarized HT29 cells, DMT1 and FPN1 mRNA levels were expressed at 2.4 and 1.4-fold lower than that of TfR1, respectively; Heph was approximately 10-fold below the expression level of TfR1; Dcytb was approximately 5% the level of TfR1; and HFE mRNA levels were even less (Figure 4.1A). Compared to HeLa cells, which have no differentiated function for iron efflux but have been previously used to examine the function of HFE (Gross et al. 1998; Corsi et al. 1999; Riedel et al. 1999; Roy et al. 1999; Salter-Cid et al. 1999; Roy et al. 2002; Davies et al. 2003), HT29 cells have over 100-fold higher FPN1 mRNA levels and endogenously express FPN1 and DMT1 at similar levels (Figure 4.1B). HT29 cells also express detectable levels of Heph mRNA, whereas HeLa cells do not (Figure 4.1A and data not shown). Thus, the expression of FPN1, DMT1, and Heph in HT29 cells is consistent with the phenotype of cells specialized for iron transport.

HT29 cells were grown on permeable filter inserts and induced to polarize to test whether they exhibited enterocyte-like behavior with respect to an expression pattern of genes involved in iron transport. RNA was isolated from HT29 cells every two days for three weeks following seeding on cell culture inserts, and the mRNA expression levels of genes related to iron metabolism were examined. Changes in mRNA at each time point relative to mRNA levels after one day of growth were plotted for each gene after samples

were normalized to the GAPDH control (Figure 4.1C). The two iron transporters, DMT1 and FPN1, showed the largest increases in mRNA levels upon polarization, approximately thirty-fold and twenty-fold respectively. This increase in mRNA levels is consistent with early iron transport studies showing that the differentiated enterocytes are responsible for iron uptake in the duodenum (Conrad and Crosby 1963).

The increase in DMT1 expression could be due to an increase in a specific isoform of this transporter. DMT1 has at least two splice variants, one containing an iron-responsive element (IRE) in the 3' untranslated region (UTR) and one without an IRE (Gunshin et al. 1997; Lee et al. 1998). IREs are stem loop structures present in the UTRs of many iron-regulated genes that bind to iron-regulatory proteins (IRPs) with high affinity when the intracellular iron concentration is low. The IRE present in one DMT1 splice form is located in the 3' UTR similar to TfR1, and has been shown to be regulated by iron in a similar manner while the isoform lacking the IRE is not responsive to iron stimulus (Gunshin et al. 2001). Using conventional RT-PCR, we found that HT29 cells expressed both isoforms of DMT1 and both isoforms increased their expression upon polarization (data not shown).

The mRNA levels of other iron-related proteins were also affected by polarization. Heph mRNA levels increased up to ten-fold and Dcytb levels increased less than five-fold, but TfR1 did not change its expression level upon polarization of HT29 cells (Figure 4.1C).

Response to Iron Treatment in Non-polarized and Polarized HT29 Cells -

Non-polarized HT29 cells responded to iron treatments in an IRP/IRE dependent manner that has previously been seen in multiple cell lines (Mullner and Kuhn 1988; Koeller et al. 1989; Klausner et al. 1993). Western blot analysis of the treated cells revealed that Ft levels vary in accordance with this mode of regulation; iron treatment increased Ft levels while Df treatment decreased the Ft levels consistent with IRPs binding to the 5' UTR of the Ft mRNA and blocking translation (Figure 4.1D, NP). Additionally, TfR1 mRNA levels decreased upon treatment with Tf and increased when the cells were iron deprived by treatment with Df, while western blot analysis also indicated similar results (data not shown). This is consistent with previous studies, which demonstrate that under low iron conditions IRPs bind to the 3' UTR of the TfR1 mRNA and protect the message from ribonucleases (reviewed in (Hentze and Kuhn 1996; Theil 1998; Eisenstein 2000)).

Ft levels in polarized cells exhibited similar responses as non-polarized cells when subjected to iron loading or deprivation. Polarized HT29 cells were able to respond to Tf, in that the Tf-treated samples showed increased Ft levels compared to untreated cells (Figure 4.1D, POL). These results also indicate that Ft levels increased in response to Tf-mediated iron uptake and thus, indirectly demonstrated that the TfR1 and IRPs remained functional once the cells were polarized. The non-Tf-mediated iron uptake pathway is also functional in polarized cells as seen in the increased Ft levels when cells were given Fe-Asc apically. The above experiments were carried out in media of a specific pH to mimic the neutral environment of the blood or the acidic environment of the intestinal lumen.

HFE Expression in HT29 Cells Increases Ft Levels -

HT29 cells were stably transfected with a previously described FLAG epitope-tagged form of wild type HFE (Feder et al. 1997; Gross et al. 1998) to determine how HFE might affect iron homeostasis in this intestinal-like cell line. HFE expression in HT29 cells (fWTHFE/HT29) resulted in increased Ft levels compared to the parent cell line (Figure 4.2A). This was the case in both non-polarized and polarized cells. Increased Ft levels are opposite to that observed in other cell lines, such as HeLa or HEK293, that are transfected with the same HFE construct (Gross et al. 1998; Roy et al. 2000). In HeLa cells, HFE expression results in decreased Ft levels due to a decrease in the intracellular labile iron pool (Riedel et al. 1999; Roy et al. 2002). The behavior of the HT29 cells is similar to monocytes and macrophages with respect to iron homeostasis. Increases in Ft resulting from HFE expression have been previously reported in human monocytes (Montosi et al. 2000) and in the macrophage-like cell line THP-1 (Drakesmith et al. 2002).

Increased Ft levels could be due to increases in intracellular iron or other factors that alter Ft mRNA levels. To further investigate the basis of the finding that HFE increased levels of Ft in HT29 cells, Ft mRNA was measured. Inflammatory factors or oxidative stress can increase Ft mRNA levels through transcriptional regulation whereas changes in iron status alter Ft translation, leaving mRNA levels unaffected (reviewed in (Torti and Torti 2002)). To distinguish between these possibilities, qRT-PCR was carried out on HT29 cells (non-polarized and polarized, with and without HFE expression) for both the heavy and light chain subunits of Ft (Figure 4.2B). Less than 1.5-fold changes

in the mRNA levels of either Ft subunit were detected with HFE expression or polarization, ruling out transcriptional regulation as the major factor in the increased Ft observed. Consistent with higher Ft levels, HFE-expressing cells accumulated more iron than untransfected HT29 cells when a 20 hour ^{55}Fe-Tf uptake was carried out to examine steady state levels of intracellular iron (Figure 4.2C). These experiments indicate that the increases in Ft observed in HT29 cells expressing HFE reflect higher intracellular iron levels.

Previous studies have demonstrated that HFE and TfR1 interact (Parkkila et al. 1997b; Feder et al. 1998; Gross et al. 1998; Corsi et al. 1999). In order to determine whether they interact in the fWTHFE/HT29 cell line, co-immunoprecipitation experiments were carried out. Cell lysates were immunoprecipitated with anti-HFE (8C10 mouse anti-human HFE (Ben-Arieh et al. 2001)) or monoclonal anti-TfR1 antibodies followed by immunodetection with sheep anti-TfR1 and rabbit anti-HFE antibodies (Figure 4.2D). In cells expressing fWTHFE, TfR1 co-precipitated with HFE providing evidence for the association of the two proteins in this cell line (Figure 4.2D, lanes 2 & 4). Re-immunoprecipitation of the supernatant with antibodies to HFE showed that HFE was in excess of the TfR1/HFE complex (Figure 4.2D, lane 5). Thus, if HFE's effect is independent of its interaction with TfR1 as has recently been demonstrated in HeLa cells (Zhang et al. 2003), there is excess HFE over TfR1 in this cell line.

HFE Inhibits Iron Efflux from Cells Independent of its Association with TfR1 -

In HeLa cells, the decrease in Tf-mediated iron uptake upon HFE expression was independent of the association of HFE with TfR1 (Zhang et al. 2003). To determine the

effect of the interaction between HFE and TfR1 on the Ft levels in the HT29 cell line, cells were transfected with fW81AHFE, which has a 5,000-fold lower affinity for TfR1 (Lebron et al. 1999). Expression of fW81AHFE in HT29 cells also resulted in increased Ft levels (Figure 4.3), which indicates that a strong association between TfR1 and HFE is not required for the increased iron accumulation in HT29 cells.

A series of Tf uptake, iron uptake, and iron efflux studies were performed to determine how HFE affects iron homeostasis in HT29 cells. First, we tested to see if HFE altered Tf endocytosis. If HFE increased the rate of Tf uptake into HT29 cells, this could result in the increased Ft levels observed. Cells were incubated with 100 nM ^{125}I-Tf for 2, 4, 6, or 8 minutes at 37 °C, 5% CO_2. Tf was stripped from the cell surface and the internal ^{125}I-Tf was counted. All three cell lines had similar numbers of receptors on the cell surface (data not shown) and there was no significant difference between rates of uptake in parent HT29 cells and either HFE expressing cell line (wild type or W81A), suggesting that the uptake of Tf was not affected by HFE expression (Table 4.2).

The effect of HFE on cellular iron uptake from Tf was tested. If HFE increased the Tf-mediated iron uptake in HT29 cells, then increased Ft levels would be observed. Parent, fWTHFE, and fW81AHFE/HT29 cells were incubated with 100 nM ^{55}Fe-Tf for up to 240 minutes. The difference in the rates of ^{55}Fe uptake from Tf between parent and either HFE-expressing cell line was not significant, suggesting that this was not the mechanism by which HFE was altering Ft levels in the cells (Table 4.2). These results demonstrate that the Tf-mediated iron uptake pathway was unaltered in HFE-expressing HT29 cells, and also validated the use of ^{55}Fe-Tf to examine steady state levels of iron in cells (Figure 4.2C). Thus, HT29 cells expressing HFE differ from HeLa cells expressing

HFE. In HeLa cells, a 30-40% reduction in ^{55}Fe uptake from Tf leads to reduced Ft (Roy et al. 1999; Zhang et al. 2003). The results in the present study suggest that HFE operates by an alternative mechanism to affect intracellular iron levels in HT29 cells than in HeLa cells.

Given that HFE had little effect on Tf-mediated iron uptake in HT29 cells, the non-Tf-mediated iron uptake pathway was examined. The higher Ft levels observed could be a result of increased iron import or decreased iron export. To assess if HFE expression increases iron import into the cells, all three cell lines were incubated with 200 nM ^{55}Fe-NTA for up to one hour. There was no significant difference between the rates of ^{55}Fe uptake in parent cells versus HFE-expressing cells (Figure 4.4A), suggesting that this iron import pathway was not affected by HFE expression.

Iron efflux experiments were carried out to determine if HFE inhibited iron export. Non-polarized cells were treated with 200 nM ^{55}Fe-NTA for three hours and washed briefly with 5 mM EDTA to remove any ^{55}Fe on the cell surface. Efflux medium was placed on the cells for 0, 5, 15, and 30 minutes to allow for ^{55}Fe export out of the cells. The amount of ^{55}Fe remaining inside the cells at each time point was counted. The results showed that the parent cells export ^{55}Fe 45% faster than fWTHFE and fW81AHFE cells (Figure 4.4B). The experiment was also repeated for the 30 minute time point with parent and fWTHFE cells polarized on filter inserts; HFE-expressing cells exported less iron than parent cells, similar to non-polarized cells (data not shown). Thus, HFE expression results in the inhibition of iron export leading to increased intracellular iron. Additionally, this inhibitory effect is not dependent on an interaction between HFE and TfR1, because the fWTHFE and fW81AHFE cell lines give similar results.

Changes in mRNA Levels with HFE Expression -

The inhibition of iron efflux from HT29 cells expressing HFE suggests that HFE imparts its function on a component of the export machinery. The iron transporter, FPN1, and the ferroxidase, Heph, are implicated in the export of iron (Vulpe et al. 1999; Abboud and Haile 2000; Donovan et al. 2000; McKie et al. 2000; Anderson et al. 2002). Additionally, other unidentified players could be involved in this step. In order to determine if HFE had an effect on the mRNA levels of genes involved in iron transport, qRT-PCR was performed on mRNA from parent and fWTHFE/HT29 cells. The message levels of the iron-related genes did not change significantly in response to HFE expression for most genes tested, except for a significant reduction in Heph mRNA (Figure 4.5). This effect was also observed when the cells were polarized (data not shown). While the reduction in Heph was not confirmed at the protein level due to limitations in antibody sensitivity, it is consistent with the idea that HFE is involved in inhibiting the iron efflux pathway.

DISCUSSION

We have demonstrated that the human HT29 cell line can be a useful model to study key players involved in intestinal iron absorption because it endogenously expresses a number of genes known to be involved in iron transport in the intestine. When induced to polarize, HT29 cells strongly upregulated the mRNA expression of the two major iron transporters, DMT1 and FPN1. Heph mRNA levels also increased substantially upon polarization while Dcytb expression had only a slight increase.

When HT29 cells were stably transfected with HFE, Ft levels increased in both non-polarized and polarized cells. Iron-independent processes, such as inflammation and oxidative stress, can increase Ft at the transcriptional level. Cytokines, hormones, growth factors, and second messengers can all cause changes in either the heavy or light-chain subunit of Ft (reviewed in (Torti and Torti 2002)). The increased Ft protein observed in response to HFE expression can be attributed to a change in the intracellular iron level of the cells, not to an alternative influence affecting transcription, because there were no substantial changes in the mRNA levels of either the heavy or light-chain subunit of Ft due to HFE expression. Additionally, the steady state intracellular iron levels were also increased in HFE-expressing cells indicating that the changes in Ft levels reflect the intracellular iron status. Notably, Ft levels increased approximately the same amount in both non-polarized and polarized cells upon HFE expression. This result is not surprising, however, because both the iron importer and exporter (DMT1 and FPN1, respectively) increased expression to similar extents upon polarization, therefore maintaining the level of internal iron.

In order to understand which step of iron cycling or transport HFE affected, we first examined the Tf-mediated iron uptake pathway. If HFE increased the rate of Tf uptake or the rate of ^{55}Fe uptake from Tf, an elevated level of Ft could occur in the cells. In contrast to HeLa cells where expression of HFE causes a 30-40% reduction in Tf-mediated iron uptake (Roy et al. 1999; Zhang et al. 2003), no significant changes in Tf-mediated iron uptake were detected in HT29 cells. Rather, a 45% decrease in the rate of ^{55}Fe efflux was detected in cells expressing either wild type HFE or the W81A mutant. In turn, this inhibition of iron export leads to a buildup of intracellular iron stored in Ft, also evidenced by increased steady state iron levels.

The increase in Ft levels upon HFE expression differs from reports that examined iron metabolism in HeLa and HEK293 cells (Gross et al. 1998; Roy et al. 2000). However, previous studies have shown increased Ft levels upon HFE expression in macrophage-like cells (Montosi et al. 2000; Drakesmith et al. 2002). Using an attenuated *Salmonella typhimurium* strain as a vector to express HFE in monocytes/macrophages from patients with Type 1 HH, Montosi and colleagues found increased iron accumulation compared to untransfected cells (Montosi et al. 2000). They proposed that this result could be due to enhanced iron uptake or reduced iron efflux from cells, and favored the latter speculation because they only observed an increased iron accumulation after 24 hours of treatment with ^{55}Fe-Tf (Montosi et al. 2000). In another study, Drakesmith and colleagues demonstrated that increased Ft resulting from decreased iron efflux occurs when HFE is expressed in the monocyte/macrophage cell line THP-1 (Drakesmith et al. 2002). The results from these studies, in addition to our own, are consistent with the idea that HFE functions differently in cell types with a specialized

function for iron metabolism compared to standard cell culture models. In cells that do not export iron, such as HeLa and HEK293, intracellular iron levels decrease with HFE expression; and in cells that export iron, such as intestinal and monocytes/macrophages, intracellular iron levels increase. This could explain why different cell types in the body accumulate iron, while others like Kupffer cells appear iron depleted. We suggest that in cells that have a differentiated role for iron export, HFE expression increases intracellular Ft levels by inhibiting iron efflux. This role for HFE is also in accord with the observation that enterocytes are iron-deprived in HH patients where a non-functional HFE is expressed (Pietrangelo et al. 1995).

Iron export from intestinal epithelial cells is proposed to occur via the transporter, FPN1, and coordinate with the ferroxidase Heph (Vulpe et al. 1999; Abboud and Haile 2000; Donovan et al. 2000; McKie et al. 2000; Anderson et al. 2002; Chen et al. 2004). We examined the mRNA levels of the genes involved in iron transport to see if HFE had an effect, especially on genes involved in iron export. We observe no significant differences in mRNA levels in response to HFE expression, except for a significant reduction in Heph message levels. This result is consistent with the model that HFE inhibits iron efflux from cells, however, a mechanism of whether this effect is direct or indirect remains to be determined.

Interestingly, HFE can exert this inhibitory function on iron export independent of its interaction with TfR1. We also see in HeLa cells that HFE affects the intracellular iron status independent of TfR1 (Zhang et al. 2003). However, the effect on the cell's iron status in response to HFE expression is different in these two cell types. While HT29 cells endogenously express DMT1 and FPN1 at equivalent levels, HeLa cells have

very low levels of FPN1, even though they express DMT1 at similar levels to HT29 cells. The different responses to HFE expression in different cell types could be due to the deficiency or presence of particular players, for example those involved in iron export. This study suggests that HFE can have multiple roles in maintaining iron homeostasis depending on the availability of other proteins. We speculate that HFE interacts with a variety of proteins and depending on their abundance, HFE can alter iron uptake or efflux in order to maintain iron balance. Further experimentation is required to tease out this multi-faceted function of HFE and to determine its target in the inhibition of iron export.

Gene	Forward Primer	Reverse Primer
GAPDH (868F/968R)	5'-ACCCACTCCTCCACCTTTGA-3'	5'-CTGTTGCTGTAGCCAAATTCGT-3'
DMT1* (1415F/1555R)	5'-ATGGACTAGGCTGGCGGATT-3'	5'-GATAAGCCACGCTGACCACA-3'
FPN1 (524F/664R)	5'-CCACAATACGAAGGATTGACCA-3'	5'-GGACGTACTCCACGCACATG-3'
Heph (1797F/1897R)	5'-TGCTATGTTGGATTTCCGACTG-3'	5'-TGGGCAGGTTAGAGAACAGAAAC-3'
HFE (151F/291R)	5'-GGCTACGTGGATGACCAGCT-3'	5'-CATGTGATCCCACCCTTTCAG-3'
TfR1 (305F/435R)	5'-CAGGAACCGAGTCTCCAGTGA-3'	5'-CTTGATGGTGCCGGTGAAGT-3'
Dcytb (283F/403R)	5'-CCATCCATGCAGGGTTAAATG-3'	5'-CCAACCCAGCTGTGCAGACT-3'
H-Ft (179F/289R)	5'-CTCATGAGGAGAGGGAACATGC-3'	5'-CGCTCTCCCAGTCATCACAGT-3'
L-Ft (740F/840R)	5'-CTGAAGGGCCCCTTGCA-3'	5'-CCATTTGGTCCAAGGCTTGT-3'

*DMT1 primers recognize both the IRE and non– IRE isoforms.

Table 4.1. Primer sets used for qRT-PCR. All primer sets were designed according to human gene sequences from GenBank to yield amplicons of approximately 100-140 base pairs.

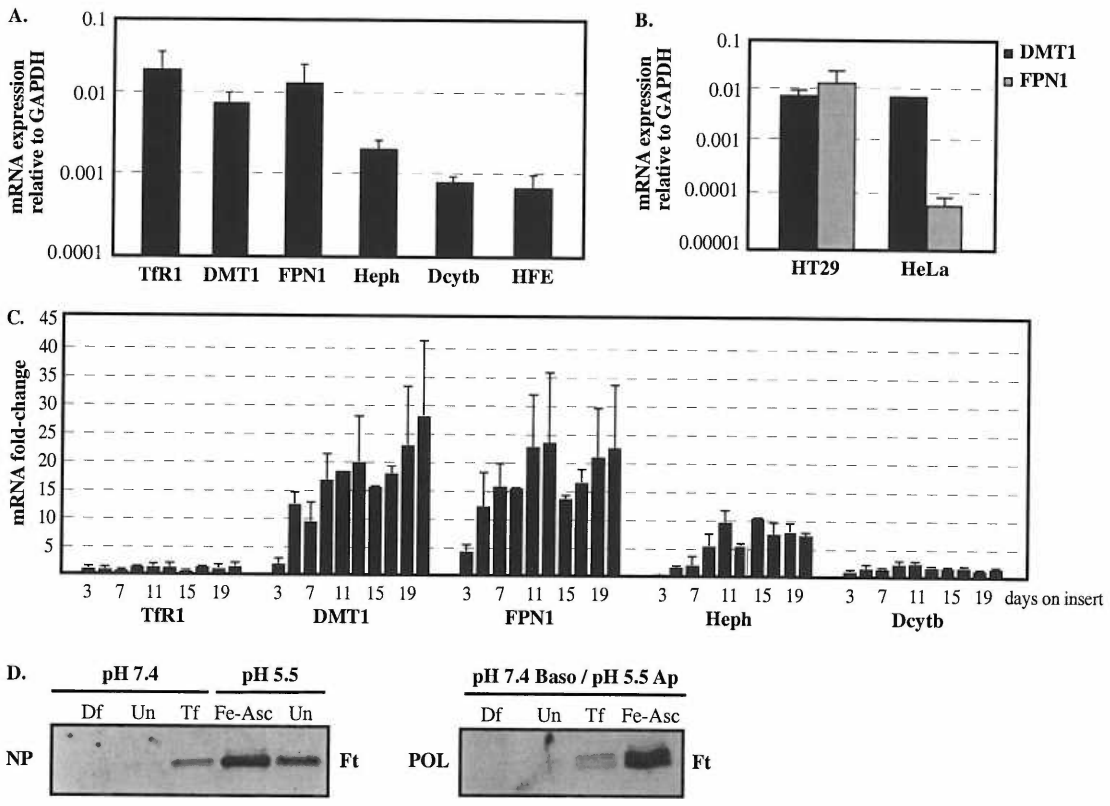


Figure 4.1. Establishment of HT29 cells as a system to study iron homeostasis. A) To establish the endogenous levels of mRNA expression for each of the genes of interest in HT29 cells, mRNA was isolated from non-polarized cells. qRT-PCR was used to quantify each gene of interest after normalizing to the internal GAPDH control. All samples were run in triplicate in at least three independent experiments and the average ± SD is depicted. **B)** qRT-PCR was carried out on untransfected HT29 or HeLa cells to determine the relative levels of DMT1 (*black*) and FPN1 (*gray*) in these cell lines. Samples were run in triplicate in at least two independent experiments and the average ± SD is depicted. The C_T values of GAPDH were similar in both cell lines, allowing for direct comparisons of mRNA levels. **C)** To assess mRNA levels at different stages of polarization, RNA was isolated from HT29 cells grown on culture inserts every two days for three weeks and subjected to qRT-PCR for each gene of interest. All data were normalized to the internal standard, GAPDH, and all mRNA levels are expressed as a fold-change relative to the level of mRNA after one day of growth for each gene. Each sample was analyzed in triplicate in two independent experiments and the average ± SD is depicted. **D)** Whole cell lysates (30 μg/lane) from different iron treatments were analyzed by western blot for Ft. Non-polarized HT29 cells were treated for 24 hours at pH 7.4 with Tf, Df, or left untreated (Un) and at pH 5.5 with Fe-Asc or left untreated. Polarized HT29 cells (cultured on inserts for 18 days) were treated for 24 hours with Fe-Asc on the apical side, Tf on the basolateral side, Df on both sides, or left untreated. The apical buffer was pH 5.5 and the basolateral medium was pH 7.4. These results are representative of three experiments without significant variation between experiments.

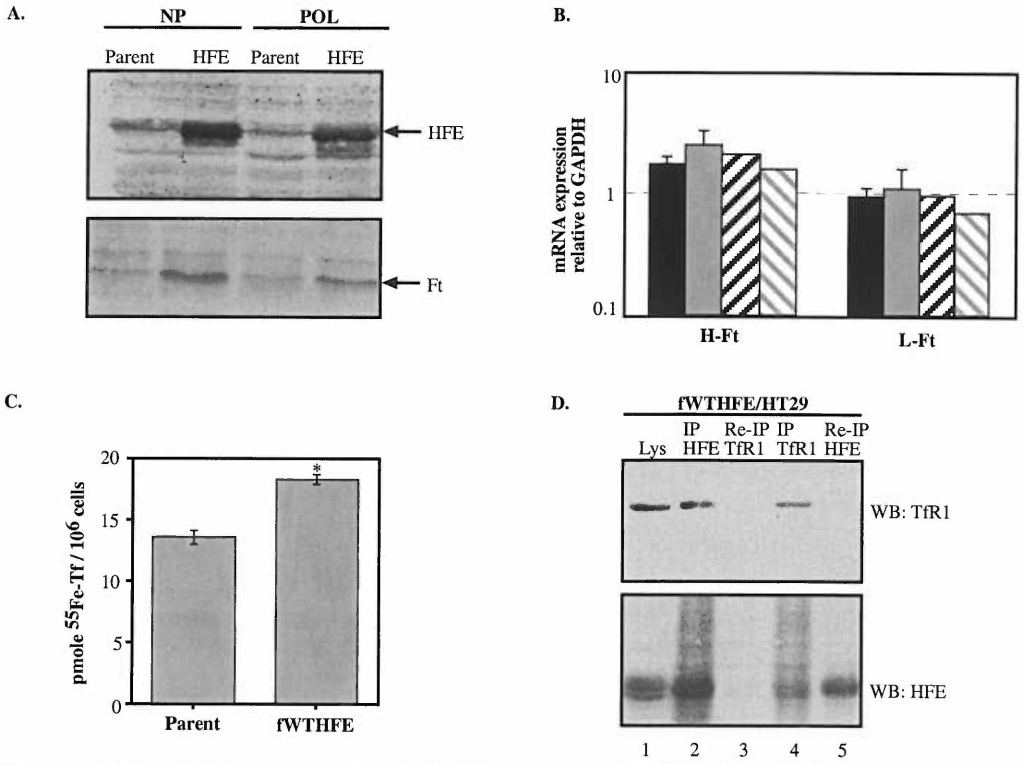


Figure 4.2. HFE expression in HT29 cells. A) Whole cell lysates (30 μg/lane) from non-polarized (NP) or polarized (POL) parent or fWTHFE/HT29 cells were analyzed by western blot for HFE and Ft. Chemiluminescence detected ~43 and ~19/21-kDa bands representing HFE and Ft respectively. HFE migrates as broad heterogeneous band presumably due to heterogeneity in glycosylation, which has been noted previously (Gross et al. 1998; Riedel et al. 1999; Salter-Cid et al. 1999; Ben-Arieh et al. 2001). These results are representative of three experiments without significant variation between experiments. **B)** qRT-PCR was carried out on duplicate samples as used in panel A to assess Ft expression in response to HFE (*Parent NP = solid black, fWTHFE NP = solid gray, Parent POL = black striped, fWTHFE POL = gray striped*). Both the heavy (H-Ft) and light (L-Ft) chain mRNA show less than 1.5-fold change in response to HFE expression or polarization. Samples were normalized to the internal control GAPDH and were run in triplicate for two independent experiments and the average ± SD is depicted. **C)** Steady state intracellular iron levels were measured in parent and fWTHFE/HT29 non-polarized cells by treatment with 200 nM ^{55}Fe-Tf for 20 hours in complete media. After acid stripping the cell surface of excess ^{55}Fe-Tf, the internal ^{55}Fe was counted. Data is expressed as the average ± SD of pmole ^{55}Fe/10^6 cells for eight samples per cell line. The HFE-expressing cells accumulated a significantly higher amount of iron than the parent cells ($*P < 0.0001$). The experiment was repeated with similar results. **D)** Lysates from fWTHFE/HT29 cells were immunoprecipitated and immunodetected with antibodies to TfR1 and HFE (Lanes 2 & 4) and re-immunoprecipitation was carried out with the other antibody on duplicate samples (lanes 3 & 5). Chemiluminescence detected ~97 (TfR1) and ~43-kDa (HFE) species (lanes 2 & 4) providing evidence for the association of HFE and TfR1 in the transfected cells. Re-immunoprecipitation samples show that HFE is in excess of TfR1 (lane 5). Lane 1 is whole cell lysate control. The experiment was repeated with similar results.

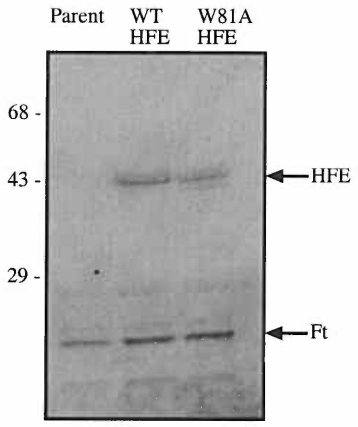


Figure 4.3. HFE expression increases Ft independently of association with TfR1. Whole cell lysates (30μg/lane) from non-polarized parent, fWTHFE, and fW81AHFE/HT29 cells were analyzed by western blot for HFE and Ft levels. Like the wild type HFE-expressing cells, Ft levels are increased in cells expressing the W81A mutant HFE, suggesting that an interaction between HFE and TfR1 is not necessary for HFE function in HT29 cells.

	---------- ^{125}I-Tf uptake ----------			---------- ^{55}Fe-Tf uptake ----------		
Cell Line	**Parent**	**WTHFE**	**W81A**	**Parent**	**WTHFE**	**W81A**
Avg. Slope	0.0253	0.0218	0.0245	0.0545	0.0520	0.0660
St. Dev.	0.002	0.011	0.010	0.014	0.014	0.017
N*	3	4	2	2	2	2

*N = number of experiments with four to six data points per time point

Table 4.2. HFE does not alter Tf-mediated iron uptake in HT29 cells. ^{125}I-Tf and ^{55}Fe-Tf uptake experiments were carried out on non-polarized parent, fWTHFE, and fW81AHFE/HT29 cells. Linear regression was determined with Cricket Graph software. Statistical analyses show the slopes (rates of uptake measured in pmole/minute/10^6cells) for the HFE-expressing cells are not significantly different from parent cells ($P > 0.05$).

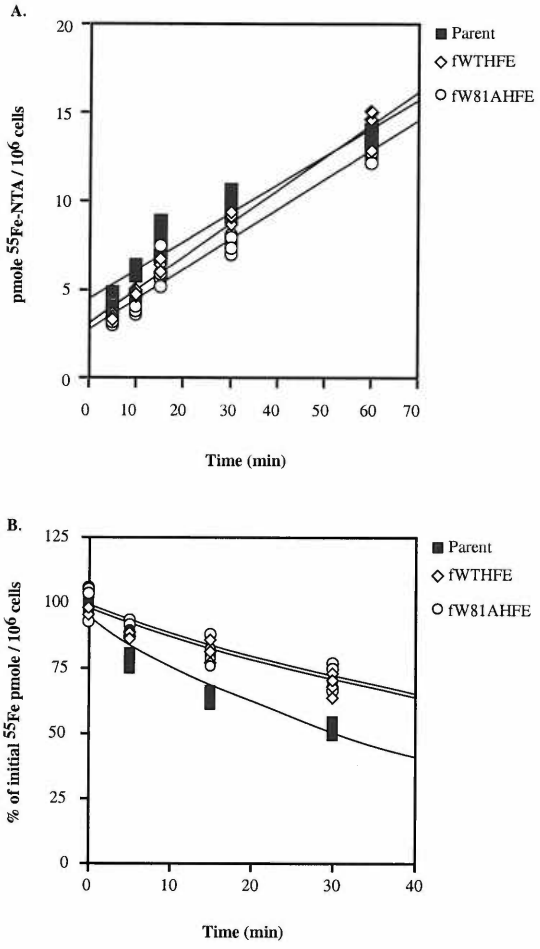


Figure 4.4. HFE does not alter ^{55}Fe import, but inhibits ^{55}Fe export. A) ^{55}Fe uptake from ^{55}Fe-NTA was measured in non-polarized parent, fWTHFE, and fW81AHFE/HT29 cells. The rates of ^{55}Fe uptake in pmole/minute/10^6 cells for this experiment were: Parent ■ *(closed squares)*: 0.159, fWTHFE ↓ *(open diamonds)*: 0.187, and fW81AHFE ○ *(open circles)*: 0.169. Linear regression was determined in the Cricket Graph program. The results shown represent one of two independent experiments performed with six data points per time point with minimal variation between experiments. The rates of ^{55}Fe uptake between parent and either HFE-expressing cell line were not significantly different ($P > 0.05$). **B)** ^{55}Fe efflux was measured from parent, fWTHFE, and fW81AHFE/HT29 non-polarized cells. The percentage of initial pmole ^{55}Fe remaining per 10^6 cells across a 30-minute efflux is graphed. Exponential curve fits are shown where the slope is equal to the rate of iron loss from cells (*Symbols are the same as in panel A;* Parent: $y = 92.598 \times 10^{-0.009x}$, fWTHFE: $y = 95.865 \times 10^{-0.005x}$, and fW81AHFE: $y = 96.632 \times 10^{-0.005x}$). The slopes demonstrate that parent cells export ^{55}Fe 45% faster than the HFE-expressing cell lines. Exponential regression was determined in the Cricket Graph program. These results represent one of two independent experiments performed with six data points per time point with minimal variation between experiments. The percentage of ^{55}Fe remaining in the transfected cells is significantly greater than in the parent cells for each time point ($P < 0.001$).

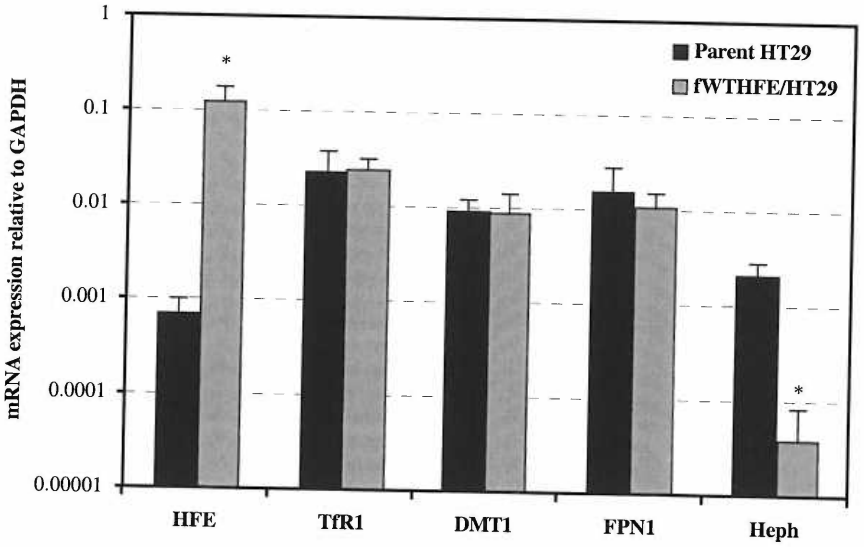


Figure 4.5. Changes in mRNA levels in response to HFE expression. qRT-PCR was carried out on non-polarized parent *(black)* and fWTHFE *(gray)* HT29 cells as described in Materials & Methods. mRNA expression is graphed as compared to the internal control GAPDH. Samples were run in triplicate in at least five independent experiments and the average ± SD is depicted. *Represents a significant difference in expression compared to parent cells ($P < 0.0001$).

SUPPLEMENARY DATA TO CHAPTER 4

RATIONALE

As demonstrated in this thesis, HFE expression either increases or decreases intracellular iron levels depending on cell type. These differences could be due to cell-specific expression of distinct proteins. We observe increased Ft in HT29 cells upon HFE expression (Figures 4.2A and 4.3) and increased intracellular iron at steady state (Figure 4.2C) due to inhibition of iron efflux (Figure 4.4B). In contrast, decreased Ft in HFE-expressing HeLa cells was measured (Roy et al. 1999; Zhang et al. 2003). HT29 cells express equivalent levels of iron transporters, DMT1 and FPN1, for iron import and export, respectively. Even though HT29 and HeLa cells express similar levels of DMT1, HeLa cells have over 100-fold lower expression of FPN1 mRNA (Figure 4.1B). Due to increased Ft levels and decreased iron efflux in HT29 cells, we hypothesized that HFE could inhibit iron export by acting on FPN1. We reasoned that if FPN1 is not present (or expressed at very low levels, as in HeLa cells), HFE would not affect iron export and might target another protein. In HeLa cells, HFE's "target protein" could be DMT1, inhibiting the transport of iron out of the endosome into the cytosol, thus yielding the decreased Tf-mediated iron uptake observed in HeLa cells (Roy et al. 1999; Zhang et al. 2003).

We hypothesized that expression of FPN1 in HeLa cells would result in a cell line that would accumulate iron in the presence of HFE. If HFE acted on FPN1 in the same manner as hypothesized in HT29 cells, Ft levels would be expected to rise due to an

inhibition of iron efflux. We designed the following experiments to determine if FPN1 was the target of HFE's inhibition of iron export.

MATERIALS AND METHODS

Cell Lines -

The fWTHFE and fW81AHFE/tTA HeLa cell lines expressing FLAG epitope-tagged wild type or W81A mutant HFE under the tet-responsive promoter have been previously described (Gross et al. 1998; Zhang et al. 2003). Cells were grown in DMEM supplemented with 10% FBS, 0.4 mg/ml G418 (Geneticin, Calbiochem), 0.2 μg/ml puromycin, and with (HFE-) or without (HFE+) 1 μg/ml Dox.

Plasmid -

The human WTFPN1-myc-his plasmid was a kind gift from Dr. Pamela Bjorkman, (California Institute of Technology; originally from Dr. Hal Drakesmith, University of Oxford). This plasmid was created by inserting the human wild type FPN1 cDNA between the *Not*I and *Xba*I restriction sites in the multiple cloning region of the pcDNA3.1+ parent vector (Invitrogen). After the last amino acid in the coding region of FPN1, six residues from the parent vector followed, then the *c-myc* tag (EQKLISEEDL), a 6-His tag, and a stop site.

Transient Transfections –

Transient transfection of the fWTHFE or fW81AHFE/tTA HeLa cells with the hWTFPN1-myc-his plasmid was accomplished using Lipofectamine (Invitrogen). Transfection was carried out in one 100 mm dish of cells at 80% confluency that had been maintained in 5 ng/ml Dox for 2 days. This low level of Dox allowed for slight

expression of HFE, but was amenable to high expression of HFE when the Dox was washed away, or suppression of HFE when higher concentrations of Dox were added. The transfection was carried out in this single dish to ensure equal efficiency of FPN1 transfection and the cells were later split into Dox+ and Dox- media.

Cells were washed twice with DMEM containing no serum and the transfection solution was added to the cells: 12μg DNA and 45μl lipofectamine, each diluted in Opti-MEM media (Invitrogen), combined and incubated at room temperature for 30 minutes, and further diluted in DMEM without serum. After incubation for 5 hours at 37°C, the lipofectamine solution was removed and fresh media was added (DMEM, 10% FBS, 0.4 mg/ml G418, 0.2 μg/ml Puromycin, 5 ng/ml Dox) to allow the cells to recover from the transfection conditions. After three hours at 37°C, the cells were washed five times with PBS, trypsinized, and split in half into the above media with or without 1 μg/ml Dox (three or four 60 mm dishes each) and incubated at 37°C for 40, 56, 72, and in some instances 88 additional hours. In some cases, 1mg/ml diferric-Tf was also added at the time of complete media replacement.

Western Immunodetection -

Cell lysates were made 48, 64, 80, or 96 hours after the start of transfection with NET-Triton (150 mM NaCl, 5 mM EDTA, and 10 mM Tris (pH 7.4) with 1% Triton X-100) and protein concentration was determined by BCA assay (Pierce). Cell lysates (100μg) of duplicate samples were diluted with Laemmli buffer (125 mM Tris-HCl (pH 6.8), 4% SDS, 20% glycerol, and 10% 2-mercaptoethanol) (Laemmli 1970). One set of the duplicates was boiled for 5 minutes and the other set was incubated at room

temperature for 15 minutes. All samples were subjected to electrophoresis on 12% SDS-polyacrylamide gels under reducing conditions and transferred to nitrocellulose. Prestained molecular weight markers (Benchmark Protein Ladder; Invitrogen) were also run on each gel. After blocking in 5% milk/TBST at room temperature for 2 hours, immunoblot analysis was carried out. The boiled samples were assessed for HFE and Ft expression (rabbit anti-HFE at 1:10,000 dilution, EX1 #137; and sheep anti-Ft at 1:100 dilution, The Binding Site), and the non-boiled samples were assessed for FPN1 expression (rabbit anti-FPN1 at 1:2500 dilution in 5% milk/TBST, generous gift from Dr. David Haile, University of Texas Health Science Center, San Antonio, TX). As with many multiple membrane spanning proteins, boiling of samples leads to aggregation of the protein and difficulty in analysis (Canonne-Hergaux et al. 2000). Detection of Ft and FPN1 both required at least 5 hours incubation at room temperature or overnight at 4°C in the primary antibody for optimal signal; a doublet is seen for Ft when using this antibody. Blots were incubated in HRP-conjugated secondary antibodies (goat anti-rabbit (Chemicon) at 1:10,000 dilution for HFE and 1:2,000 dilution in 5% milk/TBST for FPN1, or donkey anti-sheep (Chemicon) at 1:2500 dilution for Ft) followed by ECL detection (SuperSignal, Pierce).

RESULTS AND DISCUSSION

Stable transfections of wild type FPN1 were unattainable in the fWTHFE/tTA HeLa cells and colleagues in the field have also commented that they are unable to achieve stable transfections, due to cell death when wild type FPN1 is expressed for extended periods of time. To circumvent this problem, we transiently transfected human wild type FPN1 into the fWTHFE/tTA HeLa cells. In contrast to our prediction, when the lysates were examined by Western analysis, we did not observe a "switch" in Ft phenotype in cells transiently transfected with FPN1 compared to cells not expressing this transporter (Figure S4.1C). As expected, Ft levels decreased with HFE expression in the untransfected cells. Ft levels decreased further when FPN1 was expressed compared to untransfected cells, as expected due to iron being exported out of the cells by FPN1. However, we did not observe an increase in Ft levels in FPN1 expressing cells when HFE expression is turned on by withdrawal of Dox. This data suggests that the function of FPN1 is not altered by HFE expression.

If HFE were to affect FPN1 activity, it would probably do so when not bound to TfR1. To minimize the interaction of HFE with TfR1, thereby increasing the chances of binding to or affecting another protein, we carried out the same experiment in the presence of 1mg/ml Tf, which has previously been shown to be more than sufficient to saturate binding to the TfR1 and compete with HFE for binding to TfR1 (Roy et al. 1999; Zhang et al. 2003). When Ft levels are examined from this experiment, we see the same results as in Figure S4.1C in the absence of Tf supplementation. HFE expression does

not cause an increase Ft when FPN1 is also present, but a decrease in Ft levels is observed (Figure S4.2).

We took one more approach to examine the possible effect of HFE and FPN1 co-expression in HeLa cells. Although excess Tf in the media should have competed with HFE for binding to TfR1, we repeated the experiment in fW81AHFE/tTA HeLa cells where the W81A mutant HFE has a 5,000 lower binding affinity for TfR1 than wild type HFE (Lebron and Bjorkman 1999). This experiment would be a further confirmation of the previous two examples demonstrating that HFE does not affect FPN1 function when expressed in HeLa cells. Again, we see a decrease in Ft levels with FPN1 expression that is unaltered when fW81AHFE expression is turned on by withdrawal of Dox (Figure S4.3).

Together, these data suggest that FPN1 is not a direct target for HFE in inhibiting iron export from cells. Even though we do not observe HFE inhibiting iron efflux in HeLa cells, there are other proteins involved in the iron export machinery that could be affected by HFE. One example is the ferroxidase, Heph, which is thought to coordinate with FPN1 in achieving efficient iron export from cells (Vulpe et al. 1999; Chen et al. 2004). Co-transfection of FPN1 and Heph into the fWTHFE/tTA HeLa cells might resolve this question. We observe decreased Ft with FPN1 expression indicating that the transporter is functional, its function would be expected to be heightened with Heph co-expression. Indeed, the *sla* mice harboring a truncated form of Heph are viable, although anemic, suggesting that there are compensatory mechanisms to achieve iron export in the face of the Heph mutation. One possibility could be that the serum ferroxidase ceruloplasmin assumes the oxidation function at the intestinal enterocyte. Additionally,

Vulpe's group has recently demonstrated that the truncated form of Heph found in these mice still maintains limited oxidase activity, although much lower than wild type (Chen et al. 2004). This residual oxidase activity could allow for limited iron export, sufficient for the animals to live.

Since we hypothesize that HeLa cells are lacking a required protein for HFE to inhibit iron efflux, the transfection strategy to introduce the "missing protein" into cells may not be the most reasonable approach. Another possibility would be to inhibit certain players in the HT29 cells to try and switch their Ft phenotype from high to low. Using siRNA or blocking antibody techniques to knock down FPN1 or Heph levels might be the means to accomplish this. If one of these two proteins is not the target of HFE, then a more global approach might better address this question. It is likely that there are unidentified players involved in the iron export process that HFE may target.

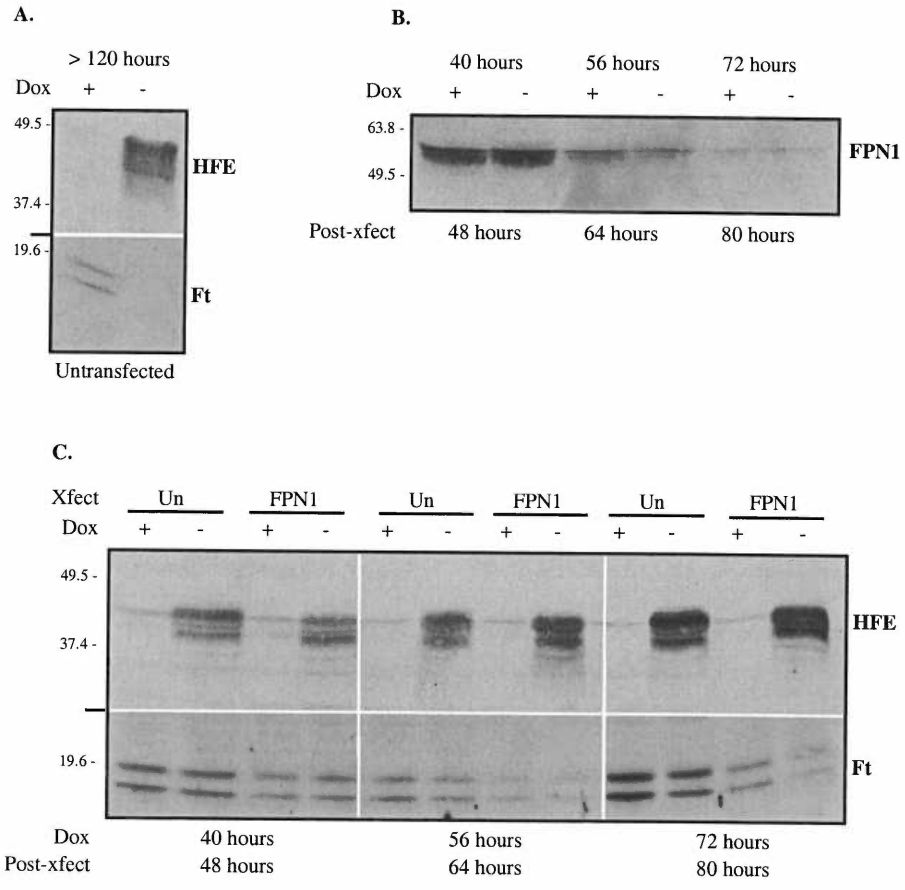


Figure S4.1. Transient transfection of FPN1 in fWTHFE/tTA HeLa cells. **A)** fWTHFE/tTA HeLa cells before transfection with FPN1; Ft levels decrease upon HFE expression. **B)** fWTHFE/tTA HeLa cells were transiently transfected with hWTFPN1-myc-his as described in the Materials & Methods. The expression of FPN1 is strong 48 hours after transfection, but decreases at 64 hours post-transfection and is only slightly expressed 80 hours after transfection. **C)** Cells expressing FPN1 have decreased Ft levels, presumably due to iron being transported out of the cells; the Ft levels do not increase upon HFE expression.

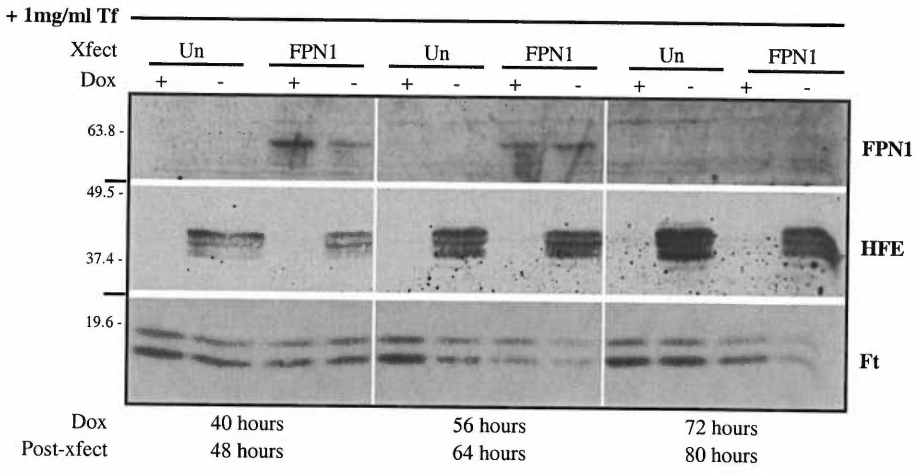


Figure S4.2. Transient transfection of FPN1 in fWTHFE/tTA HeLa cells in the presence of extracellular Tf. fWTHFE/tTA HeLa cells were transiently transfected with hWTFPN1-myc-his as described in the Materials & Methods. The culture medium was supplemented with 1mg/ml Tf to dissociate HFE from TfR1. When HFE is expressed (Dox-), Ft levels decrease. This effect is unaltered by FPN1 transfection except that the overall Ft levels are lower due to iron being transported out of the cells.

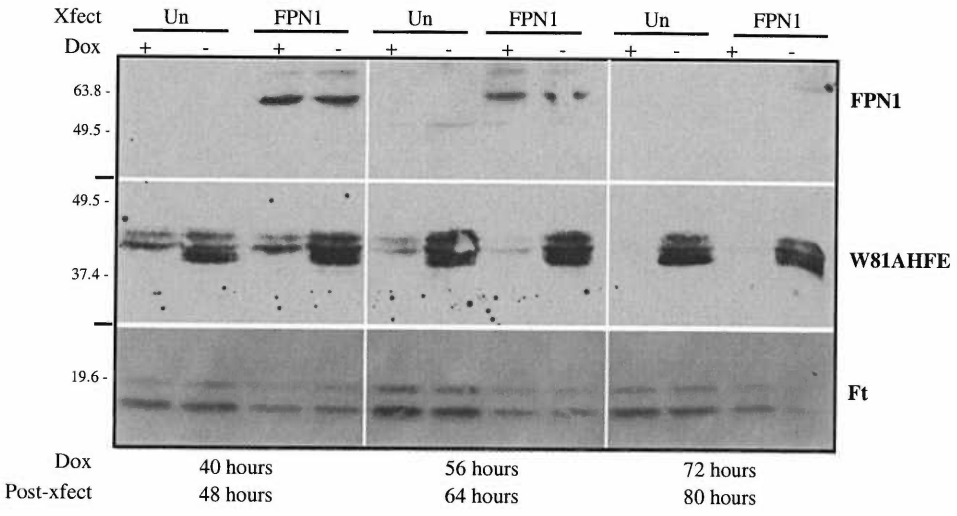


Figure S4.3. Transient transfection of FPN1 in fW81AHFE/tTA HeLa cells. fW81AHFE/tTA HeLa cells were transiently transfected with hWTFPN1-myc-his as described in the Materials & Methods. When fW81AHFE is expressed (Dox-), Ft levels decrease. This effect is unaltered by FPN1 transfection except that the overall Ft levels are lower due to iron being transported out of the cells. fW81AHFE expression does not change the effect of FPN1 expression on Ft levels.

SUMMARY AND CONCLUSIONS

This thesis depicts our evolving hypotheses regarding the role of HFE in maintaining cellular iron homeostasis. Understanding the function of HFE is important because when the protein does not fold and traffic correctly (C260Y mutant), iron accumulates in the body and, over time, leads to iron-catalyzed damage in multiple tissues. We took several approaches to determine the function of HFE in cellular iron homeostasis.

HFE Expression Lowers Intracellular Iron Levels in HeLa Cells

Previous data demonstrated that HFE expression decreases Ft levels and decreases Tf-mediated iron uptake into HeLa cells (Gross et al. 1998; Corsi et al. 1999; Riedel et al. 1999). We set out to ascertain if the HFE-specific decrease in Ft levels was due to increases in IRP binding activity in response to a reduction in the cellular labile iron pool. Using the fluorescent probe calcein, we established that HFE-expressing HeLa cells have a lower intracellular labile iron pool than cells in which HFE expression is turned off (Figure 1.6). Calcein is a fluorescent molecule whose signal is quenched when bound to iron (Cabantchik et al. 1996). When an iron-specific cell-permeable chelator is added (SIH), calcein is released from iron and the fluorescence is measured. A smaller change in the fluorescence of calcein upon addition of SIH is observed in HFE-expressing cells versus parent cells, indicating a decreased labile iron pool (Figure 1.6). This was an important piece of evidence demonstrating the effect of HFE on intracellular iron because changes in Ft as well as IRP binding activity can also occur in response to other factors besides iron levels. Such factors include signal transduction pathways (Schalinske and

Eisenstein 1996; Brown et al. 1998) or due to oxidative stress (Drapier et al. 1993; Weiss et al. 1993; Bouton et al. 1996; Pantopoulos et al. 1996; Hanson et al. 1999).

We wanted to test the mechanism by which HFE lowered intracellular iron levels. HFE-specific reduction of intracellular iron in HeLa cells takes place via the Tf-mediated uptake pathway (Corsi et al. 1999; Riedel et al. 1999; Roy et al. 1999). This effect could be attained by a variety of mechanisms. The cycling rates of TfR1 are not altered with HFE expression (Roy et al. 1999), discounting decreased receptor recycling as a means for less Tf-iron uptake. Furthermore, the competition of Tf and HFE for TfR1 binding is not an adequate explanation to account for less Tf-iron taken into the cell (Lebron et al. 1999). Even when there is sufficient Tf to saturate the TfR1, reduced Tf-mediated iron uptake is still observed (Roy et al. 1999) (Figure 3.2). These results lead to the hypothesis that HFE lowers iron uptake at the site of the endosome. To understand how HFE could accomplish this task, several hypotheses were tested. The loss of iron from receptor-bound Tf is pH dependent with the optimal pH approximately 5.6-6.0 (Sipe and Murphy 1991). HFE could increase the endosomal pH, thereby inhibiting iron release from Tf. Experiments examining the ratio of fluorescence between fluorescein, a pH-sensitive fluorophore, bound to diferric-Tf along with tetramethylrhodamine-labeled Tf, a pH-insensitive probe, show no change in endosomal pH with or without HFE expression (Figure 2.6). At the low pH of the endosome, TfR1 facilitates the release of iron from Tf (Bali and Aisen 1991; Sipe and Murphy 1991). We hypothesized that HFE might inhibit the conformational change in TfR1 at low pH that increases iron release from Tf. To examine this hypothesis, we measured the amount of iron remaining bound to Tf within the endosome by separation of apo-, monoferric-, or diferric-Tf species from the

endosomes of parent and HFE-expressing HeLa cells. No differences between the ratios of each Tf-species were detected, suggesting that HFE did not hinder the release of iron from Tf in the endosome (Figure 2.7).

The above experiments excluded potential mechanisms for how HFE reduces Tf-mediated iron uptake into cells, and led us to the hypothesis that HFE affects either the endosomal reductase or transporter (proposed to be DMT1 (Fleming et al. 1998; Su et al. 1998; Garrick et al. 1999; Gruenheid et al. 1999)) prior to transport of iron across the endosomal membrane into the cytosol. If HFE inhibits the transfer of iron from the endosome into the cytoplasm of HeLa cells, one would predict that the endosomes of HFE-expressing cells would have higher iron content than parent cells. Attempts were made to measure this difference by treatment of the two cell lines with ^{55}Fe-Tf followed by isolation of the endosomal vesicles in order to measure the radioactive iron within these compartments. This technique proved to be quite difficult, and while the expected decreased iron in the cytosolic fraction with HFE expression is observed, there is very low signal and no difference between the iron content of the endosomal isolations. The iron transport step from inside the endosome to the cytosol is probably quite fast (Gunshin et al. 1997; Nelson 1999; Sacher et al. 2001), and iron contained within the endosomes was unable to be captured. Even though this is an important remaining piece of evidence to further substantiate our data, it has proven quite problematic to address. The action of HFE in the endosome might be further clarified when the endosomal transporter and reductase are better characterized and experiments involving these proteins can be designed.

Interaction of HFE and TfR1

The first clue as to how HFE might affect iron homeostasis was the observation that HFE co-precipitates with TfR1 in cell lines expressing both proteins as well as in placental extracts (Parkkila et al. 1997b; Feder et al. 1998; Gross et al. 1998; Corsi et al. 1999; Roy et al. 1999). These two proteins can associate early in the biosynthetic pathway and interact on the cell surface (Gross et al. 1998). HFE and TfR1 co-localize in endosomal compartments (Roy et al. 1999), however, it was unclear from these studies if they remain associated once inside the cell. Binding studies using purified truncated forms of HFE and TfR1 lacking transmembrane and cytosolic domains indicate that their interaction drops sharply at a pH lower than 6.4 (Lebron and Bjorkman 1999). Since the pH of the endosome is usually between 5.6 and 6.4 depending on the cell type (Yamashiro and Maxfield 1984; Sipe and Murphy 1991), we wanted to determine whether the full length HFE and TfR1 could interact with each other in the endosome. Using the HFE-LAMP chimera protein (HFE with its cytoplasmic tail replaced with that of LAMP-1), we showed that HFE and TfR1 remain associated inside the cell. TfR1 half-life decreased in the HFE-LAMP-expressing cells compared to those expressing wild type HFE. This result implies that TfR1 remains associated with HFE upon internalization and is targeted to the lysosome along with the HFE chimera (Figure 2.3). Both TfR1 and HFE-LAMP exhibit different patterns of localization when examined by immunofluorescence, further demonstrating altered trafficking within the cells (figure 2.5). These findings were observed in the absence of any extracellular Tf. When Tf is added to the culture medium, the half-life for TfR1 increases, indicating that TfR1 is no longer targeted to lysosomes. This data suggests that HFE and TfR1 no longer associate

throughout the endocytic cycle in the presence of Tf (Figure 2.4). We then asked whether HFE and TfR1 interact at the cell surface and in endocytic pathways under physiological conditions, given that there are sufficient levels of Tf in the blood to saturate the TfR1 and compete away HFE for binding to the TfR1 (Lane 1975; Feder et al. 1998; Roy et al. 1999).

Effect of HFE on Cellular Iron Status is Independent of TfR1 Association

To ascertain if HFE could function to lower intracellular iron levels in the absence of association with TfR1, as might be expected with normal concentrations of Tf in the blood, we took advantage of an HFE mutant (W81A) that has more that 5,000-fold reduction in binding affinity for TfR1 than wild type HFE (Lebron and Bjorkman 1999). Stable transfections of this form of HFE into tTA HeLa cells gives similar results as the wild type HFE: lower Ft levels, a 30-40% reduction in Tf-iron uptake, and increases IRP binding activity (Figures 3.2 and 3.3). These findings indicated that the interaction of HFE with the TfR1 is not required for its effect on cellular iron status as had been the initial hypothesis.

HFE Increases Cellular Iron Levels when Expressed in Intestinal-like Cells

Most of the cell culture experiments that have been used to study the function of HFE are not representative cell types of those that are involved in iron homeostasis in the body. While studies in HeLa and HEK293 cells established mechanistic insight into the role of HFE in cellular iron homeostasis, a more physiologically relevant cell culture model would also be beneficial. We were interested to see what effect HFE might have

on cells of an intestinal origin. To test this, the colonic carcinoma cell line, HT29, which has many duodenal-like characteristics (Godefroy et al. 1988) was stably transfected with the fWTHFE or fW81AHFE plasmids used in our previous studies. Consistent with the HeLa cells, we observe little difference between effects of either WT or W81A HFE expression on cellular iron status, supporting the idea that HFE can have effects on iron levels independent of its interaction with the TfR1. However, the direction of the effect on iron status in response to HFE expression is opposite in HT29 cells compared to HeLa cells. In HFE-expressing HT29 cells, Ft levels increase and steady state levels of iron are higher than in the parent cells (Figures 4.2A, 4.3, and 4.2C). The increase in iron levels with HFE expression has been previously observed in both macrophages from patients and in a macrophage-like cell line (Montosi et al. 2000; Drakesmith et al. 2002); however, ours is the first data depicting the increased iron phenotype in intestinal-like cells. These results are consistent with the observation that intestinal enterocytes from patients with Type 1 HH, where HFE is not expressed, are iron-deprived (Pietrangelo et al. 1995).

Our initial findings of a high iron phenotype in HT29 cells were quite intriguing and led us to examine the expression patterns of the other genes involved in iron homeostasis in both HT29 and HeLa cells. In most cells involved in iron metabolism, two transporters are proposed to control iron influx (DMTI) and iron efflux (FPN1). HT29 cells express DMT1 and FPN1 mRNA at approximately the same level (Figure 4.1A, B, C). HeLa cells express nearly the same level of mRNA for DMT1 as HT29 cells; however, they express much less or do not express mRNA for proteins involved in iron export, FPN1 or Heph, respectively (Figure 4.1B). These observations led us to

hypothesize that the discrepancy in expression levels of iron export machinery might lead to the opposite effects on iron levels in the presence of HFE in HeLa and HT29 cells. We demonstrate that unlike HeLa cells, the Tf-mediated iron uptake pathway is unaltered in HFE-expressing HT29 cells (Table 4.2). Moreover, the rate of non-Tf bound iron uptake is unaffected with HFE expression (Figure 4.4A). Consistent with the increased iron status of the cells, we observe a decrease in iron efflux when HFE is expressed in HT29 cells (Figure 4.4B). If HFE acts to inhibit the efflux of iron from cells, this would not be apparent when studying HeLa cells because they do not export iron. In this circumstance, HFE could have an alterative effect, possibly inhibiting DMT1 transport of iron from the endosome to the cytosol, leading to decreased intracellular iron levels. The cellular iron acquisition in HeLa and HT29 cells is comparable prior to HFE transfection (Table 0.1); however, these cells differ in the ability to export iron. This suggests that the iron export pathway may be involved in yielding the opposite iron phenotypes observed when HFE is expressed in each cell line.

Multiple Roles of HFE in the Maintenance of Iron Homeostasis

Interactions between HFE and TfR1 occur *in vitro* (Feder et al. 1998; Gross et al. 1998; Bennett et al. 2000; Roy et al. 2000). However, we have evidence that this interaction may not be required for HFE to alter iron status as previously hypothesized (Feder et al. 1998; Gross et al. 1998; Roy et al. 2000; Zhang et al. 2003; Davies and Enns 2004). Given that multiple cell types express these two proteins, in addition to others involved in iron metabolism, the distinct function of HFE may be multifaceted and involve more binding partners than just TfR1. Different MHC-class I molecules use

different interfaces of the protein to interact with their ligands. For example, the T-cell receptor interacts with the peptide-binding groove formed by the α-1 and α-2 domains of the MHC class I molecule, while CD8 interacts with the base of the α-3 domain ((Garcia et al. 1999) and references therein). The Fc portion of immunoglobulin G interacts with the α-2 domain on the neonatal Fc receptor (FcRn), another MHC class I similar molecule, which is responsible for transporting maternal IgG to the fetus (Burmeister et al. 1994). Similar to the T cell receptor, TfR1 interacts with the α-1 and α-2 domains of HFE, the groove that is too narrow to bind peptide (Bennett et al. 2000). We hypothesize that HFE interacts with different molecules through its different binding interfaces to alter iron homeostasis. We propose that HFE can interact with proteins involved in both iron influx and efflux depending on expression levels of such target proteins in different cell types.

In addition to the intestine, the liver plays a fundamental role in iron homeostasis as the site for excess iron storage in the body. Communication between the storage site of the liver and the absorption site of the intestine is crucial for properly balancing the body's iron needs. Hepcidin, a peptide secreted by the liver, is hypothesized to play the part of this communicator acting as the "iron stores regulator". The effect of HFE expression on hepcidin levels remains controversial. In the β2m knockout mouse model of HH, hepcidin expression is reportedly increased (Pigeon et al. 2001). Conversely, two other reports do not detect any difference or decreased hepcidin levels with HFE expression when examining the HFE knockout mouse model (Ahmad et al. 2002; Muckenthaler et al. 2003). These results, although contradictory, suggest that HFE might

also be involved in regulation of hepcidin expression and play yet another role in iron homeostasis.

Data in this thesis rethinks the long-standing model for the requirement of an interaction between HFE and TfR1 in order to maintain iron homeostasis. We propose that HFE has multiple binding partners to exert appropriate effects to maintain cellular iron homeostasis. Alternatively, the cellular localization of HFE and other proteins involved in iron transport may differ by cell type allowing for HFE to carry out multiple effects. Forthcoming experiments should focus on determining these target proteins and their cell type-specific localization. Eight years after the long-awaited discovery of HFE, we have learned that its role in maintaining cellular and organismal iron homeostasis is both elegant and complex and its mystery provides for many exciting future experiments.

APPENDIX I – Polarized HT29 Cells as a Model for Intestinal Villus Cells

RATIONALE

We originally hypothesized that polarized HT29 cells could be used as a culture model for intestinal villus cells. When polarized, HT29 cells can form a brush border membrane and microvilli. However, we found they also tend to grow in clumps and in multiple cell layers on the filter inserts. It turns out that HT29 cells did not polarize into a uniform monolayer across the entire surface of the filter insert, therefore were not suitable for iron transport experiments. These cells are more appropriate as a model for generalized intestinal epithelial cells because they endogenously express the mRNA of proteins involved in iron transport, unlike other less differentiated cell lines such as HeLa (Figure 4.1). Some initial work was carried out, however, to determine if mRNA expression in isolated mouse villus versus crypt cells coordinated with the expression pattern in polarized compared to non-polarized HT29 cells.

MATERIALS AND METHODS

Animals –

Wild type C57BL/6 mice (4, 8, and 16 weeks of age) were kindly provided by Dr. Melissa H. Wong (Dept. of Dermatology, OHSU).

Isolation of Villus and Crypt Cells -

The small intestine was removed from a sacrificed mouse and the proximal 4 cm were used in these experiments (representing the duodenum). The tissue was flushed with PBS to remove luminal contents, cut open longitudinally, and further rinsed five times in HBSS (Hank's Balanced Salt Solution without calcium or magnesium; Invitrogen) to remove any remaining luminal contents. Villus and crypt cells were isolated following a modified version of the Weiser method (Weiser 1973). This method is based on loosening the attachments of enterocytes and their release by rotating and vortexing with DTT and EDTA-containing solutions. The removal of calcium by EDTA causes a loss of protein-mediated calcium-dependent adhesion of cells to one another and to the basement membrane. The tissue (from one or multiple mice of the same sex and age) was placed in a 50 ml conical vial with ice cold HBSS supplemented with 1mM EDTA and 1mM DTT. This was rotated at 4°C for 15 minutes and vortexed at high speed for 15 seconds. The tissue was removed and placed in a new tube containing a fresh ice-cold aliquot of the above solution. The first aliquot was spun at 1,000 rpm at 4°C for 10 min in a Beckman tabletop centrifuge. The supernatant was discarded and the pellet of villus cells was kept on ice. The 15 min incubation and 15 sec vortex was

repeated for the tissue in the second aliquot. The tissue was then removed, the remaining solution was added to the first pellet and spun as described above to combine the villus factions. The tissue that was removed was placed in a tube with a final solution of fresh ice cold HBSS supplemented with 5mM EDTA and 1mM DTT. The increased concentration of EDTA in the final solution was used to aid in removing all of the remaining cells, representing the crypts. After the 15 min incubation of the final solution, the sample was vortexed for 30 - 45 sec to fully remove the remaining cells, spun as before, the supernatant discarded, and the resulting crypt pellet was kept on ice. One piece of tissue, however, was removed after each step and placed in formalin fixative for later histological analysis.

Preparation and Staining of Intestinal Tissue –

In order to confirm that the appropriate cells were removed (villus cells in first two spins and crypt cells in final spin), hematoxylin and eosin (H&E) staining was carried out to examine tissue morphology. First, the samples that were removed at distinct stages during the villus/crypt cell isolation were placed in formalin fixative and pinned open so the villi faced upward. They were gently rocked in the fixative at room temperature for one hour, washed three times with 70% ethanol for 15 minutes each, and soaked in 70% ethanol overnight. The next day, the tissue was unpinned and prepared for paraffin embedding by stacking in 2% agarose. The tissue preparations were sent to the OHSU Cancer Institute Core Facility for paraffin embedding, sectioning, and H&E staining.

Musashi-1 PCR –

Another method used to confirm relative purity of the villus and crypt cell isolations was to examine each fraction by PCR with primers for the gene *musashi-1*. Musashi-1 is a marker of stem and early lineage progenitor cells in murine intestinal tissue with predominant expression in regenerating crypts (Potten et al. 2003). This crypt-specific marker was used to determine if our isolations were consistent with villus-enriched and crypt-enriched populations. RNA was isolated from the villus and crypt fractions, or from whole intestinal tissue flash frozen in liquid nitrogen, using the RNeasy RNA Isolation Kit (Qiagen) and treated with 10 units of DNaseI (Roche) to remove any contaminating genomic DNA. cDNA was synthesized using Oligo dT primers and Superscript II Reverse Transcriptase (Invitrogen). PCR was carried out for 30 and 40 cycles. The musashi-1 primer sequences used were forward primer: 5'-TGGTCGCTTTTATTTATTTTTGGAT-3' and reverse primer: 5'-CCGGAGGAGAGGGCAGAT-3' (Potten et al. 2003). Samples were run on a 3% agarose gel containing ethidium bromide and bands were visualized with UV light.

qRT-PCR -

Isolation of RNA, DNase-treatment, and cDNA synthesis was achieved as described above for the isolated villus and crypt pellets. Samples were diluted 1:5 after cDNA synthesis and PCR using mouse GAPDH primers spanning an intron/exon junction was performed to check cDNA yield and confirm the absence of genomic DNA contamination in samples containing no reverse transcriptase. Real-time qRT-PCR was carried out in triplicate on each sample for each gene in at least three independent

experiments using the SYBR Green detection system on an ABI PRISM 7900 machine (Applied Biosystems). Melting curve experiments established that the fluorescent signal for each amplicon was derived from product only and not from primer dimers. The primer pairs used were designed with the Primer Express Software (Applied Biosystems), synthesized by IDT Technologies, and are shown in Table AI.1. Data was analyzed as described in Chapter 4.

Confocal Microscopy of Polarized HT29 Cells -

The morphology of HT29 cells polarized on filter inserts was analyzed by confocal microscopy and a fluorescent membrane dye. Cells were seeded at approximately 7 x 10^4 cells/cm^2 0.4-micron filter inserts in 24-well plates and maintained for 14 days. Cells on the filter were washed in room temperature HANKS (without sodium bicarbonate) and fixed in 4% paraformaldehyde for 15 minutes. The cells were then washed twice in HANKS and 1ng/μl FM1-43, a fluorescent membrane dye (gift from Dr. Maggie So, OHSU; Molecular Probes) was added on either side of the filter insert for 15 minutes at room temperature. Filters were cut away from the plastic inserts with a scalpel and mounted cell-side down in a drop of ProLong Antifade (Molecular Probes) on a glass slide. The filter was folded halfway back to protrude the cells on the filter at the folded edge and a coverslip was placed on top. Alternatively, some filters were not folded and were mounted flat. Cells were imaged by Aurelie Snyder in the Oregon Health & Science University/Medical Marketing International Research Core Facility with Applied Precision Deltavision image restoration system on a Nikon microscope.

RESULTS AND DISCUSSION

A method for isolating villus-enriched and crypt-enriched cell populations from mice was established. Using the Weiser method with some modifications, I was able to sequentially remove the villus and crypt cells along the villus core and into the crypts of Lieberkuhn (Figure AI.1). Histological examination of the tissue samples after each isolation step allowed for the monitoring of cell removal. A cross-section taken prior to cell isolation demonstrates, by H&E stain, the crypt cells located in the invaginations of the basement membrane and the villus cells surrounding the villi core (Figure AI.1A). After each sequential incubation/vortex step, the villus cells were removed (Figure AI.1 B & C). Finally, the crypt cells were detached in the last fraction with the more stringent EDTA solution (Figure AI.1D).

I further examined the purity of the villus and crypt cell isolations by PCR with primers for Musashi-1, a crypt-specific marker. At 30 cycles, signal appears in the crypt fraction and no signal is detected in the villus fraction (Figure AI.2) however, by 40 cycles some signal is present in the villus fraction indicating some cross contamination in the cell isolation procedure. Judging from the intensity of the bands at 30 and 40 cycles, the contamination of villus cells with crypt cells is estimated to be 10-20%. This was also apparent in some portions of the H&E stained cross-sections, in that sometimes not all villus cells were removed prior to the crypt cell isolation step (data not shown). Even though this isolation is not complete, it does enrich for one cell type over the other.

Real-time qRT-PCR was carried out for the genes of interest on the villus and crypt fractions isolated from wild type mice. The data was analyzed for each age group

individually and then averaged together since the results were comparable between the three age groups used (4, 8, and 16 weeks). There was more TfR1 and HFE expression in crypt cells, approximately 4 and 2-fold, respectively. The overall finding, however, was that mRNA for all of the genes tested were expressed in both villus and crypt-enriched cell fractions (Figure AI.3).

Data in the literature demonstrate mRNA expression of HFE and TfR1 in the crypts with the expression ceasing at the crypt/villus junction (Jeffrey et al. 1996; Oates and Morgan 1996b), but we can detect expression of both HFE and TfR1 in our villus cell isolations. Reports in the literature from in situ hybridization experiments demonstrate that DMT1 mRNA is expressed in the lower two-thirds of the villus, but there is conflicting data on expression patterns of DMT1 message in the crypt region or tips of the villi when examining rats on control diets (Gunshin et al. 1997; Oates et al. 2000b; Trinder et al. 2000). FPN1 mRNA expression is reported to be weak or undetectable in the crypts with the intensity increasing along the length of the villi in mice fed both a control or iron-deficient diet (Donovan et al. 2000; McKie et al. 2000). *In situ* hybridization methods were used to obtain the published conclusions and are not as sensitive as qRT-PCR, so low levels of message could have been overlooked. Alternatively, there is some cross-contamination in our villus/crypt cell isolations, and the fractions obtained can only be called "villus-enriched" and "crypt-enriched". This disparity might be overtly apparent when examining precise mRNA levels. Furthermore, the C57BL/6 mice have been shown to have a low Tf saturation and liver iron content under normal diets compared to other commonly used mouse strains, which could affect

the mRNA expression levels of DMT1 and FPN1 (Dupic et al. 2002b; Dupic et al. 2002a).

When the mRNA expression levels of the iron-related genes we tested are compared between polarized HT29 cells (Figure 4.1C) and villus-enriched fractions from C57BL/6 mice (Figure AI.3), there are some similarities. TfR1 and DMT1 are expressed approximately the same amount in both the cell line and the animal. FPN1 is expressed approximately 10-fold higher in the villus cells, Hephaestin about 4-fold higher, and Dcytb approximately 2.5-fold higher. The expression patterns, for the non-polarized cells cannot be coordinated with the crypt cells, however, because there is still similar expression in the crypts as the villi, whereas we see a 20-30-fold increase in some cases upon polarization of HT29 cells. This is not surprising, however, because even though crypt cells are undifferentiated, they still maintain polarized membranes.

With more sensitive techniques available, the subtle differences in expression patterns of iron-related genes will become more apparent. What might have once been thought to be a clear, robust expression in one area of tissue and declared absent another portion, might be challenged by a method of analyzing crypt and villi populations separately. Future experiments might take advantage of laser capture microdissection to further and more purely isolate these cell types. The isolated cell populations could be analyzed by qRT-PCR to elucidate subtle expression patterns and would allow for more precise and intricate investigation of cells along the length of the crypt/villus axis. This would help clarify the data presented in the literature regarding mRNA expression patterns of these important iron-related genes and lead to a better idea of when cells express different genes throughout migration and differentiation.

Originally, we hypothesized that HT29 cells polarized on filter inserts could be a culture model for villus cells. We reasoned that the apical membranes and basolateral membranes would create a unified cell monolayer where iron transport studies could be carried out mimicking iron transport across the intestinal villus cells. When HT29 cells were polarized on filter inserts and examined by confocal microscopy, however, we see that they grow in layers of more than one cell thick (Figure AI.4). In some instances there was a true monolayer formed, however this was not the case across the entire surface area of the filter insert. This type of growth made it difficult to do iron transport studies representative of iron transport across a single layer of villus cells in the duodenum. Therefore, we decided to use HT29 cells as a general model for intestinal-like cells since they endogenously express genes involved in iron transport. Given that, a line of further experimentation to coordinate the HT29 cell culture data to the isolated mouse cells was not further pursued.

Gene	Forward Primer	Reverse Primer
mGAPDH* (MW104/MW105)	5'-AAATATGACAACTCACTCAAGATTGTCA-3'	5'-CCCTTCCACAATGCCAAAGT-3'
mDcytb (171F/291R)	5'-GTGACCGGCTTCGTCTTCAT-3'	5'-TGGCAGCCACAGCGTTTAA-3'
mDMT1 (1706F/1847R)	5'-CCGCTCAGCCTGAACTCTATCTT-3'	5'-CCGAACTAAGGGATTTGCTAACA-3'
mFPN1 (1240F/1381R)	5'-TGACAGTCCTGGGCTTTGACT-3'	5'-TTTCGACGTAGCCAGGTGAAG-3'
mHeph 2559F/2660R	5'-GCCTGGGCACAGAGACTGAT-3'	5'-AGGTGTGAGGAAAGAGCATGACT-3'
mHFE (718F/859R)	5'-TCTGGGACAGCAAGTGCCTACT-3'	5'-GGCATCCAGTGGTTGGTTGT-3'
mTfR1 (1265F/1410R)	5'-CCAGTGTGGGAACAGGTCTTC-3'	5'-CAACCACTCAGTGGCACCAA-3'
mTf (49F/124R)	5'-TGTCTGGCTGTCCCTGACAA-3'	5'-GGAAGCTGATGCATTTGGTATTC-3'

Table AI.1 Primer sets used for qRT-PCR of mouse samples. All primer sets were designed according to mouse gene sequences from GenBank to yield amplicons of ~75-140 base pairs. *mGAPDH primers were originally designed in the laboratory of Dr. Melissa H. Wong.

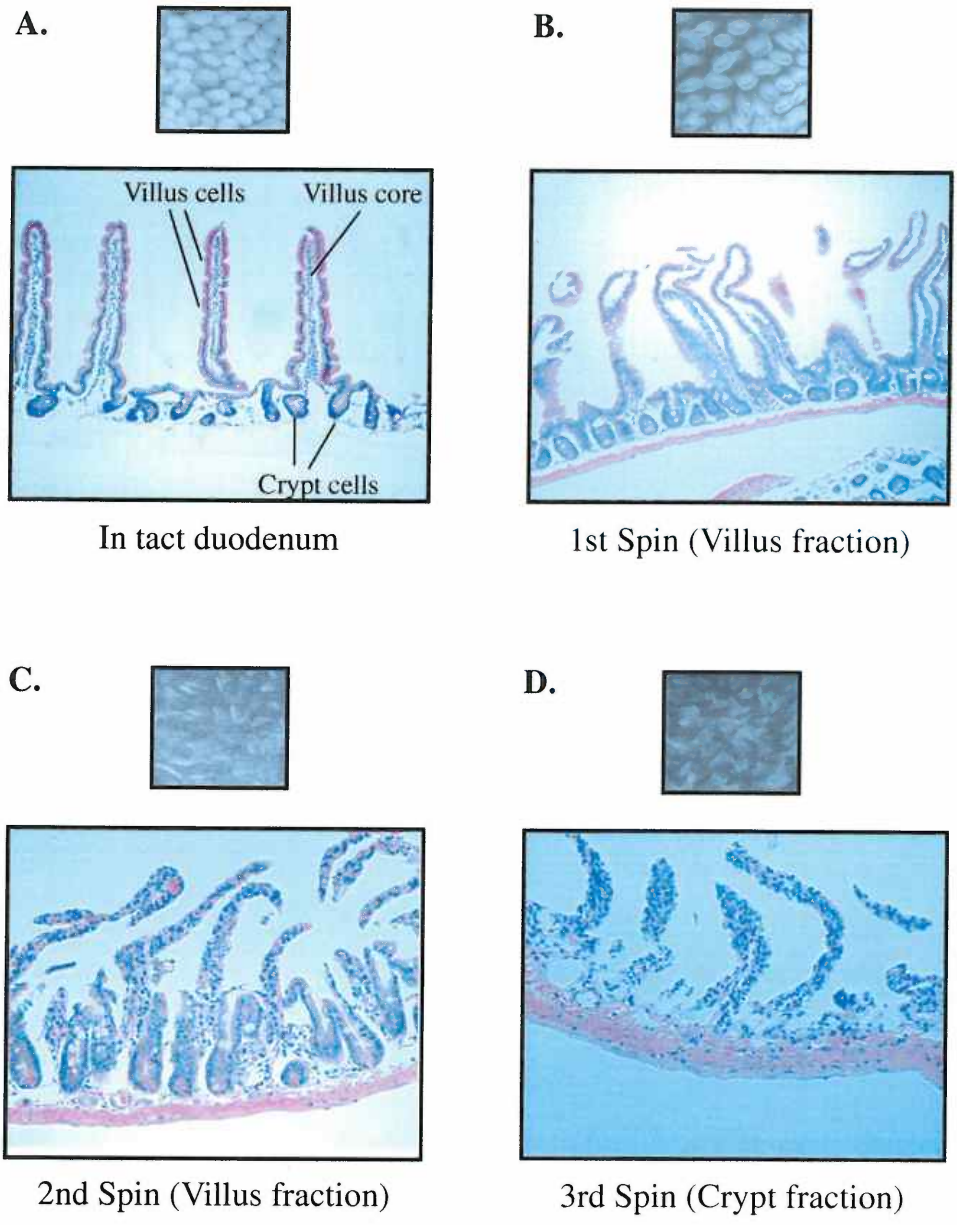


Figure AI.1. Isolation of villus and crypt cells from mouse duodenum. A modified Weiser method was used to sequentially isolate villus and crypt cells from mouse duodenum. The smaller panels are light microscopy looking down on the tissue (villi protruding from the plane). The larger panels are cross-sections of tissue that have been H&E stained to assess morphology. **A)** A sample of mouse duodenum prior to cell isolation procedures. The cross-section depicts cells lining the crypt invaginations as well as lining and surrounding the villi core all the way to the tip. **B)** After the first spin, the cells on the villi tips are removed. **C)** After the second spin, the villus cells along the length of the villi are removed; the villus core and crypt cells remain. **D)** After the final and more stringent wash and spin, the crypt cells are removed.

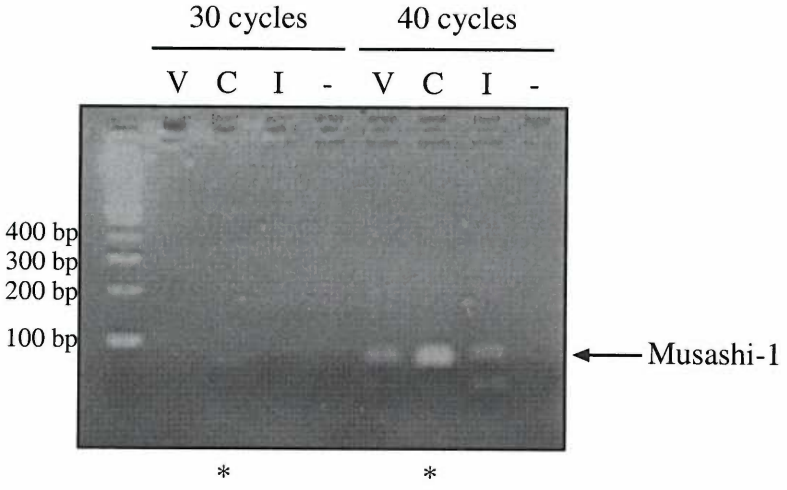


Figure AI.2. Examination of villus and crypt fractions by Musashi-1 PCR. Templates of water (-) or cDNA from mouse villus cells (V), crypt cells (C), or proximal intestine (I) were run in a 20μl PCR reaction for 30 or 40 cycles. Five μl were run on a 3% agarose gel. Musashi-1 expression is detected in the crypt fraction by 30 cycles (*), whereas no signal is detected in the other lanes. At 40 cycles, this signal in the crypt lane is quite strong (*). There is some signal coming up at 40 cycles in the proximal intestine, which would be expected due to the contribution of the crypt cell population. The signal that begins to appear at 40 cycles for the villus sample could be due to contamination of the isolated cell population with some crypt cells.

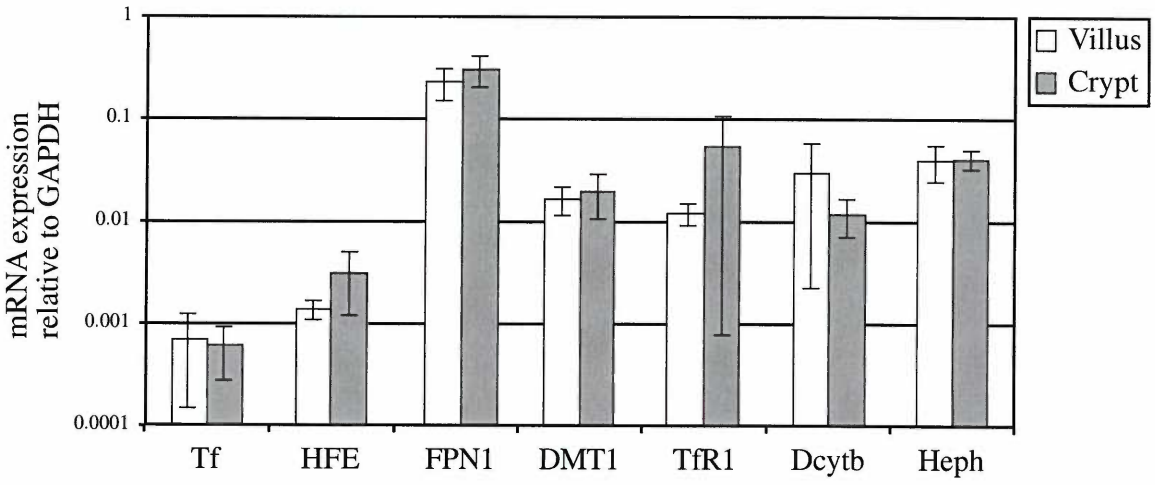


Figure AI.3. Both villus and crypt cells express mRNA of iron-related genes. Real-time qRT-PCR was carried out for genes involved in iron homeostasis on isolated villus and crypt fractions from wild type mice. Samples were run in triplicate in at least two independent experiments, normalized to the internal control GAPDH, and the average ± SD is depicted.

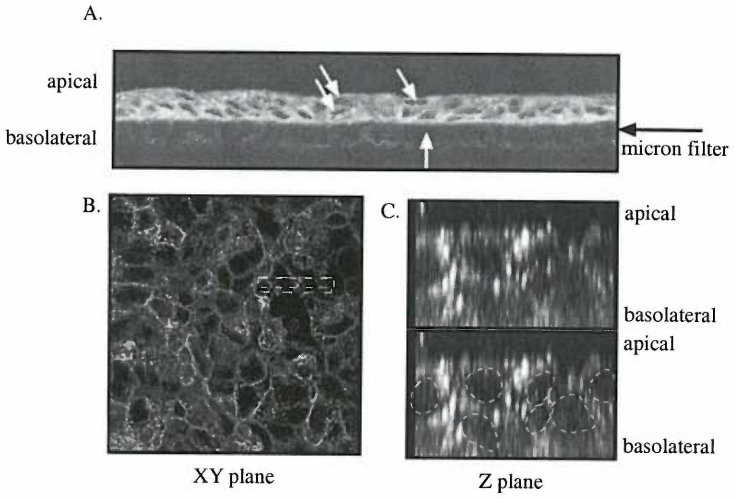


Figure AI.4. Confocal microscopy of HT29 cells seeded on filter inserts. Parent HT29 cells were grown for 14 days on polyester filter inserts and subsequently stained with FM1-43 fluorescent dye to define membrane morphology and observed by confocal microscopy. **A**) Cells were stained and the filter membrane was folded in half under a glass coverslip and the folded-edge was imaged. The cells are sitting with the basolateral membrane on the filter insert with their apical membrane facing upwards. The cells form a layer more than one cell deep as can be seen noting the multiple nuclei (arrows). **B**) Cells from a non-folded filter were imaged in an XY plane. The white-dashed box in the upper right of the panel was selected for further analysis of the Z-section. **C**) Z-section of the selected area in panel B. The lower panel is a duplicate of the upper panel with the nuclei outlined that are stacked on top of one another, demonstrating a multilayer of cells.

REFERENCES

Abboud S. and Haile D. J. (2000) A novel mammalian iron-regulated protein involved in intracellular iron metabolism. *J. Biol. Chem.* **275,** 19906-19912.

Ahmad K. A., Ahmann J. R., Migas M. C., Waheed A., Britton R. S., Bacon B. R., Sly W. S. and Fleming R. E. (2002) Decreased liver hepcidin expression in the Hfe knockout mouse. *Blood Cells Mol. Dis.* **29,** 361-366.

Aisen P. (1998) Transferrin, the transferrin receptor, and the uptake of iron by cells. *Met. Ions Biol. Syst.* **35,** 585-631.

Anderson G. J., Frazer D. M., McKie A. T., Wilkins S. J. and Vulpe C. D. (2002) The expression and regulation of the iron transport molecules hephaestin and IREG1: implications for the control of iron export from the small intestine. *Cell Biochem. Biophys.* **36,** 137-146.

Anderson G. J., Murphy T. L., Cowley L., Evans B. A., Halliday J. W. and McLaren G. D. (1998) Mapping the gene for sex-linked anemia: an inherited defect of intestinal iron absorption in the mouse. *Genomics* **48,** 34-39.

Andrews N. C. (1999) Disorders of iron metabolism. *N. Engl. J. Med.* **341,** 1986-1995.

Askwith C. and Kaplan J. (1998) Iron and copper transport in yeast and its relevance to human disease. *Trends Biochem. Sci.* **23,** 135-138.

Aziz N. and Munro H. N. (1987) Iron regulates ferritin mRNA translation through a segment of its 5' untranslated region. *Proc. Natl. Acad. Sci. U. S. A.* **84,** 8478-8482.

Bali P. K. and Aisen P. (1991) Receptor-modulated iron release from transferrin: differential effects on N- and C-terminal sites. *Biochemistry* **30,** 9947-9952.

Bali P. K. and Aisen P. (1992) Receptor-induced switch in site-site cooperativity during iron release by transferrin. *Biochemistry* **31,** 3963-3967.

Bali P. K., Zak O. and Aisen P. (1991) A new role for the transferrin receptor in the release of iron from transferrin. *Biochemistry* **30,** 324-328.

Bannerman R. M. (1976) Genetic defects of iron transport. *Fed. Proc.* **35,** 2281-2285.

Barton J. C., Sawada-Hirai R., Rothenberg B. E. and Acton R. T. (1999) Two novel missense mutations of the HFE gene (I105T and G93R) and identification of the S65C mutation in Alabama hemochromatosis probands. *Blood Cells Mol. Dis.* **25,** 147-155.

Ben-Arieh S. V., Zimerman B., Smorodinsky N. I., Yaacubovicz M., Schechter C., Bacik I., Gibbs J., Bennink J. R., Yewdell J. W., Coligan J. E., Firat H., Lemonnier F. and Ehrlich R. (2001) Human cytomegalovirus protein US2 interferes with the expression of human HFE, a nonclassical class I major histocompatibility complex molecule that regulates iron homeostasis. *J. Virol.* **75,** 10557-10562.

Bennett M. J., Lebron J. A. and Bjorkman P. J. (2000) Crystal structure of the hereditary haemochromatosis protein HFE complexed with transferrin receptor. *Nature* **403,** 46-53.

Beutler E. (2003) The HFE Cys282Tyr mutation as a necessary but not sufficient cause of clinical hereditary hemochromatosis. *Blood* **101,** 3347-3350.

Beutler E., Hoffbrand A. V. and Cook J. D. (2003) Iron deficiency and overload. *Hematology (Am. Soc. Hematol. Educ. Program)* pp 40-61.

Bezwoda W. R., Bothwell T. H., Charlton R. W., Torrance J. D., MacPhail A. P., Derman D. P. and Mayet F. (1983) The relative dietary importance of haem and non-haem iron. *S. Afr. Med. J.* **64,** 552-556.

Bomford A. (2002) Genetics of haemochromatosis. *Lancet* **360,** 1673-1681.

Bothwell T. H. and Charlton R. W. (1979) Current problems of iron overload. *Recent Results in Cancer Research* **69,** 87-95.

Bothwell T. H. and MacPhail A. P. (1998) Hereditary hemochromatosis: etiologic, pathologic, and clinical aspects. *Semin. Hematol.* **35,** 55-71.

Bothwell T. H., Charlton R. W. and Motulsky A. G., eds (1995) *The Metabolic and Molecular Basis of Inherited Disease,* Seventh Edition, Vol. II, pp 2237-2269. McGraw-Hill, Inc., San Francisco.

Bouton C., Raveau M. and Drapier J. C. (1996) Modulation of iron regulatory protein functions. Further insights into the role of nitrogen- and oxygen-derived reactive species. *J. Biol. Chem.* **271,** 2300-2306.

Bowen B. and Morgan E. H. (1987) Anemia of the Belgrade rat: Evidence for defective membrane transport of iron. *Blood* **70,** 38-44.

Bridle K. R., Frazer D. M., Wilkins S. J., Dixon J. L., Purdie D. M., Crawford D. H., Subramaniam V. N., Powell L. W., Anderson G. J. and Ram G. A. (2003) Disrupted hepcidin regulation in HFE-associated haemochromatosis and the liver as a regulator of body iron homoeostasis. *Lancet* **361,** 669-673.

Brown N. M., Anderson S. A., Steffen D. W., Carpenter T. B., Kennedy M. C., Walden W. E. and Eisenstein R. S. (1998) Novel role of phosphorylation in Fe-S cluster stability

revealed by phosphomimetic mutations at Ser-138 of iron regulatory protein 1. *Proc. Natl. Acad. Sci. U. S. A.* **95,** 15235-15240.

Brunt E. M., Olynyk J. K., Britton R. S., Janney C. G., Di Bisceglie A. M. and Bacon B. R. (2000) Histological evaluation of iron in liver biopsies: relationship to HFE mutations. *Am. J. Gastroenterol.* **95,** 1788-1793.

Burmeister W. P., Huber A. H. and Bjorkman P. J. (1994) Crystal structure of the complex of rat neonatal Fc receptor with Fc. *Nature* **372,** 379-383.

Cabantchik Z. I., Glickstein H., Milgram P. and Breuer W. (1996) A fluorescence assay for assessing chelation of intracellular iron in a membrane model system and in mammalian cells. *Anal. Biochem.* **233,** 221-227.

Cairo G., Tacchini L. and Pietrangelo A. (1998) Lack of coordinate control of ferritin and transferrin receptor expression during rat liver regeneration. *Hepatol.* **28,** 173-178.

Cairo G., Recalcati S., Montosi G., Castrusini E., Conte D. and Pietrangelo A. (1997) Inappropriately high iron regulatory protein activity in monocytes of patients with genetic hemochromatosis. *Blood* **89,** 2546-2553.

Camaschella C., Roetto A. and De Gobbi M. (2002) Juvenile hemochromatosis. *Semin. Hematol.* **39,** 242-248.

Camaschella C., Roetto A., Cali A., De Gobbi M., Garozzo G., Carella M., Majorano N., Totaro A. and Gasparini P. (2000) The gene *TFR2* is mutated in a new type of haemochromatosis mapping to 7q22. *Nat. Genet.* **25,** 14-15.

Canonne-Hergaux F., Gruenheid S., Ponka P. and Gros P. (1999) Cellular and subcellular localization of the Nramp2 iron transporter in the intestinal brush border and regulation by dietary iron. *Blood* **93,** 4406-4417.

Canonne-Hergaux F., Fleming M. D., Levy J. E., Gauthier S., Ralph T., Picard V., Andrews N. C. and Gros P. (2000) The Nramp2/DMT1 iron transporter is induced in the duodenum of microcytic anemia *mk* mice but is not properly targeted to the intestinal brush border. *Blood* **96,** 3964-3970.

Casey J. L., Di Jeso B., Roa K., Klausner R. D. and Harford J. B. (1988a) Two genetic loci participate in the regulation by iron of the gene for the human transferrin receptor. *Proc. Natl. Acad. Sci. U. S. A.* **85,** 1787-1791.

Casey J. L., Koeller D. M., Ramin V. C., Klausner R. D. and Harford J. B. (1989) Iron regulation of transferrin receptor mRNA levels requires iron-responsive elements and a rapid turnover determinant in the 3' untranslated region of the mRNA. *EMBO J.* **8,** 3693-3699.

Casey J. L., Hentze M. W., Koeller D. M., Caughman S. W., Rouault T. A., Klausner R. D. and Harford J. B. (1988b) Iron-responsive elements: regulatory RNA sequences that control mRNA levels and translation. *Science* **240,** 924-928.

Chen H., Attieh Z. K., Su T., Syed B. A., Gao H., Alaeddine R. M., Fox T. C., Usta J., Naylor C. E., Evans R. W., McKie A. T., Anderson G. J. and Vulpe C. D. (2004) Hephaestin is a ferroxidase that maintains partial activity in sex linked anemia mice. *Blood.* epub ahead of print.

Chen O. S., Schalinske K. L. and Eisenstein R. S. (1997) Dietary iron intake modulates the activity of iron regulatory proteins and the abundance of ferritin and mitochondrial aconitase in rat liver. *J. Nutr.* **127,** 238-248.

Conrad M. E. and Crosby W. H. (1963) Intestinal mucosal mechanisms controlling iron absorption. *Blood* **22,** 406-415.

Corsi B., Levi S., Cozzi A., Corti A., Altimare D., Albertini A. and Arosio P. (1999) Overexpression of the hereditary hemochromatosis protein, HFE, in HeLa cells induces and iron-deficient phenotype. *FEBS Lett.* **460,** 149-152.

Cox T. M. and Peters T. J. (1980) Cellular mechanisms in the regulation of iron absorption by the human intestine: studies in patients with iron deficiency before and after treatment. *Br. J. Haematol.* **44,** 75-86.

Daniele B. and D'Agostino L. (1994) Proliferation and differentiation of the small intestinal epithelium: from Petri dish to bedside. *Ital. J. Gastroenterol.* **26,** 459-470.

Dautry-Varsat A., Ciechanover A. and Lodish H. F. (1983) pH and the recycling of transferrin during receptor-mediated endocytosis. *Proc. Natl. Acad. Sci. U. S. A.* **80,** 2258-2262.

Davies P. S. and Enns C. A. (2004) Expression of the hereditary hemochromatosis protein, HFE, increases ferritin levels by inhibiting iron export in HT29 cells. *J. Biol. Chem.* epub ahead of print.

Davies P. S., Zhang A. S., Anderson E. L., Roy C. N., Lampson M. A., McGraw T. E. and Enns C. A. (2003) Evidence for the interaction of the hereditary haemochromatosis protein, HFE, with the transferrin receptor in endocytic compartments. *Biochem. J.* **373,** 145-153.

De Gobbi M., Roetto A., Piperno A., Mariani R., Alberti F., Papanikolaou G., Politou M., Lockitch G., Girelli D., Fargion S., Cox T. M., Gasparini P., Cazzola M. and Camaschella C. (2002) Natural history of juvenile haemochromatosis. *Br. J. Haematol.* **117,** 973-979.

Devalia V., Carter K., Walker A. P., Perkins S. J., Worwood M., May A. and Dooley J. S. (2002) Autosomal dominant reticuloendothelial iron overload associated with a 3-base pair deletion in the ferroportin 1 gene (SLC11A3). *Blood* **100,** 695-697.

Donovan A., Brownlie A., Zhou Y., Shepard J., Pratt S. J., Moynihan J., Paw B. H., Drejer A., Barut B., Zapata A., Law T. C., Brugnara C., Lux S. E., Pinkus G. S., Pinkus J. L., Kingsley P. D., Palis J., Fleming M. D., Andrews N. C. and Zon L. I. (2000) Positional cloning of zebrafish ferroportin1 identifies a conserved vertebrate iron exporter. *Nature* **403,** 776-781.

Drakesmith H., Sweetland E., Schimanski L., Edwards J., Cowley D., Ashraf M., Bastin J. and Townsend A. R. (2002) The hemochromatosis protein HFE inhibits iron export from macrophages. *Proc. Natl. Acad. Sci. U. S. A.* **99,** 15602-15607.

Drapier J. C., Hirling H., Wietzerbin J., Kaldy P. and Kuhn L. C. (1993) Biosynthesis of nitric oxide activates iron regulatory factor in macrophages. *EMBO J.* **12,** 3643-3649.

Dunn K. W., Park J., Semrad C. E., Gelman D. L., Shevell T. and McGraw T. E. (1994) Regulation of endocytic trafficking and acidification are independent of the cystic fibrosis transmembrane regulator. *J. Biol. Chem.* **269,** 5336-5345.

Dupic F., Fruchon S., Bensaid M., Loreal O., Brissot P., Borot N., Roth M. P. and Coppin H. (2002a) Duodenal mRNA expression of iron related genes in response to iron loading and iron deficiency in four strains of mice. *Gut* **51,** 648-653.

Dupic F., Fruchon S., Bensaid M., Borot N., Radosavljevic M., Loreal O., Brissot P., Gilfillan S., Bahram S., Coppin H. and Roth M. P. (2002b) Inactivation of the hemochromatosis gene differentially regulates duodenal expression of iron-related mRNAs between mouse strains. *Gastroenterol.* **122,** 745-751.

Edwards C. Q., Griffen L. M., Drummond C., Skolnick M. H. and Kushner J. P. (1988) Screening for hemochromatosis in healthy blood donors. Preliminary results. *Ann. N. Y. Acad. Sci.* **526,** 258-273.

Edwards J. A. and Bannerman R. M. (1970) Hereditary defect of intestinal iron transport in mice with sex-linked anemia. *J. Clin. Invest.* **49,** 1869-1871.

Edwards J. A., Sullivan A. L. and Hoke J. E. (1980) Defective delivery of iron to the developing red cell of the Belgrade laboratory rat. *Blood* **55,** 645-648.

Ehrlich R. and Lemonnier F. A. (2000) HFE--a novel nonclassical class I molecule that is involved in iron metabolism. *Immunity* **13,** 585-588.

Eisenstein R. S. (1998) Interaction of the hemochromatosis gene product HFE with transferrin receptor modulates cellular iron metabolism. *Nutr. Rev.* **56,** 356-358.

Eisenstein R. S. (2000) Iron regulatory proteins and the molecular control of mammalian iron metabolism. *Annu. Rev. Nutr.* **20,** 627-662.

Eisenstein R. S., Tuazon P. T., Schalinske K. L., Anderson S. A. and Traugh J. A. (1993) Iron-responsive element-binding protein. *J. Biol. Chem.* **268,** 27363-37370.

Enns C. A. (2001) Pumping iron: the strange partnership of the hemochromatosis protein, a class I MHC homolog, with the transferrin receptor. *Traffic* **2,** 167-174.

Enns C. A., Rutledge E. A. and Williams A. M. (1996) The Transferrin Receptor. *Biomembranes* **4,** 255-287.

Enns C. A., Mulkins M. A., Sussman H. and Root B. (1988) Modulation of the transferrin receptor during DMSO-induced differentiation in HL-60 cells. *Exp. Cell Res.* **174,** 89-97.

Feder J. N., Penny D. M., Irrinki A., Lee V. K., Lebron J. A., Watson N., Tsuchihashi Z., Sigal E., Bjorkman P. J. and Schatzman R. C. (1998) The hemochromatosis gene product complexes with the transferrin receptor and lowers its affinity for ligand binding. *Proc. Natl. Acad. Sci. U. S. A.* **95,** 1472-1477.

Feder J. N., Tsuchihashi Z., Irrinki A., Lee V. K., Mapa F. A., Morikang E., Prass C. E., Starnes S. M., Wolff R. K., Parkkila S., Sly W. S. and Schatzman R. C. (1997) The hemochromatosis founder mutation in HLA-H disrupts β2-microglobulin interaction and cell surface expression. *J. Biol. Chem.* **272,** 14025-14028.

Feder J. N., Gnirke A., Thomas W., Tsuchihashi Z., Ruddy D. A., Basava A., Dormishian F., Domingo R. J., Ellis M. C., Fullan A., Hinton L. M., Jones N. L., Kimmel B. E., Kronmal G. S., Lauer P., Lee V. K., Loeb D. B., Mapa F. A., McClelland E., Meyer N. C., Mintier G. A., Moeller N., Moore T., E. M., Prass C. E., Quintana L., Starnes S. M., Schatzman R. C., Brunke K. J., Drayna D. T., Risch N. J., Bacon B. R. and Wolff R. K. (1996) A novel MHC class I-like gene is mutated in patients with hereditary haemochromatosis. *Nat. Genet.* **13,** 399-408.

Feeney G. P. and Worwood M. (2001) The effects of wild-type and mutant HFE expression upon cellular iron uptake in transfected human embryonic kidney cells. *Biochim. Biophys. Acta* **1538,** 242-251.

Fleming M. D., Romano M. A., Su M. A., Garrick L. M., Garrick M. D. and Andrews N. C. (1998) Nramp2 is mutated in the anemic Belgrade (*b*) rat: evidence of a role for Nramp2 in endosomal iron transport. *Proc. Natl. Acad. Sci. U. S. A.* **95,** 1148-1153.

Fleming M. D., Trenor C. C., Su M. A., Foernzler D., Beier D. R., Dietrich W. F. and Andrews N. C. (1997) Microcytic anaemia mice have a mutation in nramp2, a candidate iron transporter gene. *Nat. Genet.* **16,** 383-386.

Fleming R. E. and Sly W. S. (2002) Mechanisms of iron accumulation in hereditary hemochromatosis. *Annu. Rev. Physiol.* **64,** 663-680.

Fleming R. E., Migas M. C., Holden C. C., Waheed A., Britton R. S., Tomatsu S., Bacon B. R. and Sly W. S. (2000) Transferrin receptor 2: continued expression in mouse liver in the face of iron overload and in hereditary hemochromatosis. *Proc. Natl. Acad. Sci. U. S. A.* **97,** 2214-2219.

Forgac M. (1999) Structure and properties of the vacuolar (H+)-ATPases. *J. Biol. Chem.* **274,** 12951-12954.

Francanzani A. L., Fargion S., Romano R., Piperno A., Arosio P., Ruggeri G., Ronchi G. and Fiorelli G. (1989) Immunohistochemical evidence for a lack of ferritin in duodenal absorptive epithelial cells in idiopathic hemochromatosis. *Gastroenterol.* **96,** 1071-1078.

Ganz T. (2003) Hepcidin, a key regulator of iron metabolism and mediator of anemia of inflammation. *Blood* **102,** 783-788.

Garate M. A. and Nunez M. T. (2000) Overexpression of the ferritin iron-responsive element decreases the labile iron pool and abolishes the regulation of iron absorption by intestinal epithelial (Caco-2) cells. *J. Biol. Chem.* **275,** 1651-1655.

Garcia K. C., Teyton L. and Wilson I. A. (1999) Structural basis of T cell recognition. *Annu. Rev. Immunol.* **17,** 369-397.

Garrick L. M., Dolan K. G., Romano M. A. and Garrick M. D. (1999) Non-transferrin-bound iron uptake in Belgrade and normal rat erythroid cells. *J. Cell. Phys.* **178,** 349-358.

Garrick M. D., Gniecko K., Liu Y., Cohan D. S. and Garrick L. M. (1993) Transferrin and the transferrin cycle in Belgrade rat reticulocytes. *J. Biol. Chem.* **268,** 14867-14874.

Gatter K. C., Brown G., Trowbridge I. S., Woolston R.-E. and Mason D. Y. (1983) Transferrin receptors in human tissues: Their distribution and possible clinical relevance. *J. Clin. Path.* **36,** 539-545.

Gavin M. W., McCarthy D. M. and Garry P. J. (1994) Evidence that iron stores regulate iron absorption--a setpoint theory. *Am. J. Clin. Nutr.* **59,** 1376-1380.

Gehrke S. G., Kulaksiz H., Herrmann T., Riedel H. D., Bents K., Veltkamp C. and Stremmel W. (2003) Expression of hepcidin in hereditary hemochromatosis: evidence for a regulation in response to the serum transferrin saturation and to non-transferrin-bound iron. *Blood* **102,** 371-376.

Geuze H. J., Slot J. W., Strous G. J. A. M., Lodish H. F. and Schwartz A. L. (1983) Intracellular site of asialoglycoprotein receptor-ligand uncoupling: Double-label immunoelectron microscopy during receptor-mediated endocytosis. *Cell* **32,** 277-287.

Geyer G. (1979) Decay of murine intestinal epithelial cells under extrusion. *Acta Histochem.* **64,** 213-225.

Godefroy O., Huet C., Blair L. A., Sahuquillo-Merino C. and Louvard D. (1988) Differentiation of a clone isolated from the HT29 cell line: polarized distribution of histocompatibility antigens (HLA) and of transferrin receptors. *Biol. Cell* **63,** 41-55.

Godefroy O., Huet C., Ibarra C., Dautry-Varsat A. and Louvard D. (1990) Establishment of polarized endocytosis in differentiable intestinal HT29-18 subclones. *New Biol.* **2,** 875-886.

Gossen M. and Bujard H. (1992) Tight control of gene expression in mammalian cells by tetracycline-responsive promoters. *Proc. Natl. Acad. Sci. U. S. A.* **89,** 5547-5551.

Gross C. N., Irrinki A., Feder J. N. and Enns C. A. (1998) Co-trafficking of HFE, a nonclassical major histocompatibility complex class I protein, with the transferrin receptor implies a role in intracellular iron regulation. *J. Biol. Chem.* **273,** 22068-22074.

Gruenberg J., Griffiths G. and Howell K. E. (1989) Characterization of the early endosome and putative endocytic carrier vesicles *in vivo* and with an assay of vesicle fusion *in vitro*. *J. Cell Biol.* **108,** 1301-1316.

Gruenheid S., Cellier M., Vidal S. and Gros P. (1995) Identification and characterization of a second mouse Nramp gene. *Genomics* **25,** 514-525.

Gruenheid S., Canonne-Hergaux F., Gauthier S., Hackam D. J., Grinstein S. and Gros P. (1999) The iron transport protein NRAMP2 is an integral membrane glycoprotein that colocalizes with transferrin in recycling endosomes. *J. Exp. Med.* **189,** 831-841.

Guarnieri F. G., Arterburn L. M., Penno M. B., Cha Y. and August J. T. (1993) The motif Tyr-X-X-hydrophobic residue mediates lysosomal membrane targeting of lysosome-associated membrane protein 1. *J. Biol. Chem.* **268,** 1941-1946.

Gunshin H., Mackenzie B., Berger U. V., Gunshin Y., Romero M. F., Boron W. F., Nussberger S., Gollan J. L. and Hediger M. A. (1997) Cloning and characterization of a mammalian proton-coupled metal-ion transporter. *Nature* **388,** 482-488.

Gunshin H., Allerson C. R., Polycarpou-Schwarz M., Rofts A., Rogers J. T., Kishi F., Hentze M. W., Rouault T. A., Andrews N. C. and Hediger M. A. (2001) Iron-dependent regulation of the divalent metal ion transporter. *FEBS Lett.* **509,** 309-316.

Guo B., Yu Y. and Leibold E. A. (1994) Iron regulates cytoplasmic levels of a novel iron-responsive element-binding protein without aconitase activity. *J. Biol. Chem.* **269,** 24252-24260.

Guo B., Phillips J. D., Yu Y. and Leibold E. A. (1995a) Iron regulates the intracellular degradation of iron regulatory protein 2 by the proteasome. *J. Biol. Chem.* **270,** 21645-21651.

Guo B., Brown F. M., Phillips J. D., Yu Y. and Leibold E. A. (1995b) Characterization and expression of iron regulatory protein 2 (IRP2). Presence of multiple IRP2 transcripts regulated by intracellular iron levels. *J. Biol. Chem.* **270,** 16529-16535.

Haile D. J., Rouault T. A., Tang C. K., Chin J. and Harford J. B. (1992a) Reciprocal control of RNA-binding and aconitase activity in the regulation of the iron-responsive element binding protein: Role of the iron-sulfur cluster. *Proc. Natl. Acad. Sci. U. S. A.* **89,** 7536-7540.

Haile D. J., Rouault T. A., Harford J. B., Kennedy M. C., Blondin G. A., Beinert H. and Klausner R. D. (1992b) Cellular regulation of the iron-responsive element binding protein: disassembly of the cubane iron-sulfur cluster results in high-affinity RNA binding. *Proc. Natl. Acad. Sci. U. S. A.* **89,** 11735-11739.

Han O., Fleet J. C. and Wood R. J. (1999) Reciprocal regulation of HFE and Nramp2 gene expression by iron in human intestinal cells. *J. Nutr.* **129,** 98-104.

Hanson E. S., Foot L. M. and Leibold E. A. (1999) Hypoxia post-translationally activates iron-regulatory protein 2. *J. Biol. Chem.* **274,** 5047-5052.

Harris E. D. (1999) Ceruloplasmin and iron: vindication after 30 years. *Nutrition* **15,** 72-74.

Henderson B. R. and Kuhn L. C. (1995) Differential modulation of the RNA-binding proteins IRP-1 and IRP-2 in response to iron. IRP-2 inactivation requires translation of another protein. *J. Biol. Chem.* **270,** 20509-20515.

Henderson B. R., Seiser C. and Kuhn L. C. (1993) Characterization of a second RNA-binding protein in rodents with specificity for iron-responsive elements. *J. Biol. Chem.* **268,** 27327-27334.

Hentze M. W. and Kuhn L. C. (1996) Molecular control of vertebrate iron metabolism: mRNA-based regulatory circuits operated by iron, nitric oxide, and oxidative stress. *Proc. Natl. Acad. Sci. U. S. A.* **93,** 8175-8182.

Hocker M. and Weidenmann B. (1998) Molecular mechanisms of enteroendocrine differentiation. *Ann. N. Y. Acad. Sci.* **859,** 160-164.

Hunt J. R. and Roughead Z. K. (2000) Adaptation of iron absorption in men consuming diets with high or low iron bioavailability. *Am. J. Clin. Nutr.* **71,** 94-102.

Ikuta K., Fujimoto Y., Suzuki Y., Tanaka K., Saito H., Ohhira M., Sasaki K. and Kohgo Y. (2000) Overexpression of hemochromatosis protein, HFE, alters transferrin recycling process in human hepatoma cells. *Biochim. Biophys. Acta* **1496,** 221-231.

Iwai K., Klausner R. D. and Rouault T. A. (1995) Requirements for iron-regulated degradation of the RNA binding protein, iron regulatory protein 2. *EMBO J.* **14,** 5350-5357.

Iwai K., Drake S. K., Wehr N. B., Weissman A. M., LaVaute T., Minato N., Klausner R. D., Levine R. L. and Rouault T. A. (1998) Iron-dependent oxidation, ubiquitination, and degradation of iron regulatory protein 2: implications for degradation of oxidized proteins. *Proc. Natl. Acad. Sci. U. S. A.* **95,** 4924-4928.

Jeffrey G. P., Basclain K. A. and Allen T. L. (1996) Molecular regulation of transferrin receptor and ferritin expression in the rat gastrointestinal tract. *Gastroenterol.* **110,** 790-800.

Kaptain S., Downey W. E., Tang C., Philpott C., Haile D., Orloff D. G., Harford J. B., Rouault T. A. and Klausner R. D. (1991) A regulated RNA binding protein also possesses aconitase activity. *Proc. Natl. Acad. Sci. U. S. A.* **88,** 10109-10113.

Kato J., Fujikawa K., Kanda M., Fukuda N., Sasaki K., Takayama T., Kobune M., Takada K., Takimoto R., Hamada H., Ikeda T. and Niitsu Y. (2001) A mutation, in the iron-responsive element of H ferritin mRNA, causing autosomal dominant iron overload. *Am. J. Hum. Genet.* **69,** 191-197.

Kawabata H., Germain R. S., Vuong P. T., Nakamaki T., Said J. W. and Koeffler H. P. (2000) Transferrin receptor 2-alpha supports cell growth both in iron-chelated cultured cells and in vivo. *J. Biol. Chem.* **275,** 16618-16625.

Kawabata H., Yang R., Hirama T., Vuong P. T., Kawano S., Gombart A. F. and Koeffler H. P. (1999) Molecular cloning of transferrin receptor 2. A new member of the transferrin receptor-like family. *J. Biol. Chem.* **274,** 20826-20832.

Ke Y., Wu J., Leibold E. A., Walden W. E. and Theil E. C. (1998) Loops and bulge/loops in iron-responsive element isoforms influence iron regulatory protein binding. Fine-tuning of mRNA regulation? *J. Biol. Chem.* **273,** 23637-23640.

Klausner R. D., Rouault T. A. and Harford J. B. (1993) Regulating the fate of mRNA: the control of cellular iron metabolism. *Cell* **72,** 19-28.

Klausner R. D., Ashwell G., van Renswoude J., Harford J. B. and Bridges K. R. (1983) Binding of apotransferrin to K562 cells: Explanation of the transferrin cycle. *Proc. Natl. Acad. Sci. U. S. A.* **80,** 2263-2266.

Koeller D. M., Casey J. L., Hentze M. W., Gerhardt E. M., Chan L. N., Klausner R. D. and Harford J. B. (1989) A cytosolic protein binds to structural elements within the iron regulatory region of the transferrin receptor mRNA. *Proc Natl Acad Sci U. S. A.* **86,** 3574-3578.

Konijn A. M., Glickstein H., Vaisman B., Meyron-Holtz E. G., Slotki I. N. and Cabantchik Z. I. (1999) The cellular labile iron pool and intracellular ferritin in K562 cells. *Blood* **94,** 2128-2134.

Kuo Y. M., Su T., Chen H., Attieh Z., Syed B. A., McKie A. T., Anderson G. J., Gitschier J. and Vulpe C. D. (2004) Mislocalisation of hephaestin, a multicopper ferroxidase involved in basolateral intestinal iron transport, in the sex linked anaemia mouse. *Gut* **53,** 201-206.

Laemmli U. K. (1970) Cleavage of structural proteins during the assembly of the head of bacteriophage T4. *Nature* **227,** 680-685.

Lane R. S. (1975) Differences between human Fe1-transferrin molecules. *Br. J. Haematol.* **29,** 511-520.

Lawson D. M., Treffry A., Artymiuk P. J., Harrison P. M., Yewdall S. J., Luzzago A., Cesareni G., Levi S. and Arosio P. (1989) Identification of the ferroxidase centre in ferritin. *FEBS Lett.* **254,** 207-210.

Lebron J. A. and Bjorkman P. J. (1999) The transferrin receptor binding site on HFE, the class I MHC-related protein mutated in hereditary hemochromatosis. *J. Mol. Biol.* **289,** 1109-1118.

Lebron J. A., West A. P., Jr. and Bjorkman P. J. (1999) The hemochromatosis protein HFE competes with transferrin for binding to the transferrin receptor. *J. Mol. Biol.* **294,** 239-245.

Lebron J. A., Bennett M. J., Vaughn D. E., Chirino A. J., Snow P. M., Mintier G. A., Feder J. N. and Bjorkman P. J. (1998) Crystal structure of the hemochromatosis protein HFE and characterization of its interaction with transferrin receptor. *Cell* **93,** 111-123.

Lee P. L., Gelbart T., West C., Halloran C. and Beutler E. (1998) The human Nramp2 gene: characterization of the gene structure, alternative splicing, promoter region and polymorphisms. *Blood Cells Mol. Dis.* **24,** 199-215.

Leibman A. and Aisen P. (1979) Distribution of iron between the binding sites of normal transferrin in serum: methods and results in normal human subjects. *Blood* **53,** 1058-1065.

Leibold E. A. and Munro H. N. (1988) Cytoplasmic protein binds in vitro to a highly conserved sequence in the 5' untranslated region of ferritin heavy- and light-subunit mRNAs. *Proc. Natl. Acad. Sci. U. S. A.* **85,** 2171-2175.

Levi S., Luzzago A., Cesareni G., Cozzi A., Franceschinelli F., Albertini A. and Arosio P. (1988) Mechanism of ferritin iron uptake: activity of the H-chain and deletion mapping of the ferro-oxidase site. A study of iron uptake and ferro-oxidase activity of human liver, recombinant H-chain ferritins, and of two H-chain deletion mutants. *J. Biol. Chem.* **263,** 18086-18092.

Levi S., Yewdall S. J., Harrison P. M., Santambrogio P., Cozzi A., Rovida E., Albertini A. and Arosio P. (1992) Evidence of H- and L-chains have co-operative roles in the iron-uptake mechanism of human ferritin. *Biochem. J.* **288,** 591-596.

Levy J. E., Montross L. K. and Andrews N. C. (2000) Genes that modify the hemochromatosis phenotype in mice. *J. Clin. Invest.* **105,** 1209-1216.

Levy J. E., Jin O., Fujiwara Y., Kuo F. and Andrews N. C. (1999a) Transferrin receptor is necessary for development of erythrocytes and the nervous system. *Nat. Genet.* **21,** 396-399.

Levy J. E., Montross L. K., Cohen D. E., Fleming M. D. and Andrews N. C. (1999b) The C282Y mutation causing hereditary hemochromatosis does not produce a null allele. *Blood* **94,** 9-11.

Lok C. N. and Loh T. T. (1998) Regulation of transferrin function and expression: review and update. *Biol. Signals Recept.* **7,** 157-178.

Lombard M., Chua E. and O'Toole P. (1997) Regulation of intestinal non-haem iron absorption. *Gut* **40,** 435-439.

Lymboussaki A., Pignatti E., Montosi G., Garuti C., Haile D. J. and Pietrangelo A. (2003) The role of the iron responsive element in the control of ferroportin1/IREG1/MTP1 gene expression. *J. Hepatol.* **39,** 710-715.

Makey D. G. and Seal U. S. (1976) The detection of four molecular forms of human transferrin during the iron binding process. *Biochim. Biophys. Acta* **453,** 250-256.

Manis J. (1971) Intestinal iron-transport defect in the mouse with sex-linked anemia. *Am J. Physiol.* **220,** 135-139.

Mann S., Bannister J. V. and Williams R. J. (1986) Structure and composition of ferritin cores isolated from human spleen, limpet (Patella vulgata) hemolymph and bacterial (Pseudomonas aeruginosa) cells. *J. Mol. Biol.* **188,** 225-232.

Mason A., He Q. Y., Tam B., MacGillivray R. A. and Woodworth R. (1998) Mutagenesis of the aspartic acid ligands in human serum transferrin: lobe-lobe interaction and conformation as revealed by antibody, receptor-binding and iron-release studies. *Biochem. J.* **330,** 35-40.

Mason A. B., Tam B. M., Woodworth R. C., Oliver R. W., Green B. N., Lin L. N., Brandts J. F., Savage K. J., Lineback J. A. and MacGillivray R. T. (1997) Receptor recognition sites reside in both lobes of human serum transferrin. *Biochem. J.* **326,** 77-85.

Mattman A., Huntsman D., Lockitch G., Langlois S., Buskard N., Ralston D., Butterfield Y., Rodrigues P., Jones S., Porto G., Marra M., De Sousa M. and Vatcher G. (2002) Transferrin receptor 2 (TfR2) and HFE mutational analysis in non-C282Y iron overload: identification of a novel TfR2 mutation. *Blood* **100,** 1075-1077.

McKie A. T., Marciani P., Rolfs A., Brennan K., Wehr K., Barrow D., Miret S., Bomford A., Peters T. J., Farzaneh F., Hediger M. A., Hentze M. W. and Simpson R. J. (2000) A novel duodenal iron-regulated transporter, IREG1, implicated in the basolateral transfer of iron to the circulation. *Molec. Cell* **5,** 299-309.

McKie A. T., Barrow D., Latunde-Dada G. O., Rolfs A., Sager G., Mudaly E., Mudaly M., Richardson C., Barlow D., Bomford A., Peters T. J., Raja K. B., Shirali S., Hediger M. A., Farzaneh F. and Simpson R. J. (2001) An iron-regulated ferric reductase associated with the absorption of dietary iron. *Science* **291,** 1755-1759.

McLaren G. D., Nathanson M. H., Jacobs A., Trevett D. and Thomson W. (1991) Regulation of intestinal iron absorption and mucosal iron kinetics in hereditary hemochromatosis. *J. Lab. Clin. Med.* **117,** 390-401.

Monsen E. R. (1988) Iron nutrition and absorption: dietary factors which impact iron bioavailability. *J. Am. Diet. Assoc.* **88,** 786-790.

Montosi G., Paglia P., Garuti C., Guzman C. A., Bastin J. M., Colombo M. P. and Pietrangelo A. (2000) Wild-type HFE protein normalizes transferrin iron accumulation in macrophages from subjects with hereditary hemochromatosis. *Blood* **96,** 1125-1129.

Montosi G., Donovan A., Totaro A., Garuti C., Pignatti E., Cassanelli S., Trenor C. C., Gasparini P., Andrews N. C. and Pietrangelo A. (2001) Autosomal-dominant hemochromatosis is associated with a mutation in the ferroportin (SLC11A3) gene. *J. Clin. Invest.* **108,** 619-623.

Morgan E. H. (1979) Studies on the mechanism of iron release from transferrin. *Biochim. Biophys. Acta* **580,** 312-326.

Morgan E. H. (1981) Transferrin: Biochemistry, physiology, and clinical significance. *Molecular Aspects of Medicine* **4,** 1-123.

Muckenthaler M., Gray N. K. and Hentze M. W. (1998) IRP-1 binding to ferritin mRNA prevents the recruitment of the small ribosomal subunit by the cap-binding complex eIF4F. *Molec. Cell* **2,** 383-388.

Muckenthaler M., Roy C. N., Custodio A. O., Minana B., DeGraaf J., Montross L. K., Andrews N. C. and Hentze M. W. (2003) Regulatory defects in liver and intestine implicate abnormal hepcidin and Cybrd1 expression in mouse hemochromatosis. *Nat. Genet.* **34,** 102-107.

Mukhopadhyay C. K., Attieh Z. K. and Fox P. L. (1998) Role of ceruloplasmin in cellular iron uptake. *Science* **279,** 714-717.

Mullner E. W. and Kuhn L. C. (1988) A stem-loop in the 3' untranslated region mediates iron dependent regulation of transferrin receptor mRNA stability in the cytoplasm. *Cell* **53,** 815-825.

Mullner E. W., Neupert B. and Kuhn L. C. (1989) A specific mRNA binding factor regulates the iron-dependent stability of cytoplasmic transferrin receptor mRNA. *Cell* **58,** 373-382.

Mura C., Raguenes O. and Ferec C. (1999) HFE mutations analysis in 711 hemochromatosis probands: evidence for S65C implication in mild form of hemochromatosis. *Blood* **93,** 2502-2505.

Nathanson M. H., Muir A. and McLaren G. D. (1985) Iron absorption in normal and iron-deficient beagle dogs: mucosal iron kinetics. *Am. J. Physiol.* **249,** G439-448.

Nelson N. (1999) Metal ion transporters and homeostasis. *EMBO J.* **18,** 4361-4371.

Nicolas G., Bennoun M., Devaux I., Beaumont C., Grandchamp B., Kahn A. and Vaulont S. (2001) Lack of hepcidin gene expression and severe tissue iron overload in upstream stimulatory factor 2 (USF2) knockout mice. *Proc. Natl. Acad. Sci. U. S. A.* **98,** 8780-8785.

Njajou O. T., Vaessen N., Joosse M., Berghuis B., van Dongen J. W., Breuning M. H., Snijders P. J., Rutten W. P., Sandkuijl L. A., Oostra B. A., van Duijn C. M. and Heutink P. (2001) A mutation in SLC11A3 is associated with autosomal dominant hemochromatosis. *Nat. Genet.* **28,** 213-214.

Oates P. S. and Morgan E. H. (1996a) Defective iron uptake by the duodenum of Belgrade rats fed diets of different iron contents. *Am. J. Physiol.* **270,** G826-832.

Oates P. S. and Morgan E. H. (1996b) Effects of dietary iron loading with carbonyl iron and of iron depletion on intestinal growth, morphology, and expression of transferrin receptor in the rat. *Anat. Rec.* **246,** 364-371.

Oates P. S., Trinder D. and Morgan E. H. (2000a) Gastrointestinal function, divalent metal transporter-1 expression and intestinal iron absorption. *Pflugers Arch.* **440,** 496-502.

Oates P. S., Thomas C., Freitas E., Callow M. J. and Morgan E. H. (2000b) Gene expression of divalent metal transporter 1 and transferrin receptor in duodenum of Belgrade rats. *Am. J. Physiol. Gastrointest. Liver Physiol.* **278,** G930-936.

Osaki S., Johnson D. A. and Frieden E. (1971) The mobilization of iron from the perfused mammalian liver by a serum copper enzyme, ferroxidase I. *J. Biol. Chem.* **246,** 3018-3023.

Pantopoulos K. and Hentze M. W. (1995) Rapid responses to oxidative stress mediated by iron regulatory protein. *EMBO J.* **14,** 2917-2924.

Pantopoulos K., Weiss G. and Hentze M. W. (1996) Nitric oxide and oxidative stress (H_2O_2) control mammalian iron metabolism by different pathways. *Mol. Cell. Biol.* **16,** 3781-3788.

Papanikolaou G., Politou M., Roetto A., Bosio S., Sakelaropoulos N., Camaschella C. and Loukopoulos D. (2001) Linkage to chromosome 1q in Greek families with juvenile hemochromatosis. *Blood Cells Mol. Dis.* **27,** 744-749.

Papanikolaou G., Papaioannou M., Politou M., Vavatsi N., Kioumi A., Tsiatsiou P., Marinaki P., Loukopoulos D. and Christakis J. I. (2002) Genetic heterogeneity underlies juvenile hemochromatosis phenotype: analysis of three families of northern Greek origin. *Blood Cells Mol. Dis.* **29,** 168-173.

Papanikolaou G., Samuels M. E., Ludwig E. H., MacDonald M. L., Franchini P. L., Dube M. P., Andres L., MacFarlane J., Sakellaropoulos N., Politou M., Nemeth E., Thompson J., Risler J. K., Zaborowska C., Babakaiff R., Radomski C. C., Pape T. D., Davidas O., Christakis J., Brissot P., Lockitch G., Ganz T., Hayden M. R. and Goldberg Y. P. (2004) Mutations in HFE2 cause iron overload in chromosome 1q-linked juvenile hemochromatosis. *Nat. Genet.* **36,** 77-82.

Park C. H., Bacon B. R., Brittenham G. M. and Tavill A. S. (1987) Pathology of dietary carbonyl iron overload in rats. *Lab Invest.* **57,** 555-563.

Park C. H., Valore E. V., Waring A. J. and Ganz T. (2001) Hepcidin, a urinary antimicrobial peptide synthesized in the liver. *J. Biol. Chem.* **276,** 7806-7810.

Parkkila S., Waheed A., Britton R. S., Feder J. N., Tsuchihashi Z., Schatzman R. C., Bacon B. R. and Sly W. S. (1997a) Immunohistochemistry of HLA-H, the protein defective in patients with hereditary hemochromatosis, reveals unique pattern of expression in gastrointestinal tract. *Proc. Natl. Acad. Sci. U. S. A.* **94,** 2534-2539.

Parkkila S., Waheed A., Britton R. S., Bacon B. R., Zhou X. Y., Tomatsu S., Fleming R. E. and Sly W. S. (1997b) Association of the transferrin receptor in human placenta with HFE, the protein defective in hereditary hemochromatosis. *Proc. Natl. Acad. Sci. U. S. A.* **94,** 13198-13202.

Pietrangelo A., Casalgrandi G., Quaglino D., Gualdi R., Conte D., Milani S., Montosi G., Cesarini L., Ventura E. and Cairo G. (1995) Duodenal ferritin synthesis in genetic hemochromatosis. *Gastroenterol.* **108,** 208-217.

Pigeon C., Ilyin G., Courselaud B., Leroyer P., Turlin B., Brissot P. and Loreal O. (2001) A new mouse liver-specific gene, encoding a protein homologous to human antimicrobial peptide hepcidin, is overexpressed during iron overload. *J. Biol. Chem.* **276,** 7811-7819.

Ponka P., Beaumont C. and Richardson D. R. (1998) Function and regulation of transferrin and ferritin. *Semin. Hematol.* **35,** 35-54.

Potten C. S., Booth C., Tudor G. L., Booth D., Brady G., Hurley P., Ashton G., Clarke R., Sakakibara S. and Okano H. (2003) Identification of a putative intestinal stem cell and early lineage marker; musashi-1. *Differentiation* **71,** 28-41.

Powell L. W., Campbell C. B. and Wilson E. (1970) Intestinal mucosal uptake of iron and iron retention in idiopathic haemochromatosis as evidence for a mucosal abnormality. *Gut* **11,** 727-731.

Ramalingam T. S., West A. P., Jr., Lebron J. A., Nangiana J. S., Hogan T. H., Enns C. A. and Bjorkman P. J. (2000) Binding to the transferrin receptor is required for endocytosis of HFE and regulation of iron homeostasis. *Nat. Cell Biol.* **2,** 953-957.

Recalcati S., Taramelli D., Conte D. and Cairo G. (1998) Nitric oxide-mediated induction of ferritin synthesis in J774 macrophages by inflammatory cytokines: role of selective iron regulatory protein-2 downregulation. *Blood* **91,** 1059-1066.

Riedel H. D., Muckenthaler M. U., Gehrke S. G., Mohr I., Brennan K., Herrmann T., Fitscher B. A., Hentze M. W. and Stremmel W. (1999) HFE downregulates iron uptake from transferrin and induces iron- regulatory protein activity in stably transfected cells. *Blood* **94,** 3915-3921.

Rivard S. R., Lanzara C., Grimard D., Carella M., Simard H., Ficarella R., Simard R., D'Adamo A. P., Ferec C., Camaschella C., Mura C., Roetto A., De Braekeleer M., Bechner L. and Gasparini P. (2003) Juvenile hemochromatosis locus maps to chromosome 1q in a French Canadian population. *Eur. J. Hum. Genet.* **11,** 585-589.

Roetto A., Totaro A., Piperno A., Piga A., Longo F., Garozzo G., Cali A., De Gobbi M., Gasparini P. and Camaschella C. (2001) New mutations inactivating transferrin receptor 2 in hemochromatosis type 3. *Blood* **97,** 2555-2560.

Roetto A., Totaro A., Cazzola M., Cicilano M., Bosio S., D'Ascola G., Carella M., Zelante L., Kelly A. L., Cox T. M., Gasparini P. and Camaschella C. (1999) Juvenile hemochromatosis locus maps to chromosome 1q. *Am. J. Hum. Genet.* **64,** 1388-1393.

Rothenberg B. E. and Voland J. R. (1996) beta2 knockout mice develop parenchymal iron overload: A putative role for class I genes of the major histocompatibility complex in iron metabolism. *Proc. Natl. Acad. Sci. U. S. A.* **93,** 1529-1534.

Rouault T. A., Hentze M. W., Caughman S. W., Harford J. B. and Klausner R. D. (1988) Binding of a cytosolic protein to the iron-responsive element of human ferritin messenger RNA. *Science* **241,** 1207-1210.

Rouault T. A., Stout D. C., Kaptain S., Harford J. B. and Klausner R. D. (1991) Structural relationship between an iron-regulated RNA-binding protein (IRE-BP) and aconitase: Functional implications. *Cell* **64,** 881-883.

Roy C. N., Penny D. M., Feder J. N. and Enns C. A. (1999) The hereditary hemochromatosis protein, HFE, specifically regulates transferrin-mediated iron uptake in HeLa cells. *J. Biol. Chem.* **274,** 9022-9028.

Roy C. N., Carlson E. J., Anderson E. L., Basava A., Starnes S. M., Feder J. N. and Enns C. A. (2000) Interactions of the ectodomain of HFE with the transferrin receptor are critical for iron homeostasis in cells. *FEBS Lett.* **484,** 271-274.

Roy C. N., Blemings K. P., Deck K. M., Davies P. S., Anderson E. L., Eisenstein R. S. and Enns C. A. (2002) Increased IRP1 and IRP2 RNA binding activity accompanies a reduction of the labile iron pool in HFE-expressing cells. *J. Cell. Physiol.* **190,** 218-226.

Rutledge E. A., Mikoryak C. A. and Draper R. K. (1991) Turnover of the transferrin receptor is not influenced by removing most of the extracellular domain. *J. Biol. Chem.* **266,** 21125-21130.

Rutledge E. A., Root B. J., Lucas J. J. and Enns C. A. (1994) Elimination of the O-linked glycosylation site at Thr 104 results in the generation of a soluble human-transferrin receptor. *Blood* **83,** 580-586.

Sacher A., Cohen A. and Nelson N. (2001) Properties of the mammalian and yeast metal-ion transporters DCT1 and Smf1p expressed in Xenopus laevis oocytes. *J. Exp. Biol.* **204,** 1053-1061.

Salter-Cid L., Peterson P. A. and Yang Y. (2000) The major histocompatibility complex-encoded HFE in iron homeostasis and immune function. *Immunol. Res.* **22,** 43-59.

Salter-Cid L., Brunmark A., Li Y., Leturcq D., Peterson P. A., Jackson M. R. and Yang Y. (1999) Transferrin receptor is negatively modulated by the hemochromatosis protein

HFE: implications for cellular iron homeostasis. *Proc. Natl. Acad. Sci. U. S. A.* **96,** 5434-5439.

Santos M., Clevers H., de Sousa M. and Marx J. J. (1998) Adaptive response of iron absorption to anemia, increased erythropoiesis, iron deficiency, and iron loading in beta2-microglobulin knockout mice. *Blood* **91,** 3059-3065.

Santos M., Schilham M. W., Rademakers L. H., Marx J. J., de S. M. and Clevers H. (1996) Defective iron homeostasis in beta 2-microglobulin knockout mice recapitulates hereditary hemochromatosis in man. *J. Exp. Med.* **184,** 1975-1985.

Schalinske K. L. and Eisenstein R. S. (1996) Phosphorylation and activation of both iron regulatory proteins 1 and 2 in HL-60 cells. *J. Biol. Chem.* **271,** 7168-7176.

Schalinske K. L., Blemings K. P., Steffen D. W., Chen O. S. and Eisenstein R. S. (1997) Iron regulatory protein 1 is not required for the modulation of ferritin and transferrin receptor expression by iron in a murine pro-B lymphocyte cell line. *Proc. Natl. Acad. Sci. U. S. A.* **94,** 10681-10686.

Schmid S. L. (1992) The mechanism of receptor-mediated endocytosis; more questions than answers. *Bioessays* **14,** 589-596.

Schumann K., Moret R., Kunzle H. and Kuhn L. C. (1999) Iron regulatory protein as an endogenous sensor of iron in rat intestinal mucosa. Possible implications for the regulation of iron absorption. *Eur. J. Biochem.* **260,** 362-372.

Shayeghi M., Halliday N., Oakhill J., Latunde-Dada G. O., Frazer D. M., Vulpe C. D., Anderson G. J., Simpson R. J. and McKie A. T. (2003) Characterization of a novel gene highly expressed in duodenum. *BioIron 2003: The International BioIron Society World Congress on Iron Metabolism Final Program and Abstract Book* p 33.

Sipe D. M. and Murphy R. F. (1991) Binding to cellular receptor results in increased iron release from transferrin at mildly acidic pH. *J. Biol. Chem.* **266,** 8002-8007.

Snider M. D. and Rogers O. C. (1985) Intracellular movement of cell surface receptors after endocytosis: Resialylation of asialo-transferrin receptor in human erythroleukemia cells. *J. Cell Biol.* **100,** 826-834.

Su M. A., Trenor C. C., Fleming J. C., Fleming M. D. and Andrews N. C. (1998) The G185R mutation disrupts function of the iron transporter Nramp2. *Blood* **92,** 2157-2163.

Tandy S., Williams M., Leggett A., Lopez-Jimenez M., Dedes M., Ramesh B., Srai S. K. and Sharp P. (2000) Nramp2 expression is associated with pH-dependent iron uptake across the apical membrane of human intestinal caco-2 cells. *J. Biol. Chem.* **275,** 1023-1029.

Ten Elshof A. E., Brittenham G. M., Chorney K. A., Page M. J., Gerhard G., Cable E. E. and Chorney M. J. (1999) Gamma delta intraepithelial lymphocytes drive tumor necrosis factor- alpha responsiveness to intestinal iron challenge: relevance to hemochromatosis. *Immunol. Rev.* **167,** 223-232.

Theil E. C. (1998) The iron responsive element (IRE) family of mRNA regulators. Regulation of iron transport and uptake compared in animals, plants, and microorganisms. *Met. Ions Biol. Syst.* **35,** 403-434.

Torti F. M. and Torti S. V. (2002) Regulation of ferritin genes and protein. *Blood* **99,** 3505-3516.

Trinder D., Olynyk J. K., Sly W. S. and Morgan E. H. (2002) Iron uptake from plasma transferrin by the duodenum is impaired in the Hfe knockout mouse. *Proc. Natl. Acad. Sci. U. S. A.* **99,** 5622-5626.

Trinder D., Oates P. S., Thomas C., Sadleir J. and Morgan E. H. (2000) Localisation of divalent metal transporter 1 (DMT1) to the microvillus membrane of rat duodenal enterocytes in iron deficiency, but to hepatocytes in iron overload. *Gut* **46,** 270-276.

Tsunoo H. and Sussman H. H. (1983) Characterization of transferrin binding and specificity of the placental transferrin receptor. *Arch. Biochem. Biophys.* **225,** 42-54.

Vulpe C. D., Kuo Y. M., Murphy T. L., Cowley L., Askwith C., Libina N., Gitschier J. and Anderson G. J. (1999) Hephaestin, a ceruloplasmin homologue implicated in intestinal iron transport, is defective in the sla mouse. *Nat. Genet.* **21,** 195-199.

Waheed A., Parkkila S., Saarnio J., Fleming R. E., Zhou X. Y., Tomatsu S., Britton R. S., Bacon B. R. and Sly W. S. (1999) Association of HFE protein with transferrin receptor in crypt enterocytes of human duodenum. *Proc. Natl. Acad. Sci. U. S. A.* **96,** 1579-1584.

Waheed A., Grubb J. H., Zhou X. Y., Tomatsu S., Fleming R. E., Costaldi M. E., Britton R. S., Bacon B. R. and Sly W. S. (2002) Regulation of transferrin-mediated iron uptake by HFE, the protein defective in hereditary hemochromatosis. *Proc. Natl. Acad. Sci. U. S. A.* **99,** 3117-3122.

Waheed A., Parkkila S., Zhou X. Y., Tomatsu S., Tsuchihashi Z., Feder J. N., Schatzman R. C., Britton R. S., Bacon B. R. and Sly W. S. (1997) Hereditary hemochromatosis: effects of C282Y and H63D mutations on association with beta2-microglobulin, intracellular processing, and cell surface expression of the HFE protein in COS-7 cells. *Proc. Natl. Acad. Sci. U. S. A.* **94,** 12384-12389.

Wallace D. F., Pedersen P., Dixon J. L., Stephenson P., Searle J. W., Powell L. W. and Subramaniam V. N. (2002) Novel mutation in ferroportin1 is associated with autosomal dominant hemochromatosis. *Blood* **100,** 692-694.

Wang J., Chen G. and Pantopoulos K. (2003) The haemochromatosis protein HFE induces an apparent iron-deficient phenotype in H1299 cells that is not corrected by co-expression of beta 2-microglobulin. *Biochem. J.* **370,** 891-899.

Ward J. H., Kushner J. P. and Kaplan J. (1982) Regulation of HeLa cell transferrin receptors. *J. Biol. Chem.* **257,** 10317-10323.

Wardrop S. L. and Richardson D. R. (1999) The effect of intracellular iron concentration and nitrogen monoxide on Nramp2 expression and non-transferrin-bound iron uptake. *Eur. J. Biochem.* **263,** 41-49.

Warren R. A., Green F. A. and Enns C. A. (1997) Saturation of the endocytic pathway for the transferrin receptor does not affect the endocytosis of the epidermal growth factor receptor. *J. Biol. Chem.* **272,** 2116-2121.

Warren R. A., Green F. A., Stenberg P. E. and Enns C. A. (1998) Distinct saturable pathways for the endocytosis of different tyrosine motifs. *J. Biol. Chem.* **273,** 17056-17063.

Weiser M. M. (1973) Intestinal epithelial cell surface membrane glycoprotein synthesis. I. An indicator of cellular differentiation. *J. Biol. Chem.* **248,** 2536-2541.

Weiss G., Goossen B., Doppler W., Fuchs D., Pantopoulos K., Werner-Felmayer G., Wachter H. and Hentze M. W. (1993) Translational regulation via iron-responsive elements by the nitric oxide/NO-synthase pathway. *EMBO J.* **12,** 3651-3657.

West A. P., Jr., Bennett M. J., Sellers V. M., Andrews N. C., Enns C. A. and Bjorkman P. J. (2000) Comparison of the interactions of transferrin receptor and transferrin receptor 2 with transferrin and the hereditary hemochromatosis protein HFE. *J. Biol. Chem.* **275,** 38135-38138.

West A. P., Jr., Giannetti A. M., Herr A. B., Bennett M. J., Nangiana J. S., Pierce J. R., Weiner L. P., Snow P. M. and Bjorkman P. J. (2001) Mutational Analysis of the Transferrin Receptor Reveals Overlapping HFE and Transferrin Binding Sites. *J. Mol. Biol.* **313,** 385-397.

Williams A. M. and Enns C. A. (1991) A mutated transferrin receptor lacking asparagine-linked glycosylation sites shows reduced functionality and an association with binding immunoglobulin protein. *J. Biol. Chem.* **266,** 17648-17654.

Wyllie J. C. and Kaufman N. (1982) An electron microscopic study of heme uptake by rat duodenum. *Lab Invest.* **47,** 471-476.

Yajima H., Sakajiri T., Kikuchi T., Morita M. and Ishii T. (2000) Molecular modeling of human serum transferrin for rationalizing the changes in its physicochemical properties

induced by iron binding. Implication of the mechanism of binding to its receptor. *J. Protein Chem.* **19,** 215-223.

Yamashiro D. J. and Maxfield F. R. (1984) Acidification of endocytic compartments and the intracellular pathways of ligands and receptors. *J. Cell. Biochem.* **26,** 231-246.

Yamashiro D. J., Fluss S. R. and Maxfield F. R. (1983) Acidification of endocytic vesicles by an ATP-dependent proton pump. *J. Cell Biol.* **97,** 929-934.

Young S. P. and Aisen P. (1981) Transferrin receptors and the uptake and release of iron by isolated hepatocytes. *Hepatol.* **1,** 114-119.

Young S. P., Bomford A. and Williams R. (1984) The effect of the iron saturation of transferrin on its binding and uptake by rabbit reticulocytes. *Biochem. J.* **219,** 505-510.

Zak O., Trinder D. and Aisen P. (1994) Primary receptor-recognition site of human transferrin is the C-terminal lobe. *J. Biol. Chem.* **269,** 7110-7114.

Zhang A. S., Davies P. S., Carlson H. L. and Enns C. A. (2003) Mechanisms of HFE-induced regulation of iron homeostasis: Insights from the W81A HFE mutation. *Proc. Natl. Acad. Sci. U. S. A.* **100,** 9500-9505.

Zhang A. S., Xiong S., Tsukamoto H. and Enns C. A. (2004) Localization of iron metabolism-related mRNAs in rat liver indicate that HFE is expressed predominantly in hepatocytes. *Blood* **103,** 1509-1514.

Zhou X. Y., Tomatsu S., Fleming R. E., Parkkila S., Waheed A., Jiang J., Fei Y., Brunt E. M., Ruddy D. A., Prass C. E., Schatzman R. C., O'Neill R., Britton R. S., Bacon B. R. and Sly W. S. (1998) HFE gene knockout produces mouse model of hereditary hemochromatosis. *Proc. Natl. Acad. Sci. U. S. A.* **95,** 2492-2497.

Zoller H., Theurl I., Koch R., Kaser A. and Weiss G. (2002) Mechanisms of iron mediated regulation of the duodenal iron transporters divalent metal transporter 1 and ferroportin 1. *Blood Cells Mol. Dis.* **29,** 488-497.